Copyright Warning & Restrictions

The copyright law of the United States (Title 17, United States Code) governs the making of photocopies or other reproductions of copyrighted material.

Under certain conditions specified in the law, libraries and archives are authorized to furnish a photocopy or other reproduction. One of these specified conditions is that the photocopy or reproduction is not to be "used for any purpose other than private study, scholarship, or research." If a, user makes a request for, or later uses, a photocopy or reproduction for purposes in excess of "fair use" that user may be liable for copyright infringement,

This institution reserves the right to refuse to accept a copying order if, in its judgment, fulfillment of the order would involve violation of copyright law.

Please Note: The author retains the copyright while the New Jersey Institute of Technology reserves the right to distribute this thesis or dissertation

Printing note: If you do not wish to print this page, then select "Pages from: first page # to: last page #" on the print dialog screen

Order Number 9426998

Engineering analysis of a packed-bed biofilter for removal of volatile organic compound (VOC) emissions

Shareefdeen, Zarook Mohamed, Ph.D.

New Jersey Institute of Technology, 1994

U·M·I
300 N. Zeeb Rd.
Ann Arbor, MI 48106

ABSTRACT

ENGINEERING ANALYSIS OF A PACKED-BED BIOFILTER FOR REMOVAL OF VOLATILE ORGANIC COMPOUND (VOC) EMISSIONS

by
Zarook M. Shareefdeen

This study dealt with removal of VOC emissions from airstreams using an evolving new technology which is known as biofiltration. The basis of this technology is biodegradation of VOCs in biofilms formed around porous solids which are placed in packed-bed reactors.

A detailed model describing steady state biofiltration of single and mixed VOCs was developed, and experimentally validated. The model takes into account biodegradation kinetics, the effect of oxygen, kinetic interactions among structurally similar compounds, and mass transfer from the gas phase to the biolayer. It was found that oxygen (a factor neglected in all previous studies) plays a very important role in biofiltration of VOCs, especially those which are hydrophilic. It was also found that the kinetics of biodegradation are complex, and that assumptions of zero or first order kinetics made by other researchers are invalid, and can lead to significant errors in biofilter design. Sensitivity studies with the model have shown that some of the kinetic parameters, and the biofilm surface area per unit volume of biofilter bed are important in all cases. For hydrophilic solvent vapors, sensitivity studies indicate that oxygen availability in the biolayer is also extremely important.

The model was experimentally validated. In the case of single VOCs, methanol, benzene, and toluene were the model compounds. Methanol data were obtained from another study, while benzene and toluene data were generated during the course of this

study from a unit 75cm-high and 10cm in diameter. For benzene removal, the residence time was varied from 2.7 min to 4.7 min, and the concentration in the inlet air from 0.07 gm^{-3} to 0.56 gm^{-3}. During the experiments for toluene vapor removal, the residence time was varied from 2.7 min to 8.6 min, and the inlet concentration from 0.62 gm^{-3} to 2.81 gm^{-3}. Validation of the model for the case of mixed VOCs was done with experiments involving mixtures of benzene and toluene. The unit was a three-stage glass column specifically designed during the course of this work. Each segment was 15.2cm in diameter and 30.5cm in height. Residence times varied from 0.9 min to 3.1 min, inlet benzene concentrations from 0.13 gm^{-3} to 0.37 gm^{-3}, and inlet toluene concentrations from 0.21 gm^{-3} to 0.52 gm^{-3}. In all cases, there was excellent agreement between model predictions and experimentally obtained concentrations. The experimental columns were continuously operated for periods over six months for single VOCs, while for mixed VOCs the column operated continuously for a year and a half. Except at start-up, in no case were additional nutrients added to the columns, while the pressure drop never exceeded 0.25" water/m of biofilter bed. Peat and perlite mixtures (2:3 volume ratio before packing) were used in all columns as solid porous support for the biofilm.

Transient operation of biofilters involves, in addition to the mass transfer and reaction processes occurring at steady state, reversible adsorption of VOCs onto the packing material. This extra process was taken into account in developing a model which describes transient biofiltration of airstreams containing a single VOC. This model was experimentally validated with data for transient removal of toluene vapor. Good agreement was found between theory and experiments.

The experimentally validated models developed in this study, can be used in (at least preliminary) scale-up and design of industrial biofilters.

ENGINEERING ANALYSIS OF A PACKED-BED BIOFILTER FOR REMOVAL OF VOLATILE ORGANIC COMPOUND (VOC) EMISSIONS

by
Zarook M. Shareefdeen

A Dissertation
Submitted to the Faculty of
New Jersey Institute of Technology
in Partial Fulfillment of the Requirements for the Degree of
Doctor of Philosophy

Department of Chemical Engineering,
Chemistry, and Environmental Science

May 1994

APPROVAL PAGE

ENGINEERING ANALYSIS OF A PACKED-BED BIOFILTER FOR REMOVAL OF VOLATILE ORGANIC COMPOUND (VOC) EMISSIONS

Zarook M. Shareefdeen

Dr. Basil C. Baltzis, Dissertation Advisor — Date
Professor of Chemical Engineering, NJIT

Dr. Gordon A. Lewandowski, Committee Member — Date
Professor of Chemical Engineering, NJIT

Dr. Piero M. Armenante, Committee Member — Date
Professor of Chemical Engineering, NJIT

Dr. Dana E. Knox, Committee Member — Date
Associate Professor of Chemical Engineering, NJIT

Dr. Richard Bartha, Committee Member — Date
Professor of Microbiology,
Department of Biochemistry and Microbiology,
Rutgers University (New Brunswick)

BIOGRAPHICAL SKETCH

Author: Zarook M. Shareefdeen

Undergraduate and Graduate Education:

- Doctor of Philosophy in Chemical Engineering
  New Jersey Institute of Technology, Newark, New Jersey, 1994

- Master of Science in Chemical Engineering
  King Fahd University of Petroleum and Minerals, Dhahran, Saudi-Arabia, 1989

- Bachelor of Science in Chemical Engineering
  King Fahd University of Petroleum and Minerals, Dhahran, Saudi-Arabia, 1985

Major: Chemical Engineering

Publications and Presentations:

Baltzis, B. C., and Z. Shareefdeen, in preparation as a Chapter in *Biological Treatment of Hazardous Waste*, G. A. Lewandowski and L. J. DeFilippi (Eds.), John Wiley & Sons Inc., New York, 1994.

Oh, Y. S., Z. Shareefdeen, B. C. Baltzis, and R. Bartha, "Interactions between Benzene, Toluene, *p*-Xylene (BTX) during Their Biodegradation." *Biotechnol. Bioeng.* (in press)

Shareefdeen, Z., and B. C. Baltzis, "Biological Removal of Hydrophobic Solvent Vapors from Airstreams." accepted for presentation at the *First International Symposium on Bioprocess Engineering*, Cuernavaca, Mexico (1994).

Baltzis, B. C., and Z. Shareefdeen, "Biofiltration of VOC Mixtures : Modeling and Pilot Scale Experimental Verification." accepted for presentation at the 87th A&WMA Meeting, paper no. 94-WP260.10P, *Air & Waste Management Association*, Cincinnati, Ohio (1994).

Shaikh, A. A., A. Jamal, and Z. Shareefdeen, "Boundary Value Problems in Reactive Gas Absorption." *Chem. Eng. Journal*, (in press).

Shareefdeen, Z., B. C. Baltzis, Y. S. Oh, and R. Bartha, "Biofiltration of Methanol Vapor." *Biotechnol. Bioeng.*, **41**, pp 512-524 (1993).

Baltzis, B. C., Z. Shareefdeen, and H. Androutsopoulou, "Solvent Emissions Control with a Packed-Bed Biofilter: Steady-State and Transient Behavior." *1993 AIChE Annual Meeting*, St. Louis, MO (November 7-12, 1993).

Baltzis, B. C., and Z. Shareefdeen, "Modeling and Preliminary Design Criteria for Packed-Bed Biofilters." pp. 1-16, in Proceedings of the 86th A&WMA Meeting, Paper No. 93-TP-52A.03, *Air & Waste Management Association*, Denver, CO, (June 13-18, 1993).

Shareefdeen, Z., and B. C. Baltzis, "Engineering Modeling of Packed-Bed Biofilters." *The Second International Symposium on In situ and On-Site Bioreclamation*, San-Diego, CA (April 5-8, 1993).

Baltzis, B. C., and Z. Shareefdeen, "Biofiltration of BTX Vapors : Data Modeling and Numerical Studies on Optimal Column Design." *1992 AIChE Annual Meeting*, Miami, FL (November 1-6, 1992).

Baltzis, B. C., Z. Shareefdeen, R. Bartha and Y. S. Oh , "Microbial Scrubbing of Solvent Emissions." *1991 AIChE Annual Meeting*, Los Angels, CA (November 17-22, 1991).

Baltzis, B. C., and Z. Shareefdeen, "Mathematical Modeling of a Biological Filter for Scrubbing Volatile Organic Carbon Emissions.", *1991 AIChE Annual Meeting*, Los Angels, CA (November 17-22, 1991).

Shaikh, A. A., and Z. Shareefdeen, "Some Remarks on the Effect of Flow Directions on Steady State Multiplicity in Bubble Column Reactors." *Chem. Eng. Sci.*, **45**, no. 4, pp 1137-1339 (1990).

Shaikh, A. A., and Z. Shareefdeen, "Closed form Solutions for the Performance of Gas-Liquid CSTRs with Second Order Reactions" *Chem. Ing. Tech.*, **60**, pp 46-48 (1988).

This dissertation is dedicated to
my wife Fareena,
my mother Ayesha,
and
to the loving memory of my father
Mohammed Shareefdeen

ACKNOWLEDGMENT

The author wishes to express his sincere gratitude to his advisor, Professor Basil Baltzis for his guidance, encouragement, and moral support throughout this research.

The author is grateful to Professors Gordon A. Lewandowski, Piero Armenante, Dana E. Knox, and Richard Bartha for serving as members of the committee.

The author appreciates the timely help and suggestions from his colleagues and friends Dr. Sitaram Dikshitulu, Mr. Socrates Ioannides, Dr. Cheng-Ming Kung, Dr. Peter Lenas, Dr. Young-Sook Oh, Dr. Nirupam Pal, and Mr. Kung-Wei Wang.

Mr. Clint Brockway, and Ms. Gwen San Augustin provided timely and expert assistance with the experimental set-up and analytical instruments. Departmental support, as well as financial support from the Hazardous Substance Management Research Center (HSMRC: A NSF Industry/University Co-operative Research Center) through funded research projects, are also greatly appreciated.

Finally, the author thanks his wife Fareena and all members of his family in Sri-Lanka, for their patience, support, and constant encouragement without which this work could not have been accomplished.

TABLE OF CONTENTS

LIST OF TABLES

LIST OF FIGURES

Figure **Page**

Figure **Page**

LIST OF SYMBOLS

A_S : biolayer surface area per unit volume of biofilter (m^{-1})

A_S^* : total surface area available for biolayer formation and adsorption per unit volume of biofilter (m^{-1})

A_{Sj} : biolayer surface area per unit volume of reactor, for VOC j (m^{-1})

b : biomass concentration in a closed vessel ($g\ m^{-3}$)

b_o : initial biomass concentration in a closed vessel ($g\ m^{-3}$)

c_j : concentration of substance j in the air at a position h along the biofilter ($g\ m^{-3}$)

c_j^* : equilibrium concentration of a pollutant j at the gas/solid interface ($g\ m^{-3}$)

$c_{j,0}$: value of c_j at $t = 0$ ($g\ m^{-3}$)

c_{je} : value of c_j at $h = H$ ($g\ m^{-3}$)

c_{ji} : value of c_j at $h = 0$ ($g\ m^{-3}$)

$c_{ji,0}$: value of c_j at $h = 0$ and $t = 0$ ($g\ m^{-3}$)

c_{jp} : concentration of substance j on the solid particle (g of pollutant j-adsorbed/g particle)

$c_{jp,0}$: concentration of substance j on the solid particle at $t = 0$ (g of pollutant j-adsorbed/g particle)

c_O : oxygen concentration in the air at a position h along the biofilter ($g\ m^{-3}$)

c_{Oi} : oxygen concentration in the air at the inlet of the biofilter ($g\ m^{-3}$)

$c_{Oi,0}$: oxygen concentration at $h = 0$ and $t = 0$ ($g\ m^{-3}$)

$\bar{c}_j$: dimensionless concentration of a compound j in the air $\left(\bar{c}_j = c_j / c_{ji}\right)$

$\bar{c}_j^*$: dimensionless equilibrium concentration of a pollutant j defined as $\bar{c}_j^* = c_j^* / c_{ji}$

$\bar{c}_{jp}$: dimensionless concentration of substance j on the solid particle defined as $(1-\upsilon)\rho_p c_{jp}/\upsilon c_{ji}$

$\bar{c}_O$: dimensionless concentration of oxygen in the air $(\bar{c}_O = c_O/c_{Oi})$

C_{gj}, C_{gq}: concentration of compounds j and q, respectively, in the head space of a closed vessel (g m^{-3})

C_{goj} : initial head space concentration of compound j in a closed vessel (g m^{-3})

C_{Lj}, C_{Lq}: concentration of compounds j and q, respectively, in the liquid phase of a closed vessel (g m^{-3})

D_j : diffusion coefficient of a compound j in the biofilm (m^2 h^{-1})

D_{jW} : diffusion coefficient of a compound j in water (m^2 h^{-1})

D_O : diffusion coefficient of oxygen in the biofilm (m^2 h^{-1})

D_{OW} : diffusion coefficient of oxygen in water (m^2 h^{-1})

e_j : effectiveness factor based on a pollutant j, defined by equation 8.18

e_O : effectiveness factor based on oxygen, defined by equation 8.19

F : flow rate of airstream (m^3 h^{-1})

$f(X_V)$: ratio of diffusivity of a compound in the biofilm to that in water

h : position in the column (m) ; h = 0 at the entrance, h = H at the exit

H : total height of the biofilter bed (m)

k_a : mass transfer coefficient between the gas and the solid surface (m h^{-1})

k_d : Freundlich isotherm parameter

K_j : constant in the specific growth rate expression (Monod or Andrews) of a culture growing on compound j (g-compound j m^{-3})

K_{sj} : half saturation constant in the Monod kinetic expression of a culture growing on compound j (g-compound j m^{-3})

K_{Ij} : inhibition constant in the specific growth rate expression of a culture growing on compound j (g-compound j m^{-3})

K_{jq} : interaction constant in the specific growth rate expression of a culture growing on compound j, due to the presence of compound q (dimensionless)

K_O : constant in the specific growth rate expression of a culture, expressing the effect of oxygen (g-oxygen m^{-3})

m_j : distribution coefficient for the substance j/water system

m_O : distribution coefficient for the oxygen-in-air/water system

M_j : total mass of compound j in a closed vessel (g)

$M_{o,j}$: initial total mass of compound j in a closed vessel (g)

n : Freundlich isotherm parameter

R : removal rate (g m^{-3}-packing h^{-1})

R' : relative value of removal rate

R_{exp} : experimentally measured removal rate of compound j vapors from air, based on the entire biofilter (g m^{-3}-packing h^{-1})

$R_{exp,i}$: experimentally measured removal rate of compound j vapors from air, in section i of a separated column; i = 1,...,4 (g m^{-3}-packing h^{-1})

R_{pred} : model predicted removal rate of compound j vapors from air, based on the entire biofilter (g m^{-3}-packing h^{-1})

s_j : concentration of substance j at a position x in the biolayer at a point h along the column (g m^{-3})

$s_{j,0}$: concentration of substance j at a position x in the biolayer when t = 0 (g m^{-3})

s_j^* : dimensionless concentration of substance j at a point θ in the biolayer; defined as $s_j(\theta) / s_j(\theta = 0)$

s_O : oxygen concentration at a position x in the biolayer, at a point h along the column (g m^{-3})

$s_{O,0}$: oxygen concentration at a position x in the biolayer when t = 0 (g m^{-3})

$\bar{s}_j$: dimensionless concentration of a compound j in the biolayer ($\bar{s}_j = s_j/K$)

$\bar{s}_O$: dimensionless oxygen concentration in the biolayer ($\bar{s}_O = s_O/K_O$)

S : cross sectional area of the biofilter column (m^2)

t : time (h)

u_g : superficial air velocity in the biofilter; ($m\ h^{-1}$)

V_l, V_g : volume of liquid and gas phase (headspace), respectively in a closed vessel (m^3)

V_P : volume of the biofilter bed (m^3)

X_V : biofilm density (g-dry cells m^{-3})

x : position in the biolayer (m)

Y_j : yield coefficient of a culture on compound j (g-biomass g^{-1}-compound j)

Y_{Oj} : yield coefficient of a culture on oxygen (g-biomass g^{-1}-oxygen), when VOC j is the carbon source

z : dimensionless position in the biofilter ($z = h/H$)

Greek Symbols

α : fraction of total surface area available for biofilm formation

β_1 : dimensionless parameter defined as $e_j \alpha \delta A_S^* X_V H \mu^* / Y_j u_g c_{ji} \upsilon$

β_2 : dimensionless parameter defined as $e_O \alpha \delta A_S^* X_V H \mu^* / Y_O u_g c_{Oi} \upsilon$

β_3 : dimensionless parameter defined as $k_a (1-\alpha) A_S^* H / u_g \upsilon$

γ : inverse dimensionless inhibition constant ($\gamma = K_j / K_{Ij}$)

δ : effective biolayer thickness (m)

δ^* : actual biolayer thickness (m)

ε_1 : dimensionless quantity which is equal to ε_j when $j \neq O$

ε_2 : dimensionless quantity which is equal to ε_j when $j = O$

ε_j : dimensionless quantity defined as $c_{ji}/K_j m_j$

ζ : dimensionless time defined as $u_g t/H$

η : dimensionless quantity defined as $A_S D_j HK/\delta u_g c_{ji}$

θ : dimensionless position in the biolayer ($\theta = x/\delta$)

λ : dimensionless quantity defined as $Y_j K_j D_j/Y_{Oj} K_O D_O$

λ_1 : dimensionless quantity defined as $D_{BW} K_B Y_B/Y_{OB} K_O D_{OW}$

λ_2 : dimensionless quantity defined as $D_{TW} K_T Y_T/Y_{OT} K_O D_{OW}$

μ : specific growth rate (h^{-1})

μ^* : constant in the specific growth rate expression (h^{-1})

μ_m : maximum specific growth rate in the Monod expression (h^{-1})

μ_{max} : maximum specific growth rate (h^{-1})

ν_O : stoichiometric coefficient of oxygen

ρ_P : density of the solid particles (g m^{-3})

σ_1 : dimensionless quantity defined as $K_{BT} K_T/K_B$

σ_2 : dimensionless quantity defined as $K_{TB} K_B/K_T$

τ : space time defined as V_P/F

υ : porosity of the biofilter bed

ϕ^2 : square of Thiele modulus based on compound j, defined as $\mu^* \delta^2 X_V/D_j K Y_j$

ϕ_1^2 : ϕ^2 when compound j is benzene, defined as $\mu_B^* X_V \delta^2/D_{BW} f(X_V) K_B Y_B$

ϕ_2^2 : ϕ^2 when compound j is toluene, defined as $\mu_T^* X_V \delta^2/D_{TW} f(X_V) K_T Y_T$

ψ : dimensionless parameter defined as $1/c_{ji}\left[\upsilon c_{ji}/(1-\upsilon)\rho_P k_d\right]^{\frac{1}{n}}$

ω : dimensionless quantity defined as $K_O D_O c_{ji}/K_j D_j c_{Oi}$

ω_1 : dimensionless quantity defined as $K_T D_{TW} c_{Bi}/K_B D_{BW} c_{Ti}$

ω_2 : dimensionless quantity defined as $K_O D_{OW} c_{Bi}/K_B D_{BW} c_{Oi}$

Subscripts

0 : refers to conditions at t = 0

g : refers to gas phase

i : refers to conditions at h = 0, or z = 0

j : compound j

j = B : compound is benzene

j = M : compound is methanol

j = O : compound is oxygen

j = T : compound is toluene

l, L : refer to liquid phase

q : compound q

CHAPTER 1

INTRODUCTION

Volatile organic compounds (VOCs) may be present in final products such as gasoline, but are primarily used as solvents and feed-stock chemicals in the pharmaceutical and chemical industry. They are also used in lacqueries and paint shops. Due to their volatility, VOCs are emitted in large amounts (75), and create not only nuisance problems (odors), but - most importantly- hazards to the ecosystem, and health effects to humans. Treatment of off-gases has been practiced for years, and is primarily based on washing in packed-columns, activated carbon adsorption, and incineration (21). Of these three methods, only incineration leads to destruction of the pollutants, but it is an expensive method due to the high temperatures required. In addition, incineration leads to NOx gas formation. Adsorption on activated carbon is an effective method, but it leads to solid waste formation since regeneration is too expensive (21). Even if regeneration is practiced, desorbed VOCs need treatment. Treatment is also needed for VOCs adsorbed in water during packed-bed column washing operations. Clearly, industry and even small operations such as dry cleaning, are faced with a serious problem regarding VOCs. The problem has become much more severe, as environmental regulations regarding VOC emissions have become much stricter in the recent years. The Clean Air Act Amendments of 1990 (CAAA) have made VOCs a priority for manufacturing operations in the US.

Because of CAAA, intense research efforts are underway, in both industrial and academic quarters, for finding new, efficient, and economical technologies to deal with the problem of VOC emissions. A number of these research efforts have focused on the use of biological means to purify contaminated airstreams. Biological treatment of industrial and municipal wastewaters has led to the development of well established and economical

pollution control technologies. To a lesser extent, biodegradation has been also successfully employed in the remediation of contaminated soils. It is hoped that biological treatment will lead to development of cost effective technologies for purification of contaminated airstreams.

A biodegradation-based process for air pollution control which has attracted a lot of attention in the recent years is biofiltration. This process is expected to be effective at low VOC concentrations (49). Such low concentrations (ppm levels, i.e., mg/Kg-air) are characteristic for emissions. Biofiltration takes place in reactors known as biofilters. A biofilter is a reactor packed with a porous solid material (e.g., peat, perlite, compost, ceramic particles) on which a proper microbial population is immobilized forming a biolayer. The contaminated air passes through the reactor, and the pollutants are transported to the biolayer where they are biodegraded. There are different types of biofilters (18, 47), and the term trickling biofilter or bioscrubber is used in cases where a recirculating water stream flows continuously through the biofilter bed. Classical biofilters, which are the topic of this work, do not have a continuous liquid phase. The required moisture is provided by saturating the airstream before it enters the unit, and/or by supplying liquid water occasionally, as required.

Although soil and compost beds have been used for years for odor control purposes, work on biofilters for elimination of industrial solvent emissions started a decade ago by Ottengraf and his co-workers in the Netherlands (22, 47, 52). Less than three years ago, Leson and Winer (39), after reviewing the existing literature, concluded that there has been little research on, and commercial use of, biofilters in the US when compared to Europe. This seems to be rapidly changing, and some studies performed in the US were published in the past two years. These studies are discussed in the next chapter of this dissertation.

An important step in development of biofiltration technology is to derive and experimentally validate mathematical models of the process, for predictive and the scale-

up calculations. Only one model was found in the literature (52), and it is very simplistic. Biofiltration is a complex process, or at least more complex than biodegradation of liquid wastes, since it involves more than one phase; thus, kinetics alone are not enough to describe it, and one needs to take into account mass transfer problems associated with the transport of the pollutants from the gas (air) phase to the biolayer, as well as the transport (diffusion) of the pollutant within the biofilm. Furthermore, transient operation of biofilters is affected by the physical adsorption of VOCs onto the packing material, a phenomenon which has never been discussed, or modeled mathematically.

The present study was undertaken with the intent to develop, and experimentally validate detailed engineering models of biofiltration. A detailed model describing steady state and transient operation of a biofilter used in purification of airstreams containing vapor of a single VOC has been developed, numerically solved, and experimentally validated. Also, a detailed model describing steady state biofiltration of VOC mixtures has been developed, and experimentally validated for the case where airstreams contain vapors of two VOCs. As opposed to approaches taken by other researchers, this study took into account the availability of oxygen, and its potential limiting effects on the process. Furthermore, at the kinetic level, actual expressions (experimentally determined) were used instead of simplistic approaches where the kinetics are assumed to be zero-, or first-order at best. For mixtures, potential interactions among solvents were also considered, rather than assuming that each pollutant in a mixture is removed in the biofilter as if no other pollutant was present. Finally, adsorption/desorption was taken into account in developing the transient model.

Experimental validation of the models was based on data from biofiltration of methanol, benzene, toluene, and benzene/toluene mixtures. Methanol, a hydrophilic compound, is an important chemical feedstock and industrial solvent. Its global annual production is approaching 20 million metric tons (34). Losses of methanol vapors to the atmosphere during manufacture, use, and disposal have not been assessed but are likely to

be substantial. Benzene and toluene, two rather hydrophobic compounds, are classified as priority environmental pollutants (25). This classification is based on their substantial toxicities, and on the carcinogenic potential of the benzene component (15). Benzene and toluene are substantive constituents of gasolines (29), and also serve as industrial solvents and/or feedstocks for synthesis (63).

Since biodegradation kinetics are important in describing the biofiltration process, a considerable effort was placed in this study in deriving appropriate kinetic expressions. Dr. Young-Sook Oh performed shake-flask, suspended culture experiments in the laboratory of Professor Richard Bartha (Rutgers University, New Brunswick, NJ). These data were analyzed during the course of the work reported in this dissertation. Methanol degradation was studied with the use of a microbial consortium. Benzene and toluene, alone and in mixtures, were degraded by a microbial consortium and a pure culture of *Pseudomonas putida*. In the case of benzene/toluene mixtures, special emphasis was placed on the potential interactions between the two structurally similar compounds. It should be mentioned that although the pathways of benzene, toluene, as well as xylene (BTX compounds) degradation are well known (31, 66), substrate interactions are not well understood, and make treatment of mixtures much less predictable (1, 4, 13, 35). The kinetic expressions derived from this part of the study, were subsequently used in describing biofiltration of these compounds by employing the same microbial cultures.

Analysis of methanol vapor biofiltration was based on data obtained by Dr. Oh in Professor Bartha's laboratory. All other biofiltration experiments were performed during the course of this dissertation. These experiments involved biofiltration of benzene vapor at steady state, biofiltration of toluene vapor both under steady state and transient conditions, and steady state biofiltration of benzene/toluene mixtures. In all cases, the packing material used was a mixture of peat and perlite particles. Experiments with methanol were performed in small scale biofilters (5cm diameter, 60cm high). Experiments with benzene and toluene (individually), were performed in intermediate scale

biofilters (10cm-diameter, 75cm high). Finally, experiments with benzene/toluene mixtures were performed in a pilot scale, three-stage unit (15cm-diameter, 100cm total height).

CHAPTER 2

LITERATURE REVIEW

2.1 Principles of Biofiltration

2.1.1 Introduction

Biofiltration technology is an adaptation of the process by which the atmosphere is cleaned naturally. Plants and soil adsorb VOCs from the atmosphere, and degrade them. Inefficient contact of soils and plants with VOCs which are in the atmosphere, lead to relatively low reaction rates. Biofiltration provides maximal contact, and allows sufficient time for VOCs to react (10). Biofiltration, currently used on the commercial scale for odor control in waste treatment, and in food, flavors, and fragrances manufacturing, is promising also for control of solvent emissions (48).

Biological systems for elimination of volatile organics have been explored both on the experimental and mathematical modeling levels primarily in the Netherlands by the pioneering contributions of Ottengraf and his associates (47, 48, 51, 52, 74). Bohn (9), Pomeroy (59), and Bohn and Bohn (12) described the use of soil and compost beds for biological treatment of malodorous emissions, but land area requirements and lack of process control restrict the industrial use of these systems. The first biofilter was patented in the US by Pomery in 1957, and this design consisted of a slotted pipe buried under a soil. It was effective in control of odors from sewage treatment plants. This type of soil bed or "earth filter" is useful when the pollutants are very easily biodegradable, and when there is sufficient land area (18).

Nowadays, there are basically three types of biofilters (47): classical biofilters, biological trickling filters, and bioscrubbers. In a classical biofilter (Figure 2.1), contaminated gas is forced to rise through a packed column. Materials used as column packing are humus earths, compost, peat, lava, woody heather, crushed oyster shells, treebark fractions, brush-wood, or mixtures of these materials (21, 27, 56, 80).

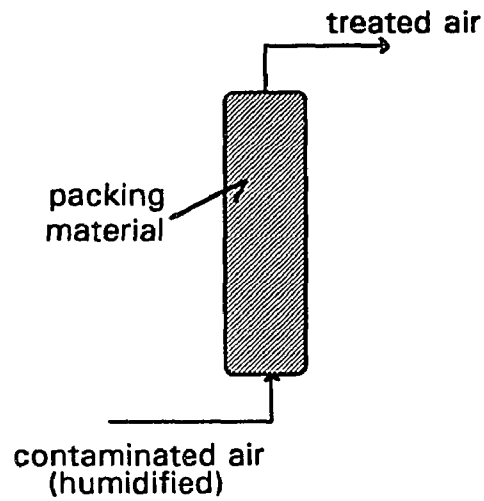

Figure 2.1 Schematic layout of a biofilter

Biological trickling filters (Figure 2.2), which are also known as "fixed-film scrubbers" (45, 55), "vapor phase bioreactors" (73), or even simply "biofilters" (73), utilize a continuous water phase which is recirculated through the bed. Bio-trickling filters employ solid (usually non-porous) support made of inorganic materials, such as plastic (20, 21, 22) or even ceramic monoliths (68). The water phase carries nutrients for the microorganisms, and is usually neutralized before recirculation, for pH-control purposes.

While classical, and trickling-bed biofilters employ immobilized organisms, bioscrubbers utilize dispersed (suspended) cultures. Bioscrubbers consist of two units: a usual scrubber in which VOCs are transported from the air to a water phase, and a classical bioreactor where the water exiting the scrubber is subjected to biological

treatment. The two units are integrated into a single system as shown in Figure 2.3. There are only few studies on bioscurbbers (54, 55).

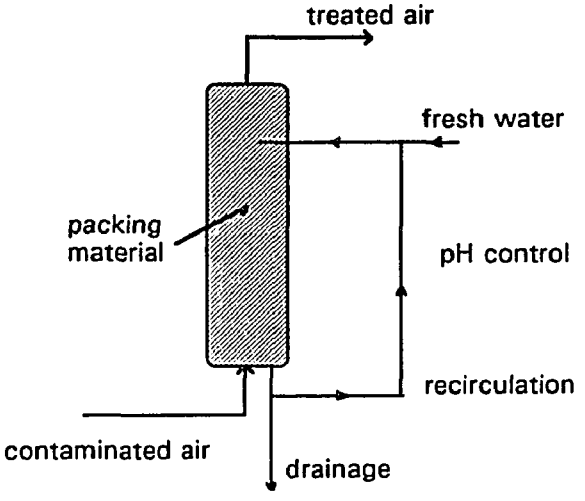

Figure 2.2 Schematic layout of a biotrickling filter

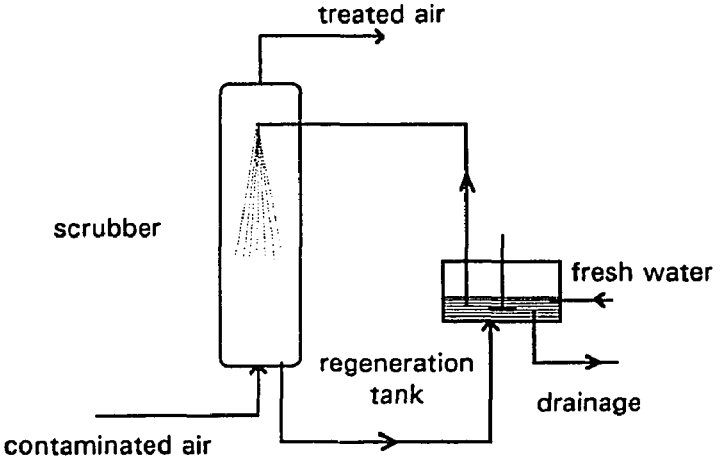

Figure 2.3 Schematic layout of a bioscrubber

2.1.2 Microorganisms

Biofiltration is based on the ability of microorganisms to oxidize (degrade) VOCs. Primarily, bacterial species are used, and to a smaller extents molds and yeasts (49). Naturally occurring packing materials such as peat and compost, contain organisms capable of biodegrading some VOCs. In most cases, the biofilter needs to be inoculated with a microbial culture. Activated sludge suspensions from sewage treatment plants can serve as inoculum (49) in cases of easily biodegradable compounds. Poorly biodegradable compounds such as chlorinated hydrocarbons (e.g., dichloromethane, vinyl chloride), and aromatics (e.g., benzene, toluene), require inoculation with specially cultivated organisms (49, 51).

Some concern was expressed a few years ago regarding presence of microbes in airstreams exiting biofilter units after treatment. A study by Ottengraf and Konings (50), has shown that there is no significant difference between the concentration of microorganisms in airstreams exiting a biofilter, and that encountered in the open air.

2.1.3 Oxygen availability and External nutrient supply

Although biofiltration is an aerobic process, the problem of oxygen availability in the biolayer where biodegradation actually occurs, has not been discussed in any detail in the literature. Diks (20), in a study with biotrickling filters, mentions that the oxygen which is dissolved in the water phase may not be enough for the process, and that a continuous supply from the gas phase may be required. Bohn (11), mentions that oxygen supply to the biofilter bed should be of concern in designing biofilters.

Survival of microorganisms, and thus biofiltration, depends not only on oxygen and carbon sources (a role played by the VOCs), but also on other nutrients such as nitrogen and phosphorus sources. These additional nutrients are not needed when materials such as peat, compost, and bark are used as solid support for the organisms. These materials contain nutrients which can be supplied to the microorganisms. When

trickling filters and bioscrubbers are used, additional nutrients are externally supplied through the water phase (20, 22).

2.1.4 Moisture and Temperature effects

In classical biofilters, the absence of a continuous water phase may create serious problems during operation. Water is required for biological activity, and is retained in the biolayer and the pore structure of the packing material. It has been reported (80), that operation of a biofilter is optimal when 50% of the pores are filled with water. Weighing sensors have been used for automating water addition to commercial biofilters (80). Due to high air volumetric rates used during biofiltration, the bed can dry-out very quickly even when the ambient temperature remains constant. To avoid this problem, contaminated airstreams are humidified before they are supplied to the biofilter. In some cases prehumidification is not enough. This is due to the fact that biodegradation is an exothermic oxidative process. Temperature rises in the biofilter bed induce evaporation of water from the pores of the solid packing. Thus, at least periodic, addition of water appears to be necessary. This has been attempted by sprinkling water at the top of the biofilter bed. Sprinkling of water has been reported to potentially create two problems: formation of anaerobic zones (53), and creation of lumps of material leading to reduction in the contact surface between the gas and the biofilter material (75). Another approach to maintaining proper moisture contents in the biofilter, is the use of steam for supersaturating the inlet gas streams. However, use of steam can lead to temperature rises such that biological activity is reduced (74). Good temperature control schemes need to be used when steam is employed. Leson et al. (38), have discussed the problem of temperature and moisture content in relation to a biofiltration demonstration project. Temperature rises, and material dry-out can also lead to channeling effects, something which leads to considerable reduction in removal rates (53), due to a decrease in the gas/solid interfacial area.

Regarding temperatures of operation for biofilter units, it has been reported that they should be between 5 and 50°C (11). Over certain temperature ranges, one could use an Arrhenius expression to describe the effect of temperature on biodegradation, and consequently on biofiltration (80). For a case of styrene vapor removal, it has been observed that the removal rate increases by a factor of 2, when the temperature increases by 7°C (49).

2.1.5 Pressure drop

Experimental studies (17, 68) have shown that pressure drop in a biofilter is very low. Typical values are around 1 to 2" water/m-filter-bed (17, 68). Estimation of pressure drop in a biofilter can be made through the Ergun equation (47, 52). Pressure drop increases have been observed in cases where a sprinkling system is used for water addition (49). This is due to the fact that excess water at the top of the biofilter leads to clogging of the packing material.

2.1.6 pH-Control

When chlorinated solvents and nitroaromatic compounds are removed from airstreams by biofiltration, maintenance of proper pH levels in the unit is of paramount importance. These units are of the trickling bed configuration, and the water stream needs to be neutralized before it is recirculated through the reactor (20, 21, 22, 46). Neutralization products such as NaCl and $CaCl_2$ have been reported to have inhibitory effects on the activity of microbial cultures used in biofiltration (20, 49).

In the case of simple solvents such ethanol, problems with the pH may arise only when acids are produced due to oxygen availability problems (38). In such cases, incomplete mineralization of the pollutant occurs, and the problem is not so much related with pH as with the proper supply of oxygen to the unit.

2.2 Feasibility of VOC Removal in Biofilters

A number of experimental studies have demonstrated that removal of various VOCs in biofilters is feasible.

Ottengraf and Van den Oever (52), using a 5-stage classical biofilter have removed mixtures of toluene, butanol, ethylacetate, and butyl acetate from airstreams. Zilli et al. (80), also with a classical biofilter which was frequently sprayed with water, have studied phenol vapor removal from airstreams. Ergas et al. (27) have removed toluene, dichloroethane, and trichloroethene, also in classical biofilters. Regarding the study of Ergas et al., it should be noted that a classical biofilter was used despite the fact that chlorinated solvent vapors were removed. The pH-drop problem was resolved by adding crushed oyster shells, a source of calcium carbonate, in the packing material. Such solutions though, are not expected to work in the long run. Ebinger et al. (24), using a soil bed without external microbial inoculation, have removed propane from airstreams. Deshusses and Hamer (17), have removed mixtures of methyl-ethyl-ketone (MEK) and methyl-isobutyl-ketone (MIBK) in classical biofilters, with packing material consisting primarily of clay spheres. Van Lith (75) conducted pilot scale experiments with classical biofilters. He reported results from three sets of experiments: one with methylformiate, one with methanol/isobutanol mixtures, and one with a complex mixture consisting of styrene, vinylcyclohexene and butadiene. Paul and Roos (56), have reported that they were able to remove tetrahydrofuran vapor in a commercial biofilter known as BIOBOX (Comprimo Co.), which was originally developed for onion odor control. They also claim that other VOCs such as toluene and ethylacetate could be removed in the same unit. Pilot demonstration studies for removal of styrene (72), and ethanol (38) using classical biofilters have been also reported.

Fewer studies exist regarding VOC removal in trickling-bed biofilters. All such studies have utilized inorganic solid support material for the microbial culture, and supply of various nutrients with the water stream. Utgikar et al. (73), have reported results from

treatment of landfill leachate offgases. Sorial et. al (68), have treated toluene vapor in a trickling bed having a monolithic channelized microbial support. Diks (20), and Diks and Ottengraf (21, 22) have removed dichloromethane in a trickling bed having plastic support. In these studies, the water stream was passed either co-currently, or counter-currently with the air-stream, but the results were the same in both cases. Ottengraf et al. (51), have studied the problem of chlorinated compound removal, as well as removal of other types of xenobiotic compounds, in trickling-bed biofilters. Phipps and Ridgeway (58), have reported preliminary results from biofiltration of gasoline fractions containing toluene, benzene, p-xylene, octane, cyclohexane and trimethylpentane. They have used an elaborate, fully computerized, system for process monitoring and control.

Overcamp et al. (55), have reported a study on methanol removal in a bioscrubber.

2.3 Studies on Modeling of the Biofiltration Process

Regarding classical biofilters, there is only one model which has been published in the literature and is due to Ottegraf and van den Oever (52). It deals with steady state biofiltration, and is based on the assumption that VOCs are in equilibrium at the air/biolayer interface. Although the authors acknowledge that based on shake-flask experiments the biodegradation kinetics of single VOCs follow the Monod model (44), they only consider two limiting cases. At high concentrations they assume zero-order kinetics, while at low concentrations they assume first-order kinetics. In cases of mixed VOCs, these authors propose to use the same model in an additive sense. Recent studies (13, 16, 17), have shown that degradation kinetics of mixtures may be significantly different from the kinetics of single compound removal, and make the last assumption of Ottengraf and Van den Oever (52), invalid, at least for cases where structurally similar compounds are biofiltered simultaneously.

The model of Ottengraf and Van den Oever has been used by other researchers (18, 27, 74), as well. The model assumes that oxygen is not exerting any limitation on the process, and that VOCs, once transported to the air/biolayer interface, diffuse into the biolayer and are biodegraded. Simple kinetics, especially zero-order, allow for distinction between diffusion- and reaction-limitation regimes. The notion of effective biolayer thickness has been also introduced (52), implying that in some cases VOCs are depleted in a fraction of the biolayer which is called "effective biolayer". In a very recent study, Deshusses and Dunn (16), have used more complex kinetic expressions for describing biofiltration of MEK and MIBK. They used modified Monod expressions for describing competitive kinetic interactions between the two solvents. This same study reports an effort to model transient biofiltration of the two solvents.

Models for biological trickling filters have been proposed by Diks (20), Diks and Ottengraf (22), Smith et al. (67), Utgikar et al. (73), and Ockeloen et al. (45). Again in most cases, zero- or first-order kinetics are used, and oxygen limitations are neglected. The main difference between these models, and those used for classical biofilters is the fact that an extra phase (water), and thus an extra mass transfer resistance is considered. Ottengraf et al. (51), claim that zero-order kinetics can be used for xenobiotic compounds which are usually treated in trickling-bed filters. This is an assumption which has not yet been tested, but it is not likely that it will prove to be generally correct.

Overcamp et al. (54, 55) have reported simulation studies with simple models describing steady-state operation of bio-scrubbers.

2.4 Transient Operation of Biofilters

Biofiltration is a technology for treating VOC emissions. The emissions level is unlikely to be constant, thus biofilters are more likely to operate under unsteady state conditions. Furthermore, biofiltration can be applied to batch processes and thus, even if the emission

level is constant, biofilters may be operating in an intermittent mode (e.g., in painting booth facilities). Hence, questions such as how well can a biofilter respond to variations in volumetric flow rate, concentration, and composition are of paramount importance for commercial application of this technology (18). The fact that biofilters are most likely operating under varying load conditions was recognized early by Ottengraf et al. (53); the load is defined as the rate of VOC mass supply per unit volume of biofilter bed. There are very few published studies on the transient performance and response of biofilters. Togna and Frish (72), in a demonstration study for styrene vapor removal, observed that intermittent operation caused no problem in the performance of biofilters; biofilters inactive over the weekend period achieved normal removal rates within a few hours. Zilli et al. (80), observed that their biofilter could be inactive for a period of 10 days, and subsequently be restored to pre-interruption performance levels within a day. Finally, as reported earlier, Deshusses and Dunn (16), have studied transient biofiltration of MEK and MIBK mixtures.

2.5 Economics of Biofiltration

Biofiltration is a new technology and for this reason, there are no reports on its cost, or even estimates of it. It is expected that it may have a substantial capital cost due to the large volumes of filter-bed required for 99% plus, removal of VOCs which are present at low concentrations. On the other hand, operating and maintenance costs are expected to be minimal.

Although VOCs, especially recalcitrant ones, are very much different from inorganic gases such as H_2S, it is mentioned here that Ergas et al. (26), quote the following claim by Neff. H_2S removal from offgases coming from a POTW (Publicly Owned Wastewater Treatment) facility in a biofilter, had a capital cost of $97,300, and a yearly operating/maintenance cost of $7,870 (1990 US dollars). The design was for

treatment of 10,000 cfm of air carrying H_2S at a concentration of 20ppm. Exit concentrations were less than 1ppm. Bohn (10), also gives some costs for biofiltration, and his numbers seem to indicate that the cost of biofiltration is two orders of magnitude less than the cost of incineration, and one order of magnitude less than the cost of activated carbon adsorption.

CHAPTER 3

OBJECTIVES

The key objective of this study was to derive and experimentally validate, detailed engineering models of the biofiltration process. These models should incorporate as many aspects of the process as possible, and should be in a form which could be eventually used in design and scale-up calculations. As the subject of general process modeling is too complex, and since there was only one (very simplistic) model in the literature, it was decided to address the following problems in this study.

I. Biofiltration of single VOCs under steady state conditions.

This objective was met by deriving a detailed model which considers reaction, mass transfer, and oxygen effects on the process. The model was validated with three solvents: methanol -a hydrophilic solvent- [experiments performed by Dr. Oh (46)]; benzene and toluene -two hydrophobic solvents- experiments performed as part of the present study.

II. Biofiltration of mixed VOCs under steady state conditions.

This objective was met by deriving a detailed model which considers reaction, mass transfer, oxygen effects, as well as kinetic interactions among solvents (if such interactions do in fact exist). As model system for validation of the theory, a mixture of benzene and toluene was selected. Although this mixture can be viewed as simple since it involves only two components, in reality it is complex since it involves kinetic interactions between the two structurally similar pollutants. Experiments were performed with a pilot-scale biofilter which was operated continuously over a period of a year and a half.

III. Biofiltration of single VOCs under transient conditions.

No mathematical modeling study on biofiltration under transient conditions existed in the literature. Furthermore, a transient biofiltration model cannot be a simple extension of the steady state models, since transient biofiltration involves an extra process (adsorption/desorption), which is not present under steady-state conditions. For this reason, a detailed model was derived for the case where airstreams contain a single VOC. The model was solved, and experimentally validated with toluene as the model compound.

To meet the three objectives above, two more objectives had to be set.

IV. Accurate determination of biodegradation kinetics.

Since biofiltration depends strongly on the kinetics of biodegradation, it was felt that objectives I-III could not be met unless good, and accurate kinetic expressions were available. Dr. Oh performed kinetic experiments, and her data were analyzed as part of this dissertation. Seven sets of experiments with suspended cultures were analyzed: methanol degradation by a mixed culture which was used also in the biofiltration experiments; benzene, toluene, and benzene/toluene mixtures biodegradation (3 sets) by a pure strain of *Pseudomonas putida* (PPO1); biodegradation of benzene, toluene, and benzene/toluene mixtures (3 sets) by a microbial consortium which was subsequently utilized in the biofiltration experiments performed during the course of this dissertation.

V. Determination of the toluene adsorption isotherm.

As mentioned before, biofiltration under transient conditions involves adsorption/desorption of VOCs on the packing material. Since toluene was selected as the model compound for the transient experiments, independent experiments were performed for determining the toluene adsorption characteristics (adsorption isotherm) on the packing material used in the biofiltration experiments.

CHAPTER 4

EXPERIMENTAL APPROACH AND PROCEDURES

4.1 Materials and Apparatus

4.1.1 Chemicals and microorganisms

Benzene (B414-1, Certified, Fisher Scientific, Springfield, NJ) and toluene (T289-4, Certified, Fisher Scientific, Springfield, NJ) were used as VOCs to be treated. The chemicals used for media preparation were: sodium phosphate -dibasic-, Na_2HPO_4 (S374-500 Fisher Scientific, Springfield, NJ); potassium phosphate -monobasic-, KH_2PO_4 (P285-500 Fisher Scientific, Springfield, NJ); ammonium chloride, NH_4Cl (A661-500 Fisher Scientific, Springfield, NJ); magnesium sulfate, $MgSO_4 \cdot 7H_2O$ (M63-500 Fisher Scientific, Springfield, NJ); ferric ammonium citrate, $FeNH_4$-citrate (I72-500 Fisher Scientific, Springfield, NJ); and calcium chloride, $CaCl_2$ (C77-500 Fisher Scientific, Springfield, NJ). The packing materials used were peat moss (Hyponex, Marysville, OH), and perlite (A. H. Hoffman Inc., Landisville, PA). The original bacterial consortium used in the biofiltration experiments was obtained from Dr. R. Bartha's Laboratory, Rutgers University, New Brunswick.

4.1.2 Medium preparation

The medium consisted of two solutions. Solution No. 1 was prepared by adding 4g of sodium phosphate -dibasic-, Na_2HPO_4, 1.5g of potassium phosphate -monobasic-, KH_2PO_4, 1g of ammonium chloride, NH_4Cl, and 0.2g of magnesium sulfate, $MgSO_4 \cdot 7H_2O$, in one liter of distilled water. Solution No. 2 was prepared by adding 0.05g

of ferric ammonium citrate, $FeNH_4$-citrate, and 0.1g of calcium chloride, $CaCl_2$, in 100 ml of distilled water. The actual mineral medium was prepared by adding 1% (by volume) of solution No. 2 into solution No. 1, after autoclaving both solutions separately.

4.1.3 Experimental set-up

The biofilter bed used in the pilot-scale experiments consisted of three equal glass segments connected in series. Each segment (Custom made, ACE Glass Inc., Vineland, NJ), had a diameter of 15.2 cm and a height of 30.5 cm. The segments were connected through spacers (Custom made, ACE Glass Inc., Vineland, NJ), of a diameter equal to that of the column segments, and of height equal to 7.0 cm. The biofilter also involved a head-top (Custom made, ACE Glass Inc., Vineland, NJ), and a head-bottom (Custom made, ACE Glass Inc., Vineland, NJ). Individual parts were connected via quick release clamps (6517-27, ACE Glass Inc., Vineland, NJ), and by using krytox grease (8115-08, ACE Glass Inc., Vineland, NJ). Each spacer, the head-top, and the head-bottom had several ports allowing for sampling of the airstream, measurement of pressure and temperature, as well as for supplying water whenever the packing looked dry. The packing material was a mixture of peat and perlite particles (2:3 volume ratio before mixing). At the bottom of each segment, a stainless steel screen 1.5 to 2mm mesh size (Custom made, ACE Glass Inc., Vineland, NJ), was placed as support for the packing material, and as distribution system for the airstream. The culture used was originally developed at Rutgers University, in the microbiology laboratory of Professor R. Bartha, and is a consortium of various species. A rotameter assembly (75-350, Gow-Mac Instrument Co., Bound Brook, NJ), was used to vary inlet solvent vapor concentrations independently, by directing a greater or smaller part of the airstream through the solvent tanks. The major portion of the air was passed through a water tank to partially humidify the airstream. After humidification, the main airstream was mixed with the airstreams

carrying the solvent vapors, to create the contaminated airstream which was fed to the biofilter. The contaminated stream contacted only glass, teflon, and stainless steel structural elements. Total air flow rate was measured by a flow meter (Matheson Inc., Morris Plains, NJ). A schematic of this experimental unit is shown in Figure 4.1.

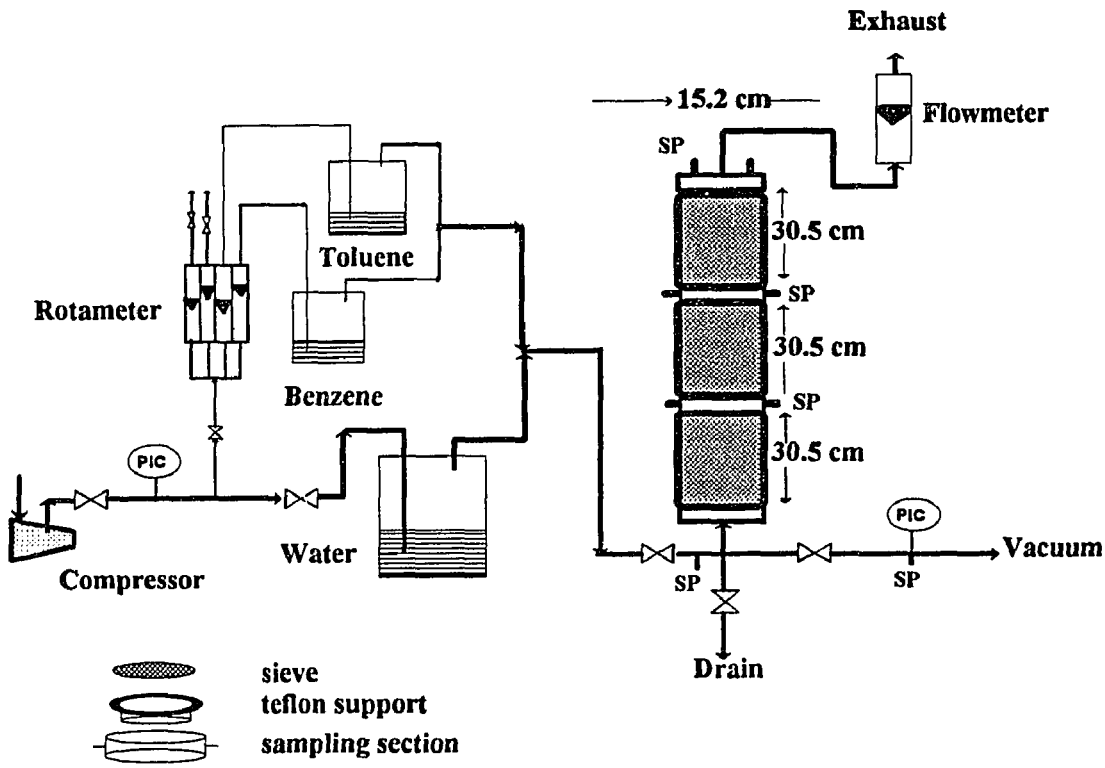

Figure 4.1 Schematic of the experimental packed-bed pilot biofilter unit. Total biofilter consists of three segments and each segment is 30.5cm high, and 15.2cm in diameter. The segments were connected through spacers of a diameter same as that of the biofilter column. SP refers to sampling ports. PIC refers to pressure indicator/controller.

The intermediate biofilter unit used for single VOC removal, was very much similar to, but a simpler version of the set-up described above. This unit consisted of a non-separated plexiglass column of diameter 10.2cm and height 76.2cm. The column had

a number of sampling ports along its length. This column was again packed with a mixture of peat and perlite (2:3 volume ratio before mixing). The height of the biofilter bed was 50.8cm for the experiments with benzene, and 68.6cm for the experiments with toluene vapor. A soap bubble flow meter (Hewlett-Packard, Paramus, NJ), was used for measuring the air flow rates. A schematic of the intermediate experimental unit is shown in Figure 4.2.

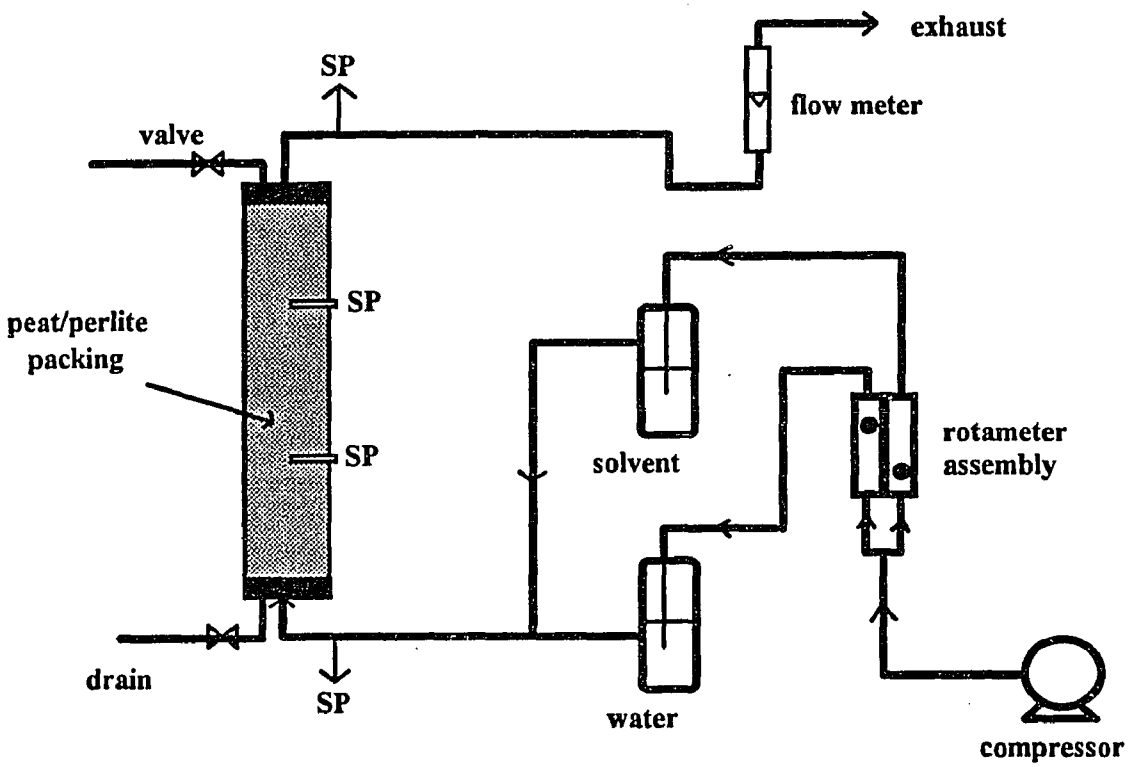

Figure 4.2 Schematic of the intermediate biofilter unit. The unit was 76.2cm high, and 10.2cm in diameter. The valve at the bottom allows for draining of water, the valve at the top allows for addition of water when the bed gets dry, and both valves allow for pressure measurements. SP refers to sampling ports (at the inlet, outlet, and intermediate levels).

4.2 Experimental Procedures

4.2.1 Preparation of the packing material

For all experiments a mixture of peat/perlite (2:3 volume ratio) was used as packing material. The reason for selecting this packing material has been discussed elsewhere (46, 64). Steam sterilized peat was used to avoid unintended variations in microbial activity. This was necessary because the peat moss contained considerable microbial activity even in the absence of inoculum. For preparing a biofilter, sufficient dry support was weighed out to pack the column. For the experiments with benzene, biomass was developed by growing an inoculum of the consortium in a simple mineral medium containing benzene as the sole carbon and energy source. After a small amount of biomass was grown in a shake-flask, it was transferred to a 10 liter sealed fermentor (New Brunswick Scientific Co., New Brunswick, NJ). The volume of the suspended culture was about 4L allowing for excess oxygen presence in the headspace. Thus, air-to-liquid ratio was kept high enough to avoid any oxygen limitations. Benzene was added in small quantities over a period of two weeks. The culture was finally harvested through centrifugation (5,000 rpm, 25 min), and was resuspended in fresh mineral medium (Na_2HPO_4 4g, KH_2PO_4 1.5g, NH_4Cl 1g, $MgSO_4 \cdot 7H_2O$ 0.2g, $CaCl_2$ 0.01g, $FeNH_4$-citrate 0.005g per liter H_2O, pH=7.0), not containing benzene. For the biofiltration experiments with toluene, and benzene-toluene mixtures, the same procedure was used except for the use of toluene, and benzene/toluene mixtures, respectively, instead of benzene, in preparing the biomass from an inoculum of the original culture. Sufficient suspension (about 30% by volume) was added to the dry packing material to fill the pore space partially with the liquid, leaving the other void space for air circulation. Water loss from the filters by evaporation, was replaced by addition of water as needed. Except when packing the biofilter, supplemental nutrients were never added to the bed.

4.2.2 Biofilter experiments

Benzene and toluene concentrations in airstreams were measured using a Hewlett-Packard Model 5890 (series II, Hewlett-Packard, Paramus, NJ) gas chromatograph equipped with a 6'x1/5" stainless steel column packed with 5%SP-1200/ 5% Bentone 34 on 100/120 Supelcoport packing (Supelco, Inc., Bellefonte, PA), and flame ionization detector. Operating conditions were: injector 120°C, oven 90°C, detector 200°C, carrier gas (N_2) 20.4 ml/min. Under these conditions, the retention times of benzene and toluene were 1.6 and 3.0 min, respectively. Standard curves were prepared as follows. First, known volumes or precise amounts of a compound were injected into several serum bottles (160 ml) using a 10µl liquid syringe (14-824, Fisher, NJ). The bottles were closed with teflon-faced silicon septa and aluminum crimp caps. The solvent was allowed to evaporate completely at room temperature within the enclosed space. Subsequently, air samples were taken from the bottles with a gas-tight, 0.5ml pressure-LOK® syringe (Precision Sampling Corp., Baton Rouge, Louisiana), and injected to the GC. During biofiltration experiments, the same type of gas-tight syringes were used for obtaining air samples from various ports of the columns. These samples were subjected to GC analysis, and concentrations were read from the calibration curves. GC calibration was repeated every two to three weeks.

During experiments, the flowrate (or residence time) of the airstream was varied, as well as the absolute and relative composition of the inlet airstream regarding benzene and toluene. Each experiment, under a given set of conditions, lasted over a long period of time in order to reach a steady state. Under each set of conditions, experiments lasted for a period of three weeks for the pilot scale unit, and about 8 to 10 days for the intermediate columns. Although experiments were performed at the room temperature, occasional temperature extremes of 60 to 85°F were recorded, but could not be prevented. The pressure drop was measured by using a pressure meter (G-07350-70, Cole

Parmer Instrument Company, Niles, Illinois). For both units, pressure drop was practically negligible as it never exceeded a value of 0.25" water/m-packing.

4.2.3 Adsorption experiments

Adsorption of toluene on the peat/perlite packing material was studied as follows. An amount of packing material was prepared exactly as described in section 4.2.1, except for the fact that instead of adding suspension, a quantity of sterile medium was added to the packing. Equal amounts (10 g) of packing material were placed in several serum bottles (160 ml). The bottles were closed with teflon-faced silicon septa and aluminum crimp caps. Using a 10µl liquid syringe (14-824, Fisher Scientific, Springfield, NJ), precise volumes of toluene were added to the bottles, and the solvent was allowed to evaporate and reach equilibrium within the enclosed space. Head-space samples were taken with a gas-tight 0.5ml pressure-LOK® syringe, and were subjected to GC analysis. Samples were taken on a daily basis, until the concentration of toluene in the air reached a constant value. Unchanging concentrations indicated that equilibrium had been reached, and these equilibrium toluene concentrations were used in deriving the adsorption isotherm. It was assumed that toluene does not adsorb on the walls of the serum bottles.

CHAPTER 5

KINETICS OF BIODEGRADATION

An important step in the development of more reliable and detailed biofiltration models is to obtain accurate kinetic expressions which describe the kinetics of biodegradation in the biofilm. Despite the fact that bacterial physiology and growth can change upon immobilization, Karel et al.(37) in a review paper, argue that the use of the same specific growth rate expression for freely suspended cells and microbial aggregates is the best assumption. This assumption was also made in the present study. In this chapter, the mathematical analysis of biodegradation data from closed-flask, suspended culture experiments is presented. The data were obtained from Dr. Oh's work (46). Biodegradation experiments involving methanol were performed by using a methanol utilizing consortium, aspects of the composition of which have been discussed elsewhere (46, 64). Experiments with benzene, toluene, and benzene/toluene mixtures were performed with a consortium, as well as with a pure culture of *Pseudomonas putida* (PPO1).

5.1 Modeling of Biodegradation Kinetics

In general, biodegradation of N volatile compounds each one of which can serve as primary carbon and/or energy source for the culture employed, can be described by the following mass balances written for a closed vessel,

$$\frac{db}{dt} = \sum_{j=1}^{N} \mu_j(C_{Lj})b, \qquad j = 1,...,N \qquad (5.1)$$

$$\frac{dM_j}{dt} = -\frac{1}{Y_j}\mu_j(C_{Lj})bV_L, \qquad j = 1,...,N \qquad (5.2)$$

In determining kinetic constants of a volatile compound, care should be taken to include the amount of VOCs in the head-space (51). Neglecting the amount which is present in the head space, may lead to unrealistic parameters (e.g., yield coefficients) when the volatility of the compound is very high. The total mass balance for a VOC present in a closed shake-flask should be written as,

$$M_j = V_L C_{Lj} + V_g C_{gj}, \qquad j = 1,...,N \qquad (5.3)$$

Assuming that each volatile compound is at all times distributed between the gas and liquid phase as dictated by thermodynamic equilibrium (Henry's law), i.e.,

$$C_{gj} = m_j C_{Lj}, \qquad j = 1,...,N \qquad (5.4)$$

and that the volume of the liquid phase is unaffected by the sampling procedure, one can show that the process can be described by the following three equations,

$$\frac{dC_{gj}}{dt} = -\frac{m_j V_L}{V_L + m_j V_g}\frac{1}{Y_j}\mu_j(C_{Lj})b, \qquad j = 1,...,N \qquad (5.5)$$

$$b = b_o + \frac{1}{V_L}\sum_{j=1}^{N}\left[Y_j M_{o,j} - \frac{Y_j\left(V_L + m_j V_g\right)C_{gj}}{m_j}\right], \quad j = 1,...,N \qquad (5.6)$$

$$Y_j = \frac{m_j\left(b - b_o\right)V_L}{\left(C_{go,j} - C_{gj}\right)\left(V_L + m_j V_g\right)}, \qquad j = 1,...,N \qquad (5.7)$$

In the case of methanol, frequent sampling of the liquid phase during all experimental runs yielded data on methanol and biomass concentrations. For benzene and toluene, sampling of the liquid phase for determination of the biomass concentration was less frequent than that of the gas phase for determination of C_{gj}. For this reason, the biomass data were first used, along with the corresponding gas phase concentration data, to determine the yield coefficients, Y_j, through equation (5.7). Then, equation (5.6) was employed for calculating biomass, b, from C_{gj} data at points in time where b was not actually measured. The experimental and/or calculated b values for each run were semilogarithmically plotted as a function of time. Points corresponding to the initial stage of each experiment were regressed to a straight line with correlation coefficients exceeding 0.99. The slope of each one of these lines was taken as the specific growth rate (μ) of the population, at the liquid phase concentration (C_L) of the biodegradable compound at the beginning of the particular experiment. The specific growth rate is defined as the rate of biomass production per unit amount of biomass. Then, the μ versus C_{Lj} data were fitted either to the Monod (44) model (Equation 5.8) through linear regression, or to the Andrews (2) (Haldane) inhibitory kinetic expression (Equation 5.9) using a non-linear regression routine.

$$\mu(C_L) = \frac{\mu_m C_L}{K_s + C_L}, \tag{5.8}$$

$$\mu\ (C_L) = \frac{\mu^*\ C_L}{K\ + C_L + \frac{C_L^2}{K_I}}, \tag{5.9}$$

5.2 Biodegradation Kinetics of Individual VOCs

5.2.1 Kinetics of methanol utilization

The values of the specific growth rate data (μ) obtained from shake flask experiments with methanol were plotted versus the corresponding methanol concentration values as shown in Figure 5.1. The data indicated a drop in μ at high methanol concentrations, i.e., they suggested substrate inhibition kinetics. The data were regressed to the Andrews (or Haldane) kinetic model, and it was found that $\mu^* = 0.22\ h^{-1}$, $K = 0.63$ kg m^{-3}, and $K_I = 20$ kg m^{-3}. Based on these constants, the curve representing the specific growth rate has been generated and is plotted in Figure 5.1. As can be seen from the graph, there is excellent agreement with the data. Differentiating expression (5.9) with respect to C_L one can see that the derivative becomes zero at $C_L = (KK_I)^{0.5}$ at

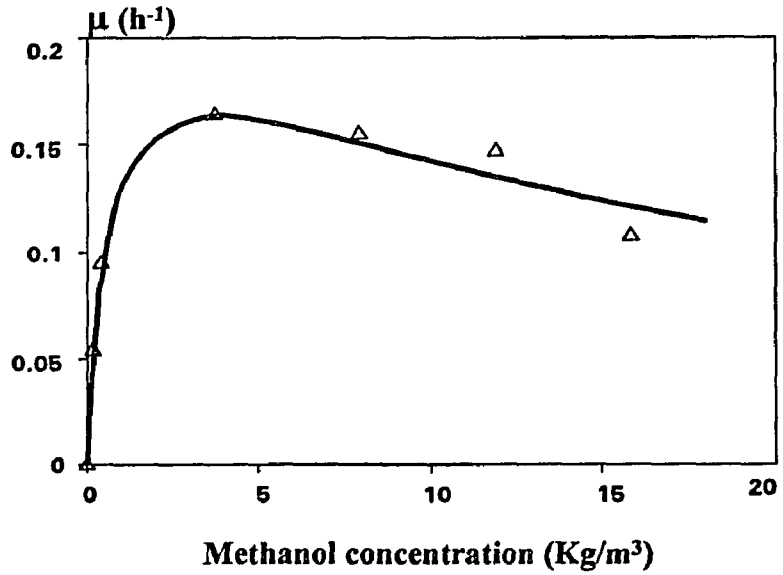

Figure 5.1 Specific growth rate of biomass on methanol under no oxygen limitation. Data from suspended culture experiments were fitted to an Andrews (Haldane) inhibitory expression.

which value, the specific growth rate becomes maximum (μ_{max}). The maximum specific growth rate is then given by

$$\mu_{max} = \frac{\mu^*}{1+2(K/K_I)^{0.5}} \qquad (5.10)$$

Based on the experimental values, equation (5.10) yields μ_{max} = 0.162 h^{-1} as can be also seen from Figure 5.1. The value of μ_{max} (or even μ^*) falls in the 0.075-0.5 h^{-1} range of values reported for maximum specific growth rates of methanol utilizers (14).

5.2.2 Kinetics of benzene and toluene utilization

Experimental data were obtained with a pure culture (*Pseudomonas putida* strain) designated as PPO1, and the consortium. Both the pure culture and the consortium exhibited a qualitatively similar behavior towards each one of the compounds. Both cultures degraded benzene following Monod kinetics. Both cultures degraded toluene following Andrews (Haldane) inhibitory kinetics. Values of the kinetic constants and yield coefficients are given in Table 5.1. Figure 5.2 shows specific growth rate data along with the predicted curves based on the kinetic constants determined. In all cases, the data fell very close to the curves. For the case of toluene, where a non-linear regression routine was used for determining the constants, it should be mentioned that convergence to the reported values was obtained regardless of the values used as initial guesses. Although comparisons between kinetic constants is rather futile when experiments have been performed with different cultures, the values obtained in this study are compared to those reported by Chang et al. (13), since this is probably the only other study which led to determination of kinetic constants for benzene and toluene removal. It should be also mentioned that Chang et al. used two pure strains of *Pseudomonas* in their experiments. Regarding the type of kinetics, between the results reported in this dissertation, and those

obtained by Chang et al., there is agreement for benzene (Monod), but a difference regarding toluene as they found Monod-type kinetics. The maximum specific growth rate on benzene by strain PPO1 is close to the upper limit of the values reported by Chang et al. The consortium studied here has a much higher μ_{max}. The maximum specific growth rate values on toluene (Table 5.1) are calculated as the maximum of the specific growth rate functions, and are considerably higher than those of Chang et al., for both cultures used here. Regarding yield coefficients, values found in this work are lower; for bioremediation, this is an advantage as the biomass disposal problem is less severe.

Table 5.1 Growth characteristics and parameters of the bacterial consortium and strain PPO1 on benzene and toluene.

	Benzene (Monod Kinetics)			**Toluene (Andrews Kinetics)**		
		[a]I	[b]II		[a]I	[b]II
Kinetic parameters	μ_m (h^{-1})	0.68	0.44	μ^*(h^{-1})	1.50	1.56
	K_S(mg/L)	12.22	3.36	K(mg/L)	11.03	15.07
	K_{BT} (-)	4.50	8.40	K_I (mg/L)	78.94	44.43
				K_{TB} (-)	0.20	0.35
Maximum specific growth rate (h^{-1})		0.68	0.44		0.86	0.72
Yield coefficient (g/g)		0.71	0.65		0.71	0.64

[a]values for the consortium; [b]values for strain PPO1

5.2.3 Dependence of kinetics on oxygen

All kinetic experiments with individual, and mixed VOCs were carried out with excess oxygen. In order to account for any oxygen limitations that may be encountered in biofiltration experiments, equations (5.8) and (5.9) were modified based on the notion

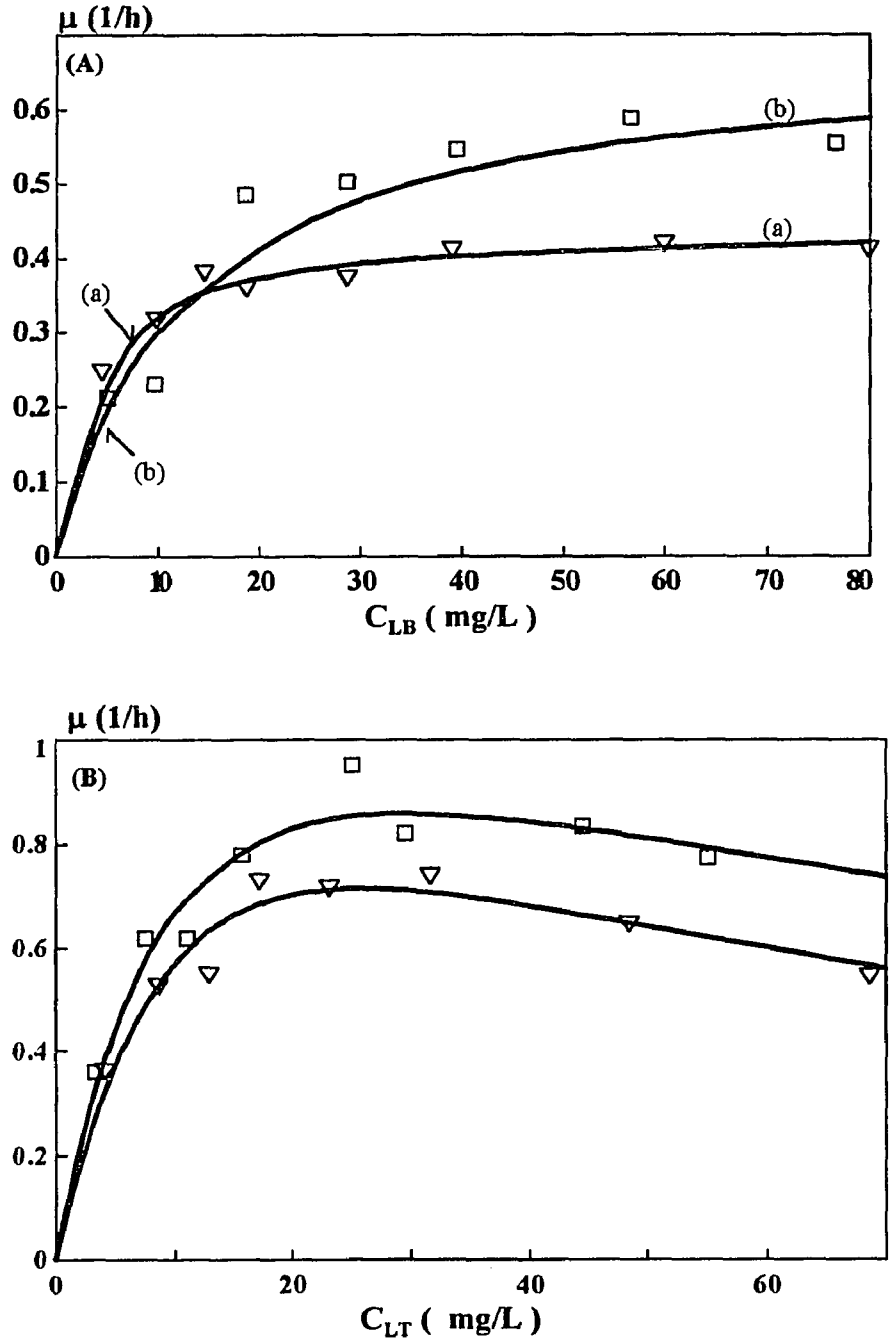

Figure 5.2 Specific growth rates of strain PPO1 (▽) and the consortium (□) on benzene (A) and toluene (B). Symbols represent values based on experimental data. Curves were generated by using the values of the kinetic constants shown in Table 5.1.

of interactive models (5). With a Monod-type kinetic dependence on oxygen, equations (5.8) and (5.9) were modified as,

$$\mu(C_L) = \frac{\mu_m C_L}{K_s + C_L} \frac{C_o}{K_o + C_o}, \tag{5.11}$$

$$\mu\ (C_L) = \frac{\mu^*\ C_L}{K\ + C_L + \frac{C_L^2}{K_I}} \frac{C_o}{K_o + C_o}, \tag{5.12}$$

The oxygen kinetic constant, K_o, was not experimentally determined in the present study. Williamson and McCarty (78) have measured a value of 0.30 g m^{-3} for *Nitrosomonas* and *Nitrobacter* cultures. Livingston (41) checked the available literature and concluded that K_o values fall in the range of 0.032-0.523 g m^{-3}. A value of 0.26 g m^{-3}, which is approximately the middle point of the aforementioned range, was used in all calculations made in this study. As will be discussed in Chapter 6, even if the actual value of K_o is one order of magnitude smaller than 0.26, biofiltration rates remain practically unaltered.

5.3 Biodegradation Kinetics of Mixed VOCs

Biodegradation of mixtures of two compounds involved in a cross-inhibitory (or competitive) interaction was described with the equations which are given in Section 5.1, along with specific growth rate expressions modified as follows.

$$\mu_j(C_{Lj}) = \frac{\mu_{mj} C_{Lj}}{K_{sj} + C_{Lj} + K_{jq} C_{Lq}}, \quad j \neq q \tag{5.13}$$

$$\mu_q(C_{Lq}) = \frac{\mu_q^* C_{Lq}}{K_q + C_{Lq} + \frac{C_{Lq}^2}{K_{Iq}} + K_{qj} C_{Lj}}, \quad j \neq q \tag{5.14}$$

Knowing the values of all model parameters -except for the interaction constants K_{jq}, K_{qj}- from single compound degradation experiments, the two new constants were determined by fitting the biodegradation data, C_{gj} and C_{gq} versus time, to the solution of equations (5.5)-(5.7) along with expressions (5.13)-(5.14), through a non-linear algorithm for minimization of the square of the errors.

5.3.1 Utilization of benzene-toluene mixtures

As in the case of individual compounds, both PPO1 and the consortium exhibited a qualitatively similar behavior towards mixtures of benzene and toluene. In mixtures, benzene and toluene were utilized competitively. The interaction parameters were determined and are given in Table 5.1. For benzene, where the kinetics are similar, (Monod-type) values obtained in the present study deviate from those reported by Chang et al. (13). According to these authors, the interaction constants should be equal to 1 in the model formulation given by equations (5.13) and (5.14). In Figure 5.3(a), experimental data were plotted against the model predictions based on the assumption that there is no interaction at the kinetic level (values of interaction parameters K_{BT} and K_{TB} set as zero). The same experimental data as a function of time, along with model predictions (curves) based on the interaction constants reported in Table 5.1 are shown in Figure 5.3(b). Clearly the data cannot be described unless interaction between benzene and toluene is considered. Similarly, for another set of experimental conditions, (Figure 5.4), the model predictions and experimental data agree excellently when kinetic interactions are considered. This agreement was found in all experimental sets. The values of the parameters show that the interaction is almost 50% less intense with the consortium as

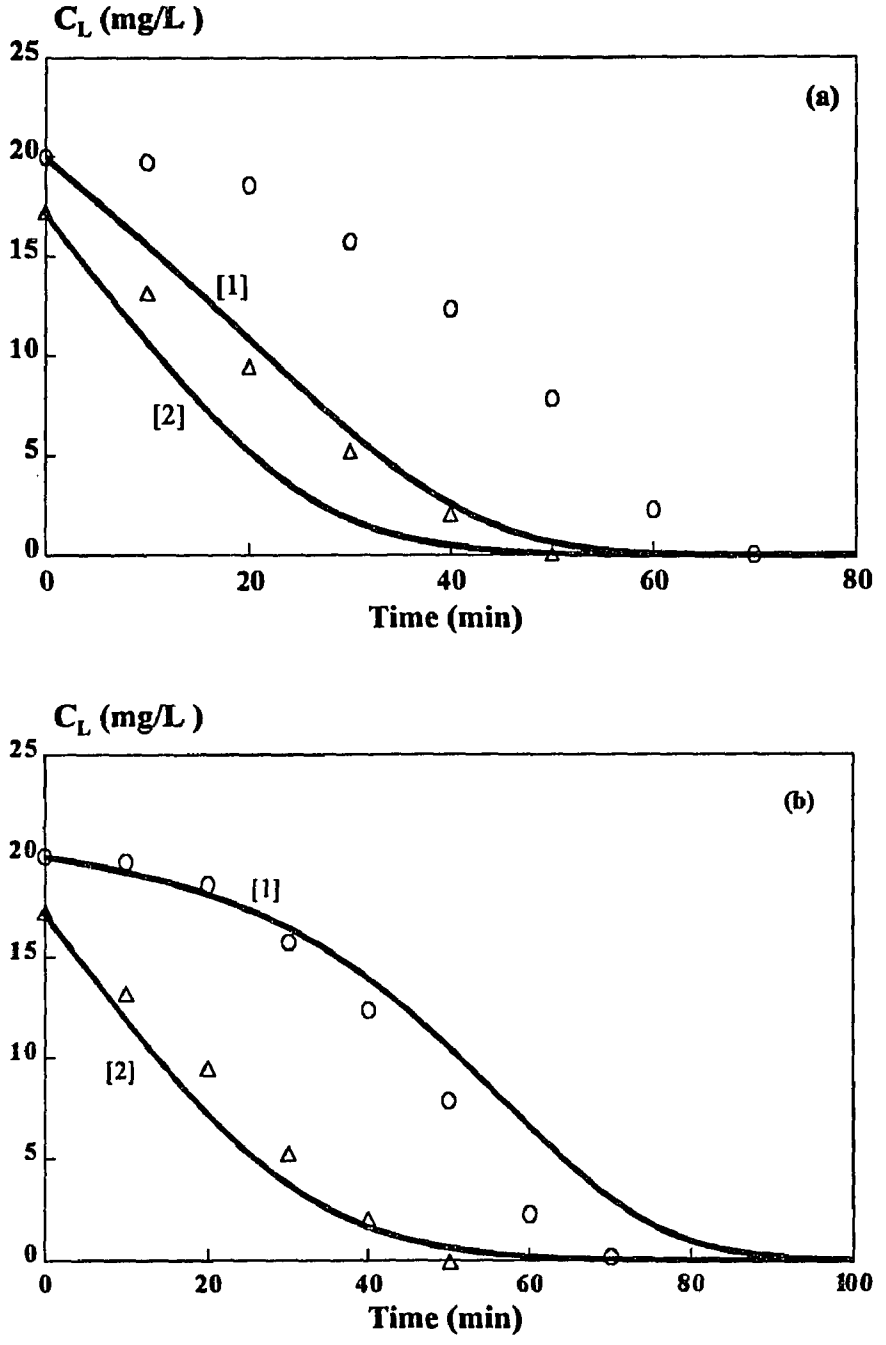

Figure 5.3 Comparison of model predictions and experimental data from a biodegradation experiment with a benzene/toluene mixture. Benzene (1 μL) and toluene (1 μL) were added. Curves in graph (a) have been prepared by assuming no kinetic interaction and in graph (b) by considering interaction effects. The values of model parameters are given in Table 5.1. It is clear that benzene data shown as O, follow curve [1], and toluene data shown as Δ, follow curve [2] only in the case of graph (b).

compared to pure strain PPO1 for both benzene and toluene. Furthermore, parameter values for PPO1 and the consortium indicate that toluene inhibits the utilization of benzene much more than benzene inhibits the utilization of toluene. Actually K_{BT} is over 20 times higher than K_{TB}, indicating that utilization of benzene is severely inhibited in the presence of toluene.

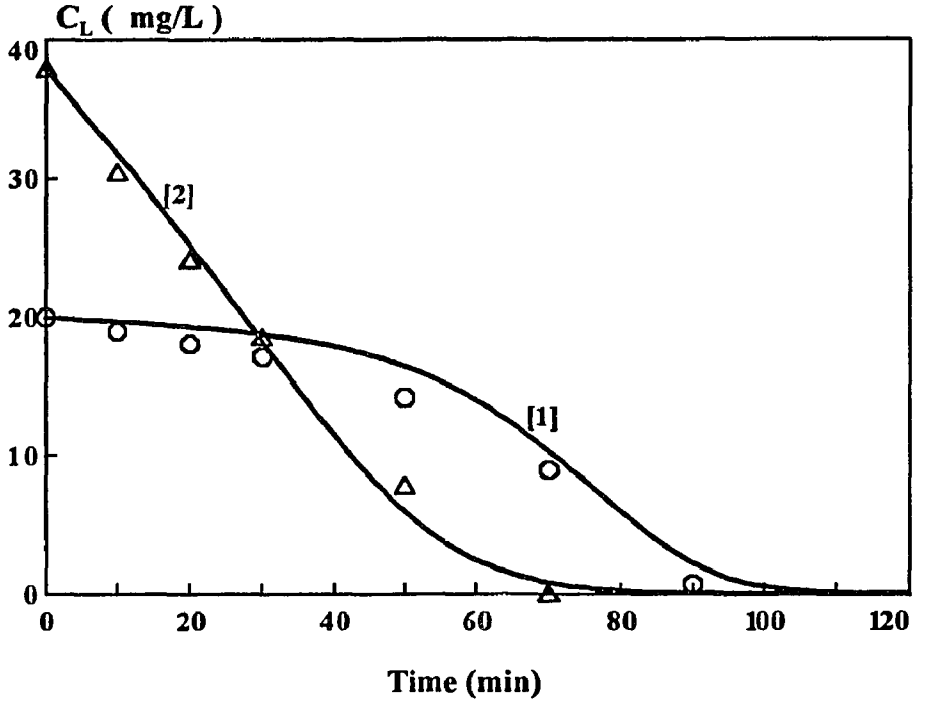

Figure 5.4 Comparison of model predictions and experimental data from a biodegradation experiment with a benzene/toluene mixture. Benzene (1 μL) and toluene (2 μL) were added. Benzene data shown as O, follow curve [1] and toluene data shown as Δ, follow curve [2]. Curves have been prepared by solving the model equations assuming that there are kinetic interactions.

CHAPTER 6

STEADY-STATE BIOFILTRATION OF SINGLE VOCs

In this chapter, a detailed model describing steady-state biofiltration of airstreams containing vapor of a single VOC, is introduced, analyzed, and experimentally validated. Validation is based on experimental data from methanol, benzene, and toluene biofiltration. Data on methanol were obtained from the work of Oh (46), while data on the hydrophobic solvents (benzene and toluene) were generated in the present study.

The model accounts for mass transfer of the VOC and oxygen from the gas phase to the biolayer, as well as within the biolayer through a diffusional process. Reaction kinetics are based on expressions which incorporate potential limitations from both the VOC and oxygen.

6.1 Mathematical Model Development

The model proposed here has been derived based on the following assumptions:

1. Oxygen and the VOC which is to be biodegraded, are the only substances affecting the reaction rate.
2. Oxygen and the VOC are transported within the biolayer by a diffusional process.
3. Reaction in the biolayer follows an interactive model as described in Chapter 5. Kinetics of biodegradation in the biolayer are the same with those when the same culture is used in suspension to biodegrade the same compound.
4. The biolayer is formed on the exterior surface of the particles, and its thickness (δ^*) is small when compared to the particle size; hence, planar geometry can be used. At least one of the rate-limiting substrates gets depleted before it reaches the biolayer/solid

support interface. Thus, there is an effective biolayer thickness (δ) in the sense of Williamson and McCarty (77).

5. There is no boundary layer at the air/biolayer interface, and the concentration of component j (j : VOC, oxygen), c_j , in the gas phase is related to the concentration of that component in the biolayer (at the air/biolayer interface), through the expression $s_j = c_j/m_j$, where m_j is the distribution coefficient for the component j /water system, as also assumed by Ottengraf and Van den Oever (52).

A schematic representation of the biolayer under assumptions 4 and 5 is given in Figure 6.1.

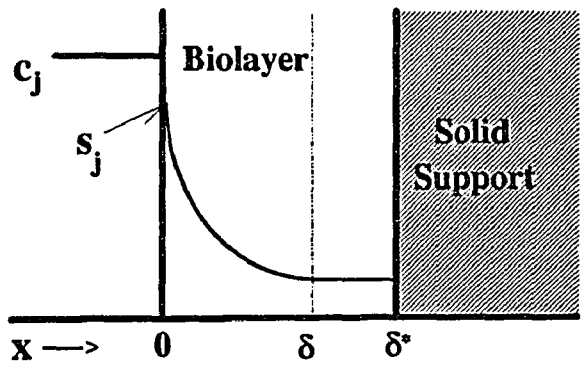

Figure 6.1 Schematic of the biofilm model concept at a cross-section along the biofilter column.

6. In the gas phase, there are no concentration variations in the radial direction of the column (plug flow).
7. The biofilm density, X_V , is constant throughout the column. X_V is the amount of dry biomass per unit volume of biofilm.

8. After the initial stages of the process, biomass accumulation in the column is either negligible, or it occurs very slowly so that, at least over substantial periods of time, one can assume that a steady state, or more specifically a quasi-steady state, is established in the unit.

Under the above assumptions, the process can be described by four mass balances, two on the pollutant, and two on oxygen as given below.

I. In the biolayer :

$$D_j \frac{d^2 s_j}{dx^2} = \frac{X_v}{Y_j} \mu(s_j, s_o) \tag{6.1}$$

$$D_o \frac{d^2 s_o}{dx^2} = \frac{X_v}{Y_{oj}} \mu(s_j, s_o) \tag{6.2}$$

with corresponding boundary conditions

$$s_j = \frac{c_j}{m_j} \qquad \text{at} \qquad x = 0 \tag{6.3}$$

$$\frac{ds_j}{dx} = 0 \qquad \text{at} \qquad x = \delta \tag{6.4}$$

$$s_o = \frac{c_o}{m_o} \qquad \text{at} \qquad x = 0 \tag{6.5}$$

$$\frac{ds_o}{dx} = 0 \qquad \text{at} \qquad x = \delta \tag{6.6}$$

$$\text{with} \quad \mu(s_j, s_o) = \mu(s_j) \frac{s_o}{K_o + s_o} \tag{6.7}$$

where $\mu(s_j)$ is the specific growth rate of the biomass used, on the VOC which is to be removed, under no oxygen limitation; $\mu(s_j)$ can be either a Monod, or an Andrews expression as discussed in Chapter 5. The specific form of $\mu(s_j)$, and the values of the kinetic constants associated with it should be revealed from independent shake-flask experiments as explained in Chapter 5.

II. Along the column :

$$u_g \frac{dc_j}{dh} = A_{sj} D_j \left[\frac{ds_j}{dx}\right]_{x=0} \tag{6.8}$$

$$u_g \frac{dc_o}{dh} = A_{sj} D_o \left[\frac{ds_o}{dx}\right]_{x=0} \tag{6.9}$$

with corresponding boundary conditions

$$c_j = c_{ji} \qquad \text{at} \qquad h = 0 \tag{6.10}$$

$$c_o = c_{oi} \qquad \text{at} \qquad h = 0 \tag{6.11}$$

For the case where the biodegradation kinetics of the VOC under no oxygen limitation follow either Andrews or Monod kinetics, the equations can be written in dimensionless form as follows.

$$\frac{d^2\bar{s}_j}{d\theta^2} = \phi^2 \frac{\bar{s}_j}{1+\bar{s}_j+\gamma\bar{s}_j^2}\frac{\bar{s}_o}{1+\bar{s}_o} \tag{6.12}$$

$$\frac{d^2\bar{s}_o}{d\theta^2} = \phi^2\lambda\frac{\bar{s}_j}{1+\bar{s}_j+\gamma\bar{s}_j^2}\frac{\bar{s}_o}{1+\bar{s}_o} \tag{6.13}$$

$$\frac{d\bar{c}_j}{dz} = \eta\left[\frac{d\bar{s}_j}{d\theta}\right]_{\theta=0} \tag{6.14}$$

$$\frac{d\bar{c}_o}{dz} = \eta\omega\left[\frac{d\bar{s}_o}{d\theta}\right]_{\theta=0} \tag{6.15}$$

$$\frac{d\bar{s}_j}{d\theta} = \frac{d\bar{s}_o}{d\theta} = 0 \qquad \text{at} \qquad \theta = 1 \tag{6.16}$$

$$\bar{s}_j = \varepsilon_1\bar{c}_j; \qquad \bar{s}_o = \varepsilon_2\bar{c}_o \qquad \text{at} \qquad \theta = 0 \tag{6.17}$$

$$\bar{c}_j = \bar{c}_O = 1 \qquad \text{at} \qquad z = 0 \tag{6.18}$$

where

$$\bar{s}_j = \frac{s_j}{K_j}, \qquad \theta = \frac{x}{\delta}, \quad \phi^2 = \frac{\mu^* \delta^2 X_v}{D_j K_j Y_j}, \qquad \gamma = \frac{K_j}{K_{Ij}}, \qquad \bar{s}_O = \frac{s_O}{K_O},$$

$$\lambda = \frac{D_j K_j Y_j}{D_O K_O Y_{Oj}}, \qquad \bar{c}_j = \frac{c_j}{c_{ji}}, \qquad z = \frac{h}{H}, \quad \eta = \frac{A_s D_j H K_j}{u_g \delta c_{ji}} \qquad \bar{c}_O = \frac{c_O}{c_{Oi}},$$

$$\omega = \frac{K_O D_O c_{ji}}{K_j D_j c_{Oi}}, \qquad \varepsilon_1 = \frac{c_{ji}}{K_j m_j}, \quad \varepsilon_2 = \frac{c_{Oi}}{K_O m_O}$$

Equations (6.12) and (6.13) along with boundary conditions (6.16) and (6.17) yield

$$\bar{s}_j = \varepsilon_1 \bar{c}_j + \frac{\bar{s}_O - \varepsilon_2 \bar{c}_O}{\lambda} \tag{6.19}$$

Because of equation (6.19), equations (6.14) and (6.15), along with boundary conditions (6.18) yield

$$\bar{c}_j = \frac{\bar{c}_O - 1}{\lambda \omega} + 1 \tag{6.20}$$

Combining equations (6.19) and (6.20) one gets

$$\bar{s}_j = \frac{\bar{s}_O}{\lambda} - \varepsilon_1 \left(\frac{1}{\lambda \omega} - 1 \right) - \frac{1}{\lambda} \left(\varepsilon_2 - \frac{\varepsilon_1}{\omega} \right) \bar{c}_O \tag{6.21}$$

From the foregoing analysis it becomes clear that the process can be described by equations (6.13) and (6.15) only, provided that expression (6.21) is substituted for $\bar{s}_j$ in equation (6.13). Of the boundary conditions (6.16) through (6.18) one needs only those concerning $\bar{s}_O$ and $\bar{c}_O$. Clearly, due to symmetry one could use equations (6.19) and (6.20) to get expressions for $\bar{s}_O$ and $\bar{c}_O$ which could then be substituted into equations (6.12) and (6.14). In such case, the process is described by equations (6.12), (6.14), and

those boundary conditions among expressions (6.16) through (6.18) which concern $\bar{s}_j$ and $\bar{c}_j$. Reduction in the number of model equations facilitates the numerical work needed for solving the model.

6.2 On the Solution of the Model

The model proposed in the previous section contains a total of 16 parameters. More specifically, up to 4 kinetic constants (μ^* or μ_{max}, K_j, K_{Ij}, K_O), which can be determined as shown in Chapter 5; 2 yield coefficients (Y_j, Y_{Oj}); two distribution coefficients (m_j, m_O); two diffusion coefficients (D_j, D_O); the biofilm density (X_V); the effective biolayer thickness (δ); the biolayer surface area per unit volume of reactor (A_S); and three operating parameters (u_g, c_{ji}, c_{Oi}), which can be easily measured in any specific experiment or application. In order to solve the model equations, one needs to determine, or estimate the 13 out of the 16 parameters.

6.2.1 Determination/Estimation of Model Parameters

6.2.1.1 Kinetic parameters

The kinetic parameters are characteristic of the culture used, and the type of VOC treated. For the solvents studied here (methanol, benzene, and toluene), these parameters have been determined as discussed in Chapter 5.

6.2.1.2 Yield coefficients

The yield coefficients (Y_j, Y_{Oj}), are again characteristic of the culture used, and the type of VOC treated. Their values can be found from the data obtained during the kinetic runs. The values of the yield coefficient on the VOC (Y_j) were experimentally obtained for the solvents studied in this dissertation. In fact, the values for Y_B and Y_T are given in Table

5.1. The value of the yield coefficient on methanol (Y_M), was also determined from the kinetic runs discussed in Chapter 5. Its value was found to be 0.28 kg-dry biomass/kg-methanol-consumed. Values of yield coefficients on methanol reported in the literature (6, 14) fall in the range of 0.30-0.54, hence the value determined in this study compares relatively well with them.

Since the kinetic runs reported in Chapter 5 were performed under excess oxygen conditions, hence oxygen consumption was not measured, the values of the yield coefficients on oxygen (Y_{Oj}), were estimated from the values of Y_j, as follows.

According to Shuler and Kargi (65), a typical cellular composition can be represented as $CH_{1.8}O_{0.5}N_{0.2}$. Taking into account the fact that in the kinetic runs NH_4Cl was the nitrogen source, using the values of Y_j (0.28 for methanol, 0.71 for benzene, 0.71 for toluene), one can write the following equations

$$CH_4O + 1.12\ O_2 + 0.07\ NH_4Cl \rightarrow 0.36\ CH_{1.8}O_{0.5}N_{0.2} + 1.78\ H_2O + 0.64\ CO_2 + 0.07\ HCl \qquad (6.23)$$

$$C_6H_6 + 5.14\ O_2 + 0.45\ NH_4Cl \rightarrow 2.25\ CH_{1.8}O_{0.5}N_{0.2} + 1.65\ H_2O + 3.75\ CO_2 + 0.45\ HCl \qquad (6.23a)$$

$$C_7H_8 + 5.97\ O_2 + 0.53\ NH_4Cl \rightarrow 2.65\ CH_{1.8}O_{0.5}N_{0.2} + 1.91\ H_2O + 4.35\ CO_2 + 0.53\ HCl \qquad (6.23b)$$

From equation (6.23) one can calculate the yield coefficient of biomass on oxygen when methanol is the carbon source, as Y_{OM} = 0.25 kg-dry-biomass/kg-O_2. Similarly, from equations (6.23a) and (6.23b) one can calculate the yield on oxygen as Y_{OB} = 0.336, Y_{OT} = 0.341 when benzene and toluene, respectively, are the carbon sources.

In order to check if the approach discussed above leads to reasonable estimates of Y_{Oj}, data from the literature on methanol (6), reporting experimentally measured values of both Y_M and Y_{OM} were used as follows. Y_M values were used in balancing equation (6.23). Estimated Y_{OM} values were compared to the reported ones. The method proved very good, especially when applied to *Pseudomonas* and *Methylomonas* species.

6.2.1.3 Biofilm density

Biofilm density, X_V, was not measured during this study. The construction of the experimental apparatus was such that it would allow for solid sampling only at the exit, in all experiments with single VOCs. Even if sampling was possible at various column locations, it could easily lead to disturbances in the air/solids contact pattern. Furthermore, the solids had a wide size distribution and were irregular in shape, something which would had made the biolayer volume determination almost impossible. In the literature, while there is a wealth of information about biofilm densities for three-phase (solid-liquid-gas) systems, e.g., Fan et al. (28, 29), Tang and Fan (69), Tang et al.(70), Livingston and Chase (42), there is no information regarding two-phase (solid-gas) systems, possibly because interest and research on biofiltration has started only recently. In the aforementioned studies, the biofilm densities reported range from 23 to 220 kg m^{-3}, while it is also established that X_V decreases as the thickness of the biofilm increases. In the present study, some microscopic observations of particles at the end of experiments with methanol (after columns had run for up to 12 weeks), have indicated that the biolayer thickness was well in the sub-millimeter range. A value of X_V = 100 kg m^{-3} was used in the calculations. This value is at about the middle point of the reported values, and was used in the absence of a better estimate.

6.2.1.4 Distribution coefficients

As discussed in the preceding section, a value of 100 kg m^{-3} was used for the biofilm density. This value implies that 100 kg of dry biomass is present in 1 m^3 of biofilm. Given

the fact that wet biomass has the same density with water, a value of X_V = 100 kg m^{-3} implies that 90% of the biofilm is made of water. For this reason, the distribution coefficients of VOCs, and oxygen, between air and biofilm were assumed to be equal to the corresponding distribution coefficients between air and water (assumption 5 for model derivation).

For methanol, vapor/liquid equilibrium data (1 atm, 25°C) for the methanol/water system from the literature (32) were used, and a value of $m_M = 0.0035$ was determined.

For benzene and toluene, values of $m_B = 0.23$, and $m_T = 0.27$ were taken from the literature (43).

The solubility of oxygen (1 atm, 25°C) in water is reported (6) as 1.26 mmol/l. Assuming a linear relationship between solubility and pressure, water when it is in equilibrium with air contains oxygen at 8 gm^{-3}. Assuming ideal gas behavior, the oxygen concentration in the air is 275 g m^{-3}. The distribution coefficient for the oxygen (in air)/water system, m_W, was then determined as 275/8 = 34.4. The concentration of oxygen in the air at the reactor entrance, c_{Oi}, was also taken as 275 g m^{-3} in all cases thus, any small changes in this value due to the VOC vapor presence in the air were disregarded.

6.2.1.5 Diffusion coefficients

The diffusivities in water of oxygen (D_{OW}), benzene (D_{BW}), and toluene (D_{TW}), at 25°C were obtained from the literature (62), and are reported in Tables 6.2 and 6.5. The diffusivity of methanol in water at 15°C was also obtained from the same reference, and then converted to a value for 25°C through the Stokes-Einstein equation (8). The value of D_{MW} at 25°C is reported in Table 6.2.

Fan et al (29) have proposed an empirical equation for predicting the diffusivity of a substance in a biofilm, relative to the diffusivity of that substance in water. The ratio of the two values, i.e., the relative diffusivity, depends on the biofilm density. For the value of X_V

= 100 kg m^{-3}, this correlation predicts a relative diffusivity of 0.195, and this value was used in all calculations made in the present work.

6.2.1.6 Effective biolayer thickness

If the actual biolayer thickness, δ^*, and its variation along the column were known, the solution of equations (6.13), (6.15), and (6.21) would indicate if one of the substrates gets practically depleted before the biolayer/solid support interface and thus, the effective biolayer thickness would be revealed. Consequently, assumption 4 would not be needed in the model derivation. Since δ^* was not known and could not be estimated, it was decided to use the notion of effective biolayer thickness in the sense of Williamson and McCarty (77), i.e., make assumption 4. This means that in solving the coupled boundary value problem a trial and error procedure was followed at each step, in order to determine the effective biolayer thickness, δ. The value of δ was taken as the distance in the biolayer which would first lead to depletion of either oxygen or the VOC. A substrate was assumed to be depleted when its value dropped to about 1% of its corresponding value at the air/biolayer interface (i.e., $\theta = 0$).

6.2.1.7 Specific biofilm surface area

The only model parameter which could neither be measured, nor estimated from the literature, is the biolayer (or biofilm) surface area per unit volume of reactor (A_{Sj}). For this reason the following approach was adopted. With each one of the VOCs tested experimentally, some column experiments were used as basis for model calibration; that is, the data were fitted to the model by varying the A_{Sj} value. A single value of A_{Sj} which minimized the sum of the squares of the error between experimental and model predicted gas phase concentration profiles in all sets used for model calibration, was taken as the A_{Sj} value associated with the particular VOC. Subsequently, this A_{Sj} value, without any adjustment, was used in predicting biofiltration of that VOC under other experimental

conditions. As will be discussed later, this approach could nicely predict experimental data not used in the model calibration.

6.3 Numerical Methodology

Equations (6.13) and (6.15), along with the corresponding boundary conditions, constitute a coupled boundary value problem. A computer code was developed for solving this problem, and is given as Appendix A of this dissertation. The logic of this code is as follows. Equation (6.13), at a given value of z, is solved by using a multiple shooting technique (subroutine BVPMS of the IMSL library). Once $\bar{s}_o(\theta)$ is evaluated at a given z, equation (6.15) is solved by a 4th-order Runge-Kutta method to produce $\bar{c}_o$ at a point $z+\Delta z$ at which, equation (6.13) is solved again. This procedure is repeated (100 times, $\Delta z = 0.01$) up to the exit of the reactor ($z = 1$). The VOC concentration profiles in the biolayer and along the column are calculated via the algebraic relations (6.21) and (6.20), respectively.

As mentioned in section 6.1 of this chapter, instead of equations (6.13) and (6.15), one could equivalently use equations (6.12) and (6.14). This requires a slight modification of the expressions appearing in the computer code.

It was found that when oxygen is depleted in the biolayer much faster than the VOC, it is better to use equations (6.13) and (6.15). This was the case with methanol. When the VOC is depleted before oxygen in the biolayer, it was found that it was better to solve equations (6.12) and (6.14). This was the case with both benzene and toluene.

It should be also mentioned that instead of using the multiple shooting technique, one could use the method of orthogonal collocation (30,76). This was the method used for solving the steady state biofiltration model for VOC mixtures. This problem is discussed in Chapter 7, and the computer code is given in Appendix B. This code could

be used instead of the one given in Appendix A, for solving the model for one VOC, provided that all but one VOC inlet air concentrations are set equal to zero.

6.4 Biofiltration of Methanol

The data on biofiltration of methanol vapor which were analyzed in the present study, were obtained from the laboratory of Professor R. Bartha (Rutgers University). The experiments were performed by Dr. Y.-S. Oh (46), in glass columns 5cm in diameter, and 60cm in height. A mixture of 40% peat and 60% perlite was used as packing material. Biomass was immobilized on the solids, and in preparing the columns, the packing was moistened to fill 50% of the available pore space. Columns exhibited an initial pressure drop of 0-1 mmHg m^{-1} which increased to a maximum of 10 mmHg m^{-1} after 8-12 weeks of use (64). Two types of column experiments were performed. In the first type, the VOC concentration was measured only at the inlet and outlet, and the column contained no other solid but peat and perlite. In the second type of experiments, concentrations of methanol were measured at the entrance, exit, and three equally spaced locations along the column length. Polyurethane foam plugs were used as spacers around sampling ports. For the data analysis, it was assumed that polyurethane is unfavorable for biofilm formation and thus, it is not considered as solid packing where biofiltration of methanol takes place. Experimentally, it was observed that the columns reached steady-state conditions in 7-10 days after start-up. Only steady state data were used in the analysis presented here.

6.4.1 Removal rates at various flow rates and inlet concentrations

The steady state data were used in calculating removal rates. The removal rate is defined as the concentration difference between inlet and outlet, multiplied by the volumetric flow

rate of the air and divided by the volume of the reactor occupied by the solid packing material.

Table 6.1 Removal rates of methanol vapors at constant inlet concentration and varying air flow rates.

case	u_g	c_{Mi}	V_P	R_{exp}	R_{pred}	Error
	$m\ h^{-1}$	$g\ m^{-3}$	$m^3 \times 10^{-6}$	$g\ h^{-1}\ m^{-3}$-packing		%
			Separated Column			
1	6.42	6.56	782	93.3	86.1	-7.7
2	7.90	6.56	932	92.8	86.6	-6.7
3	8.52	6.11	932	92.8	85.8	-7.5
4	9.52	6.32	932	104.2	88.2	-15.4
			Non-Separated Column			
5	6.42	6.33	706	112.8	86.7	-23.1
6	7.55	6.44	706	94.1	89.1	-5.3
7	9.38	6.45	706	100.8	90.7	-10.0
8	12.75	6.57	706	65.1	92.4	41.9

In the first series of experiments with separated columns, the inlet methanol concentration (c_{Mi}) was kept constant, while the superficial air velocity changed from one experiment to the other. The conditions for these experiments, along with the achieved removal rates, are shown in the first four entries of Table 6.1. These data were used in order to calibrate the model as explained in section 6.2.1.7. The value of H (reactor height) is given as V_P/S, where V_P (reported in Table 6.1) is the volume of the packing (reactor), and S is the cross sectional area of the column. Table 6.2 shows the values used for the model parameters. The value of A_{SM} giving the best fit for each of the four cases individually, is slightly different but very close to the value of 85.15 m^{-1} which was found by following approach described in section 6.2.1.7. This value is relatively low, but it is consistent with the substantial pressure drop of about 10 mmHg m^{-1}. The results of this approach are presented in Figure 6.2. The curves (solid lines) shown in these diagrams represent model predictions or more specifically in this case, the best fit. The

experimentally measured removal rates (based on exit concentrations) and those predicted by the model are shown in Table 6.1, and the agreement is good.

Table 6.2 Parameter values used for solving the model equations

Model Parameter	Numerical Value	Units
μ^*	0.22	h^{-1}
K	0.63	kg m^{-3}
K_I	20.0	kg m^{-3}
K_O	0.26×10^{-3}	kg m^{-3}
Y_M	0.28	kg kg^{-1}
Y_O	0.25	kg kg^{-1}
X_v	100.0	kg m^{-3}
m_M	0.0035	--
m_O	34.4	--
D_{MW}	1.30×10^{-9}	$m^2 s^{-1}$
D_{OW}	2.41×10^{-9}	$m^2 s^{-1}$
D_M/D_{MW}	0.195	--
D_O/D_{OW}	0.195	--
c_{Oi}	275.0×10^{-3}	kg m^{-3}
S	19.63×10^{-4}	m^2
A_{SM}	85.15	m^{-1}

The model predicts an almost linear methanol concentration profile along the column and thus, a practically constant removal rate for each section of a particular column. Removal rates for each one of the four sections of the separated columns have been calculated and are shown in Table 6.3. These data indicate a tendency for the removal rate to increase in the direction of flow. This could be due to lower surface area towards the bottom of the column resulting from compaction of the solids, or due to a lower

biomass density resulting from a possibly larger actual biofilm thickness, δ^* (as has been discussed earlier, results from the literature indicate that X_V decreases as δ^* increases).

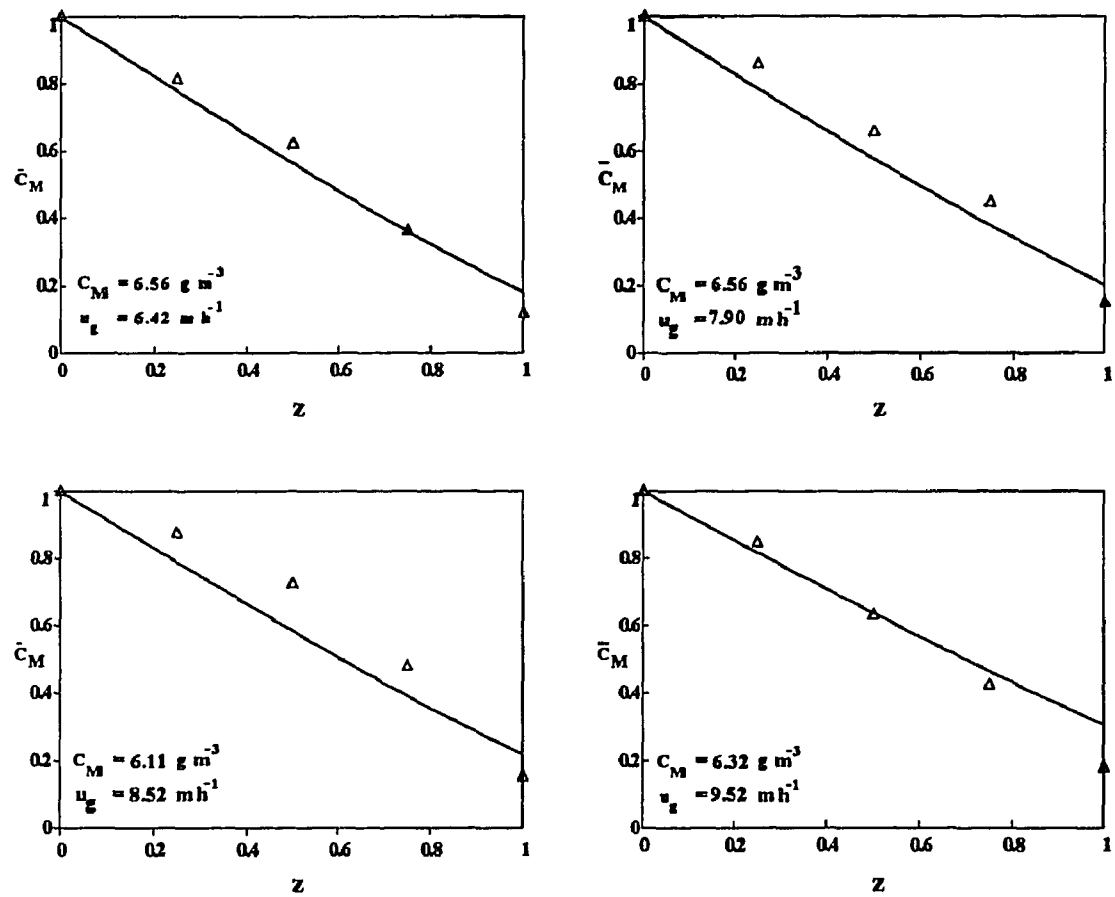

Figure 6.2 Concentration profiles of methanol vapor in the air along a biofilter column at constant inlet concentrations and increasing superficial air velocities. Experimental data shown as Δ. The curves represent model predictions.

Table 6.3 Experimentally measured removal rates of methanol vapors in individual sections of a biofilter (see also Table 6.1)

u_g m h^{-1}	c_{MI} g m^{-3}	$R_{exp,1}$	$R_{exp,2}$	$R_{exp,3}$	$R_{exp,4}$
		g h^{-1} m^{-3}-packing			
6.42	6.56	78.6	81.6	109.0	104.0
7.90	6.56	61.0	88.6	91.2	130.5
8.52	6.11	54.3	66.6	107.7	142.8
9.52	6.32	77.6	109.0	105.0	125.2

The value of 85.15 m^{-1} for A_{SM} was used for predicting other experimental sets of data. Such predictions for cases of non-separated columns are shown in Table 6.1 (cases 5-8). The agreement between data and model predictions is very good in cases 6 and 7. In case 8, the agreement is very poor but as can be seen from the data, something in this column was significantly different from all others. Severe channeling is one possible explanation. In fact, the experimentally measured value could be matched with the model prediction if a lower value of A_{SM} was used. Another possibility is that the biological activity of the organisms was damaged due to a high temperature in the laboratory during part of the period of operation of this column.

One could think of comparing the performance of separated versus non-separated columns in order to determine which type of design is preferable. Operating conditions for cases 1 and 5 are practically the same, and the data seem to indicate that the non-separated column performs better. This could be possibly explained if some of the pores in the polyurethane plugs used in positions along the separated column get clogged either by microbes or water, thus leading to some channeling problems. In fact, the experimental value for the removal rate in case 5 can be predicted by the model if a higher A_{SM} value is used. Cases 2 and 6 have very similar operating conditions, as do also cases 4 and 7. For these two pairs one can see that the removal rates are practically the same for separated and non-separated columns. A general conclusion cannot be reached but it seems that if a separated column is to be used, sieves rather than polyurethane plugs should be used.

In another series of experiments with separated columns, the value of u_g was kept constant while the methanol inlet concentration varied from column to column. The columns were packed in the same fashion as in the experiments reported in Table 6.1, were operated over the same length of time and similar pressure drops were observed. Hence, the value of A_{SM} = 85.15 m^{-1} should be valid. In fact, as can be seen from Table 6.4 and Figure 6.3, the agreement between experimental data and model predictions is

Table 6.4 Removal rates of methanol vapors at constant air flow rate and varying inlet concentrations in separated columns[1]

c_{Mi} g m^{-3}	R_{exp} g h^{-1} m^{-3} -packing	R_{pred}	Error %
2.67	53.3	53.3	0.0
6.98	92.3	90.2	-2.3
8.72	101.6	93.7	-7.8

[1]For these experiments, u_g = 9.48 m h^{-1} and V_p = 932 x 10^{-6} m^3

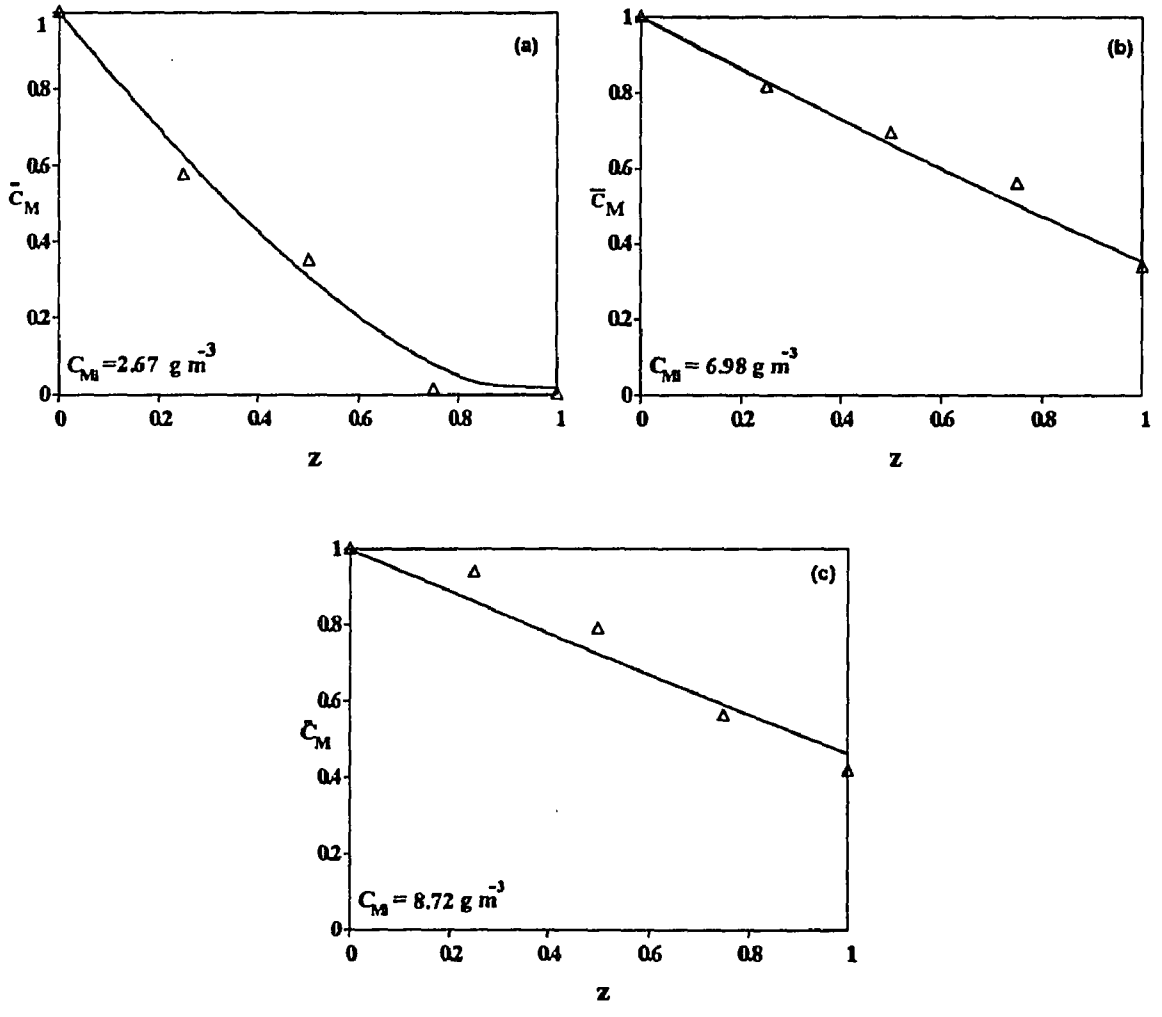

Figure 6.3 Concentration profiles of methanol vapor in the air along a biofilter column, at constant superficial air velocity of 9.48 m h^{-1}, and increasing inlet concentrations, c_{Mi}. Data shown as Δ. The curves represent model predictions.

excellent not only regarding the overall removal rate, but for concentration values along the column as well. It is worth noticing that for low inlet methanol concentrations (top left of Figure 6.3) the data show, and the model predicts, a concentration profile along the column which drastically deviates from the practically linear profiles observed at higher c_{Mi} values; this point will be discussed again later.

6.4.2 The model, its assumptions and implications

The model proposed here is much more complex than the model of Ottengraf and van den Oever (52). This complexity arises not only from the fact that the kinetic expressions are much more involved -first or zero order kinetics assumed by the aforementioned authors-, but also because oxygen and the VOC are considered. If a complex model such as the one proposed here, is to be used in practical applications, its complexity needs to be justified. More specifically, one may wonder whether it could be simplified by considering only one of the two rate limiting substrates, either the VOC or oxygen. Since methanol was the first compound compared against the theory developed here, it was decided to investigate the foregoing question.

Williamson and McCarty (77) have derived two criteria for determining if biodegradation in a biofilm can be described by considering only the electron donor, or only the electron acceptor, i.e., methanol or oxygen, respectively, for the case considered here. These two criteria written for the methanol/oxygen system are as follows.

$$s_O(0) < \frac{D_M \nu_O}{D_O} s_M(0) \tag{6.24}$$

$$\bar{s}_O(\theta) < \frac{\bar{s}_M(\theta)}{1+\gamma \bar{s}_M^2(\theta)} \tag{6.25}$$

where ν_O is the stoichiometric coefficient of oxygen in equation (6.23), i.e., $\nu_O = 1.12$.

Condition (6.24) involves the concentrations of the rate-limiting substances in the biolayer at the air/biolayer interface and if satisfied, it implies that oxygen is flux limiting. Condition (6.25) involves concentrations of the two substances throughout the biolayer; if satisfied at every position in the biolayer (from $\theta = 0$ to $\theta = 1$), it implies that oxygen is substrate (kinetic) limiting. If both conditions (6.24) and (6.25) are satisfied, biodegradation can be described by considering oxygen only. If both conditions are violated, consideration of methanol only is enough to describe the process. In any other case both substrates need to be considered.

Using equations (6.3), (6.5), and (6 20) one can show that condition (6.24) can be written as

$$1 - \frac{Y_M c_{Mi}}{Y_O c_{Oi}} < \left(\frac{\nu_O D_M m_O}{D_O m_M} - \frac{Y_M}{Y_O} \right) \frac{c_{Mi}}{c_{Oi}} \bar{c}_M \qquad (6.26)$$

When the values of the model parameters are substituted for in condition (6.26), one gets

$$\bar{c}_M > \frac{1 - 0.00407 c_{Mi}}{21.59 c_{Mi}}, \qquad (c_{Mi} \text{ in g m}^{-3}) \qquad (6.27)$$

For the values of c_{Mi} used in the experiments, condition (6.27) is satisfied throughout the column except for the case of 2.67 g m^{-3}. In the latter case, condition (6.27) is satisfied up to the point where $\bar{c}_M$ drops to about 2% of its original value. These considerations may be used as an explanation for the practically linear concentration profiles along the columns, except for the case of $c_{Mi} = 2.67$ g m^{-3} which shows a curvature towards the end of the column (Figure 6.3a). One can conclude then, that at low methanol levels in the inlet air, methanol becomes flux limiting. In fact, one can easily calculate that if c_{Mi} is less than 0.046 g m^{-3} (which corresponds to about 40 ppm), methanol is flux limiting throughout the column.

Using equation (6.21) and the values for the model parameters from Table 6.2, one can show that condition (6.25), when c_{Mi} is in g m^{-3}, can be written as

$$1463.9\bar{s}_M - 664.5c_{Mi}\bar{c}_M + 30.75 - 0.125c_{Mi} < \frac{\bar{s}_M}{1 + 0.0315\bar{s}_M^2} \qquad (6.28)$$

Since at $\theta = 0$, $\bar{s}_M = \varepsilon_1\bar{c}_M = 0.454c_{Mi}\bar{c}_M$, one can conclude from simple calculations that condition (6.28) is never satisfied at the air/biolayer interface for any value of c_{Mi} used in the experiments, and for any $\bar{c}_M$. Furthermore, the numerical calculations have shown that in almost all cases considered here, condition (6.28) is satisfied in a small portion of the biolayer close to the biolayer/solid support interface. The exception occurs again at the upper part of the column which was operated at c_{Mi} = 2.67 g m^{-3}. In the latter case, condition (6.28) was never satisfied implying that at very low methanol concentrations in the air, oxygen never becomes the kinetic-limiting substrate in any part of the biolayer.

From the foregoing discussion it can be concluded that criteria (6.24) and (6.25) were never simultaneously satisfied, except at a very small section close to the exit of the column which was operated at c_{Mi} = 2.67 g m^{-3}. Thus the model needed in fact to be written in terms of both methanol and oxygen. The process was oxygen-flux-limited and methanol-kinetic-limited. This can be seen from Figure 6.4 where typical concentration profiles (normalized with the concentration at the air/biolayer interface, i.e., at θ=0) have been plotted. The same conclusion could be reached in an alternate fashion as follows.

According to assumption 4, the effective biolayer thickness is equal to the biolayer thickness within which either methanol or oxygen gets depleted. This thickness was numerically calculated as explained in section 6.2.1.6. The numerical calculations for the case of methanol have shown the following. For c_{Mi} = 8.72 gm^{-3}, the value of δ is almost constant along the column, and equal to about 27.5 μm; furthermore, oxygen was depleted before methanol, at any position in the column. For values between 6.11 and 6.98 gm^{-3}, δ

varied from about 28 μm at the entrance of the column, to about 36 μm at the exit; again, oxygen was depleted first, at all locations in the column. Finally for $c_{Mi} = 2.67\ gm^{-3}$, the

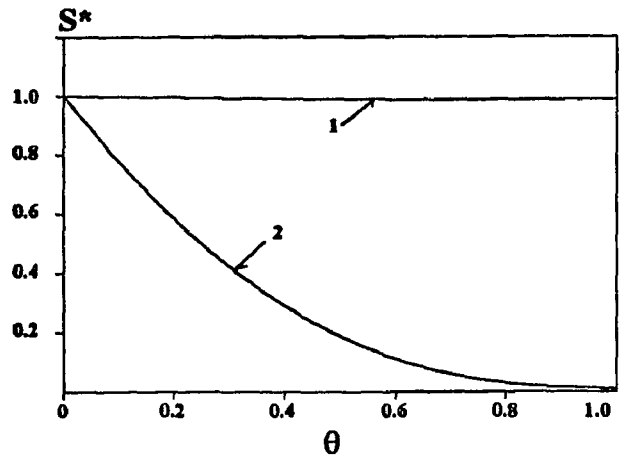

Figure 6.4 Characteristic dimensionless concentration profiles in the biolayer. Specific conditions: $u_g = 6.42\ m\ h^{-1}$, $c_{Mi} = 6.56\ g\ m^{-3}$, middle point of the column ($z = 0.5$). Curves are for methanol (1) and oxygen (2).

value of δ varied from about 31 μm at the entrance, to about 110 μm at the exit of the column; in this case, oxygen gets consumed first in the biolayer, except at positions very close to the exit where methanol gets depleted first. From these results, one can conclude that except for the case of $c_{Mi} = 2.67\ gm^{-3}$, the value of δ does not exceed 36 μm. Based on this value, one can calculate $\phi^2 = 0.18$ and $\phi^2\lambda = 260$. One can argue that ϕ is a measure of the Thiele modulus based on methanol, while $\phi\lambda^{0.5}$ is a measure of the Thiele modulus based on oxygen. Their corresponding values are 0.42 and 16.1; these values seem to indicate that the process is limited by the kinetics of methanol and diffusion of oxygen. Similarly, when $c_{Mi} = 2.67\ g\ m^{-3}$ and δ can reach about 110 μm, the corresponding Thiele moduli are 1.28 and 49.2. The value of 1.28 seems to indicate that diffusion of methanol is important. In fact, the numerical calculations show that at the very end of the column, the biolayer methanol concentration profile is not as flat as the one shown in Figure 6.4. It should be also mentioned that the values of δ reported above, well justify both parts of assumption 4.

Regarding some of the assumptions made in developing the model, one can say the following. The assumption that a steady (or quasi-steady) state is reached can be defended as follows. The time scale of events in the biolayer depends on the characteristic thickness, and the diffusivity of the substrates (37). If δ is taken as the characteristic thickness, and the slower diffusing substrate (methanol) is considered, one can easily show that the time scale δ^2/D_M is up to two orders of magnitude less than the residence time; hence, time variations in the biolayer can be neglected for long periods of time. The model also does not consider biomass accumulation in the column. Biomass accumulation would affect (in time) the values of X_V and A_{SM}. Experimentally it was observed that after an initial period, concentration profiles did not change with time, thus implying that biomass accumulation is, if not zero, very small. One could describe this effect by introducing one more equation for the total mass balance in the reactor, and assuming a biomass rate of decay. This would introduce one more parameter which would have had to be fitted. Since in most of the cases it is predicted that oxygen cannot penetrate the biolayer for more than 40 μm, it is reasonable to expect that cells die quickly due to oxygen deprivation. Although a large excess of nitrogen source was added to the column in the beginning of the experiments, death and lysis of cells can be also viewed as a possible source for nutrients other than carbon and oxygen, thus eliminating the need for them to be externally supplied. Even if biomass decay is not considered, the proposed model would be very accurate over long periods of time as can be seen from the following example. Consider the case of the non-separated column which resulted in the highest removal rate of 112.8 g m^{-3} h^{-1}. The void fraction was not measured, but it is estimated at about 40% in the beginning of the experiments. Over a period of 100 h one can calculate the volume of biomass formed as 22 cm^3 (based on $Y_M = 0.28$ and $X_V = 100$ kg m^{-3}), i.e., a change in the void fraction of about 8%. In view of the above, it is believed that the quasi-steady state assumption is quite reasonable.

6.4.3 An alternate representation of the results, and sensitivity studies with the model

In practical applications, a parameter used in determining the performance of a biofilter is its elimination capacity (18, 52), symbolized by EC, and given -for a VOC j- by the following equation.

$$(EC)_j = \frac{1}{\tau}(c_{ji} - c_{je}) = \frac{V_P}{F}(c_{ji} - c_{je}) = \frac{V_P S}{u_g}(c_{ji} - c_{je}) \qquad (6.29)$$

The EC is also known as the removal rate. If one specifies the exit concentration values so that the processed airstream meets the regulatory requirements, the model can be used for predicting the size of the required biofilter unit. Similarly, for given u_g and V_P one could calculate, through the model, the EC. Relations (6.29) can be presented in various graph forms which could facilitate design calculations; e.g., from values of EC, F, c_{ji}, and regulatory requirements defining c_{je}, one could easily calculate through equations (6.29) the size (V_P) of the required biofilter. Some graphs are presented in the following parts of this section.

Figure 6.5 shows the removal rate as a function of the superficial air velocity u_g. The form of the curve is characteristic of first-order processes. The only way in which a process having a complex kinetic dependence such as the one given by expression (6.7) reduces to a first-order type, is when it is diffusion or transport limited. Of the two substances, methanol has a solubility in water (or biofilm) which is orders of magnitude higher than that of oxygen. Thus, diffusion limitation is due to oxygen. Another way of interpreting the diagram of Figure 6.5 is the following. At low u_g values, the contact time is enough to allow for complete removal, i.e., $c_{Me} = 0$. From equation (6.29) then, one gets :

$$EC = \frac{Su_g}{V_P} c_{Mi} \qquad (6.30)$$

Equation (6.30) implies that at low u_g values there is a linear relationship between removal rate and u_g with a slope Sc_{Mi}/V_P. At high values of u_g, the contact time is not enough to allow for complete methanol removal; the model predicts and the data confirm that the removal rate is independent of the contact time. One can then argue that at low values of contact time the process behaves as if it is practically of order zero.

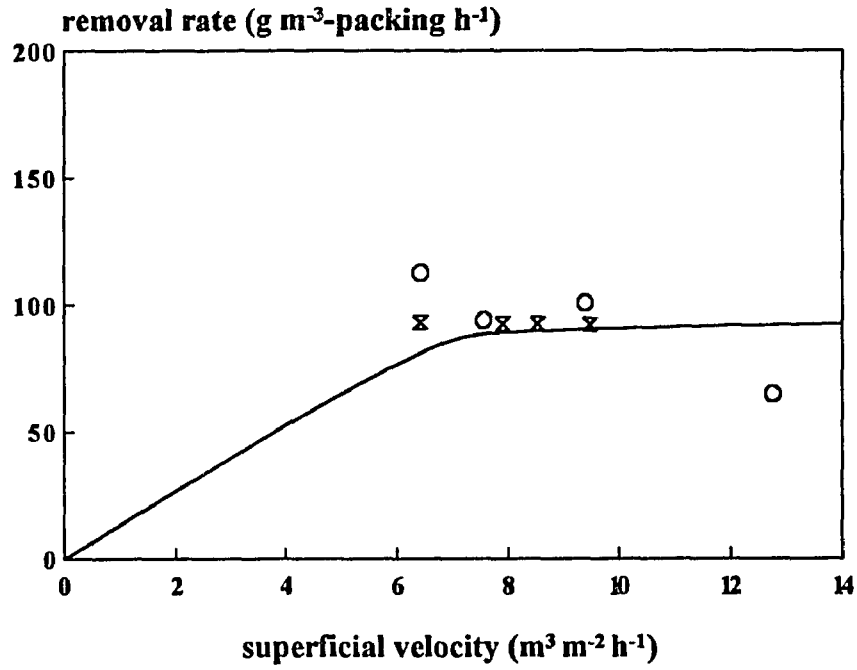

Figure 6.5 Methanol removal rate as a function of u_g : Comparison between model predictions (curve) and experimental data for c_{Mi} = 6.5 gm^{-3}; V_p = 932 cm^3 for data shown as ⧗, and 706 cm^3 for data shown as O.

Figure 6.6 shows the percent methanol removal, defined as $100(c_{Mi} - c_{Me})/c_{Mi}$, as a function of inlet concentration for three values of the residence time. As expected, when the residence time increases the percent removal increases. For a residence time of three minutes the model predictions agree nicely with experimental data.

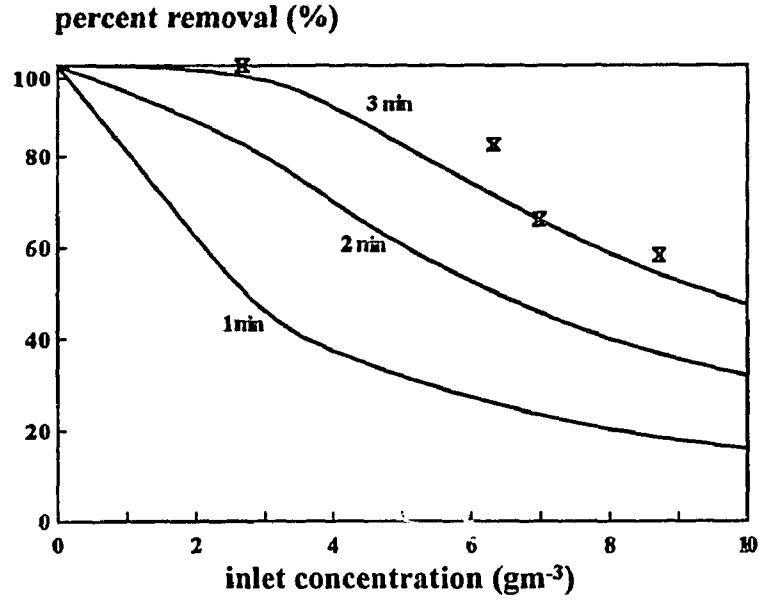

Figure 6.6 Model predictions for methanol percent removal as a function of c_{Mi} for three values of τ. Predictions are in excellent agreement with data from four 932 cm^3 columns operated at $\tau = 3$ min.

Figure 6.7 shows the percent removal as a function of space time for a particular value of methanol concentration in the inlet air. The agreement between experimental data and model predictions is very good. Hence, the model can predict the required space time (or biofilter size for a given flowrate) for complete removal.

A number of simulation studies were performed with the model in order to determine its sensitivity to the various model parameters. The rationale of these studies is the following. Suppose that one model parameter, say kinetic parameter K, is not exactly known. More, specifically assume that the value of K used in the calculations is twice the value of the real K. In this case one can define the ratio of the used value divided by the real one as relative K. In this example, relative K is equal to 2. The question is the following. Using a value of K which is twice the real one, what is the error made in estimating the removal rate. Again, one can calculate through the model two values for the removal rate: one based on the "wrong" K and one based on the "real" K. The ratio of these two values is defined as the relative removal rate (R').

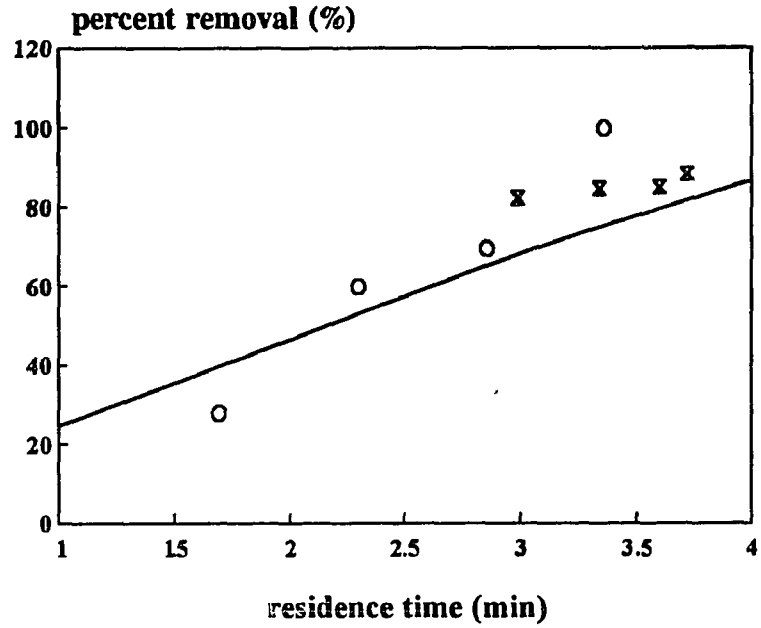

Figure 6.7 Methanol percent removal as a function of τ: Comparison between model predictions (curve) and experimental data for $c_{Mi} = 6.5\ gm^{-3}$. $V_p = 932\ cm^3$ for data shown as ⧗, and 706 cm^3 for data shown as O.

The first set of studies dealt with the kinetic parameters and the results are shown in Figure 6.8. In this graph, the relative removal rate has been plotted versus the relative values of four kinetic parameters. As basis for these studies a methanol biofiltration experiment was used. For that experiment, $V_P = 932\ cm^3$, when $c_{Mi} = 6.56\ gm^{-3}$, and $u_g = 7.90\ mh^{-1}$. The experimentally observed -hence real- value for the removal rate was about 93 g m^{-3}-packing h^{-1}. It should be mentioned that when comparisons are based on the same u_g and c_{ji} values, the relative removal rate can be also viewed as the relative percent removal. From Figure 6.8 one can conclude that out of the four kinetic parameters, only two (μ^* and K) need accurate determination. Parameters K_I and K_O even if they are not accurately known, will not lead to severe errors in predicting the removal rate. There is one more way in which this diagram could be interpreted. Consider biofiltration of a compound other than methanol. The diagram indicates that if the new compound has μ^* and K values similar to those of

methanol, and considerably similar or, different K_O and K_I values, this new compound will be removed in the biofilter at rates as those for methanol.

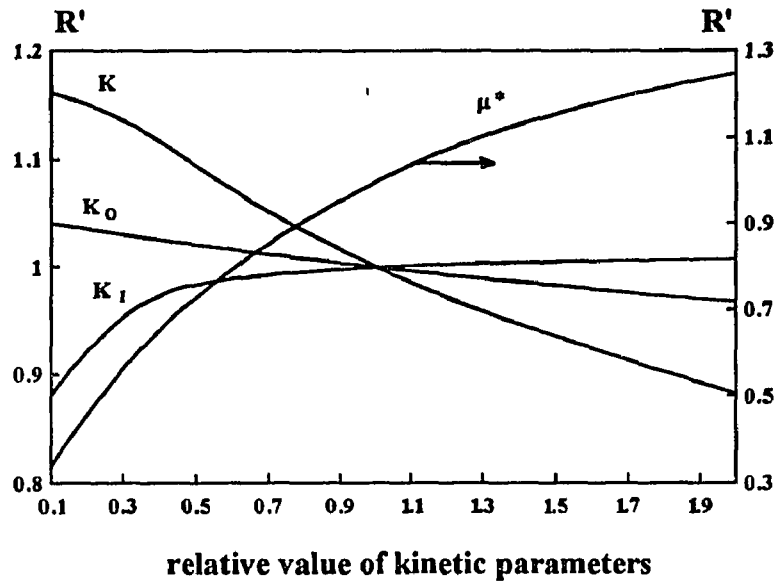

Figure 6.8 Sensitivity analysis of the effect of kinetic parameters on the removal rate of a single substance when c_{ji} = 6.5 g m^{-3} and τ = 3.6 min. The (1,1) point corresponds to methanol with an actual removal rate of about 86.6 g m^{-3}-packing h^{-1}.

Figure 6.9 shows the relative removal rate (defined above) as a function of the relative oxygen concentration in the airstream. A value larger than 1 on the x-axis implies that the airstream contains oxygen at levels higher than the atmospheric air. Calculations have been performed for two inlet methanol concentrations. When c_{Mi} = 2.67 g m^{-3} the (1,1) point corresponds to an actual removal rate of 53.3 g m^{-3}-packing h^{-1}, while when c_{Mi} = 6.98g m^{-3} the (1,1) point corresponds to an actual removal rate of about 90 g m^{-3}-packing h^{-1}. The diagram indicates that at low inlet methanol concentrations (curve a), enriching the airstream with oxygen does not lead to an improved removal rate. This is due to the fact that 100% removal is achieved in such cases. When c_{Mi} is high (curve b), enriching the air with oxygen leads to improved

rates. This is in agreement with the fact, discussed previously, that the process is in most cases limited by oxygen transfer. This graph also implies that, at least in some cases, one could keep the contact time (or biofilter size) at reasonable or desired values by enriching the air with oxygen in order to get complete removal of a pollutant.

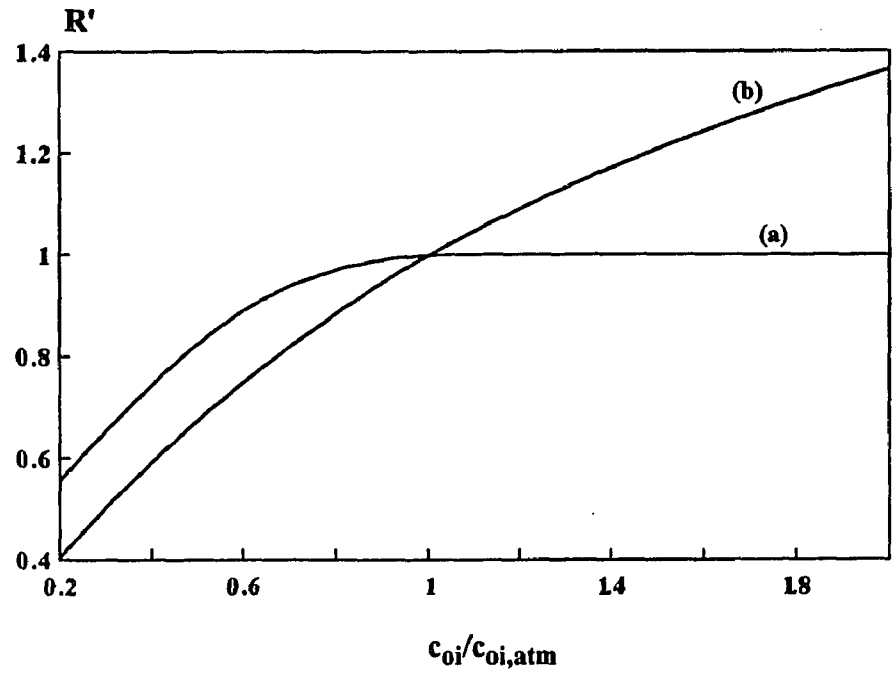

Figure 6.9 Effect of oxygen on the removal rate of methanol when τ = 3 min, and c_{Mi} = 2.67 g m^{-3} (curve a) or 6.98 g m^{-3} (curve b). The (1,1) point corresponds to removal rates discussed in the text.

Figure 6.10 shows results of sensitivity studies with the following three parameters : biofilm density (X_V), distribution coefficient (m), and the biolayer surface area (A_S). The notion of relative values here is exactly the same as that discussed earlier in conjunction with Figure 6.8. The curves of Figure 6.10 imply the following: as expected, when the biolayer surface area per unit volume of the biofilter increases, the removal rate increases and levels off when 100% removal is achieved; what is more important is that the removal rate decreases drastically with A_S and it looks as if there

is a linear relationship between the two quantities for values of R' less than 1. The biofilm density (X_V) is an important parameter only when its value is low. The graph indicates that if X_V is high (or at least above 100 kg m^{-3}), knowledge of its actual value is not important for sizing a biofilter. From the curve for the effect of the distribution coefficient, one can conclude that the more volatile a substance is (high m or low 1/m values), the larger is the size of the biofilter required, assuming that the kinetics of the two substances compared are similar. Also from the same curve one could say that as the temperature increases (and m becomes higher), removal rates for methanol will drop, assuming that the effect of temperature on the kinetic parameters is not profound.

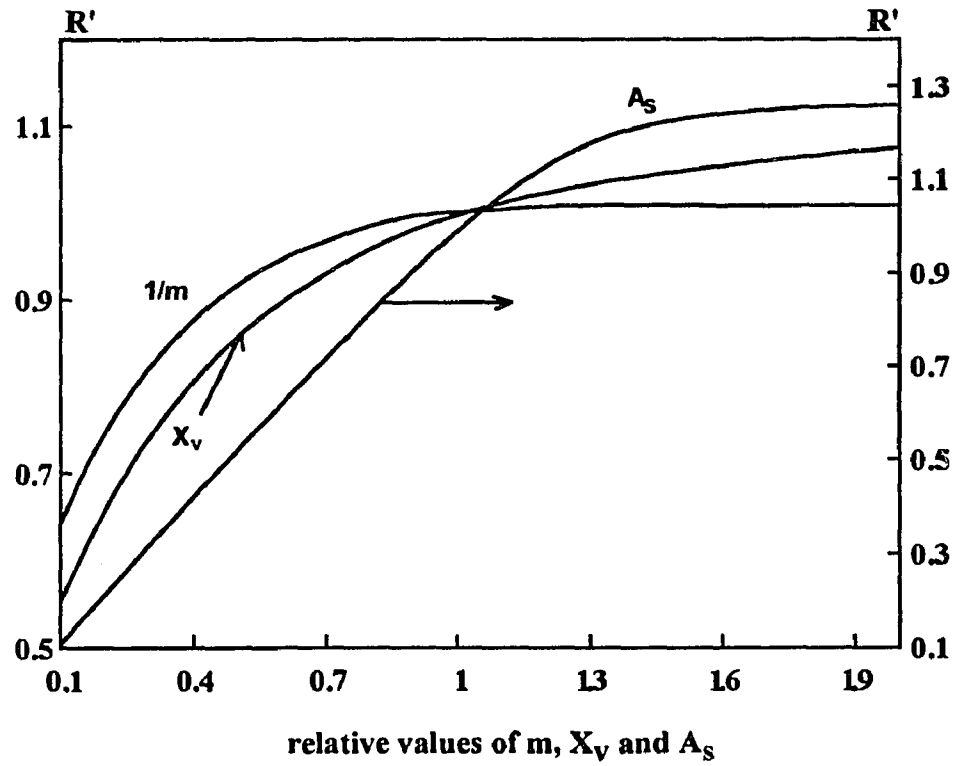

Figure 6.10 Sensitivity analysis of the effect of parameters m, X_V, and A_S on the removal rate of a single substance when c_{ji} = 6.5 g m^{-3} and u_g = 7.9 m h^{-1}; R' = 1 corresponds to an actual rate of about 86.6 g m^{-3}-packing h^{-1}.

6.5 Biofiltration of Benzene and Toluene

Once the proposed model was validated with data from experiments with methanol (data obtained from another source), experiments were performed with two hydrophobic solvents, benzene and toluene. Both substances are classified as primary pollutants by the US EPA. The objective of this part of the work was not only to demonstrate feasibility of benzene and toluene vapor biofiltration, but to also investigate if the mathematical model proposed, can describe biofiltration of hydrophobic compounds as well. As described in section 4.2, the biofilter was packed with a mixture of peat and perlite particles (volume ratio 2:3). The column (10cm in diameter, 75cm in height) was not completely filled with packing material. In the case of benzene, the length of the biofilter bed was 51cm, while for toluene the bed length was 69cm. Experiments with benzene at space times between 2.7 and 4.7 min, and inlet concentrations between 0.07 and 0.56 gm^{-3} led to a maximum removal rate of 4.5 g-benzene m^{-3}-packing h^{-1}. The maximum observed removal rate for toluene was 24.8 g-toluene m^{-3}-packing h^{-1}. Experiments with toluene were performed with inlet concentrations and space times in the range of 0.62-2.81 gm^{-3} and 2.7-8.6 min, respectively. The specific conditions for each experiment, and the measured concentrations values are reported in Table 6.6 for benzene, and Table 6.7 for toluene.

Figure 6.11 shows a characteristic response of the biofilter during start-up. Initially, an amount of the contaminant is adsorbed on the solid packing material, or simply dissolved in the water retained in the pores of the solids. Eventually, after about eight days in the case shown in Figure 6.11, the unit reaches a steady state. The data analyzed in this section are from steady state conditions.

Experiments with benzene vapor were performed under different inlet benzene concentrations, c_{Bi}, and space times, $\tau = V_P/F$. Each experiment was run for a period of at least two weeks. The values of the model parameters used in the calculations are listed

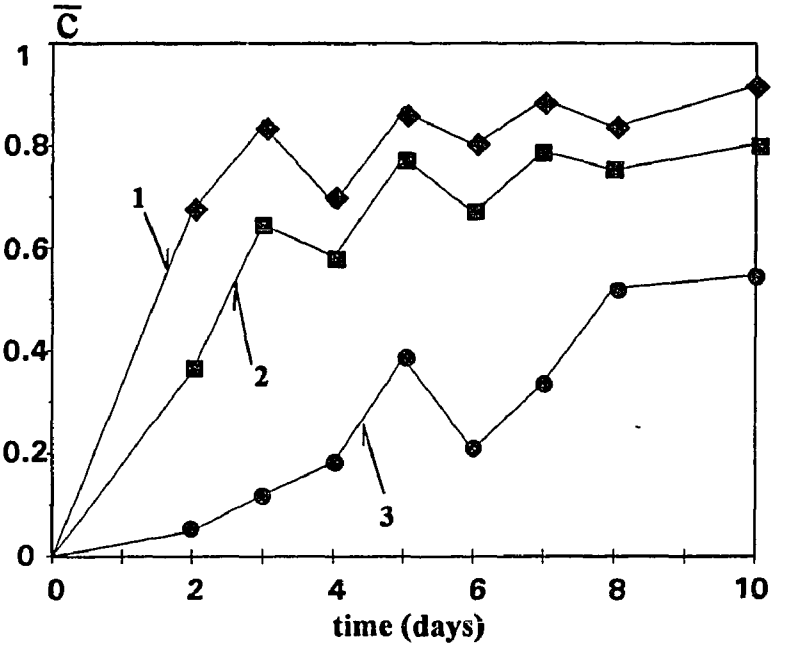

Figure 6.11 Characteristic transient response of a biofilter during start-up; dimensionless concentrations at 0.35H, 0.8H, and at the exit of the biofilter (curves 1, 2, 3, respectively), as a function of time. Data from an experiment with benzene vapor fed at 0.434 gm^{-3}, $\tau = 4.5$ min, $V_P = 4119$ cm^3, $H = 51$ cm.

in Table 6.5. Equations (6.12) and (6.14), along with the corresponding boundary conditions, were used for determining the concentration profiles. The methodology used in numerical calculations has been discussed in earlier sections of this chapter.

Table 6.6 shows the conditions for the experiments, and the measured exit concentration values of benzene. In the same table, the values of the observed removal rate, R_{exp}, which is defined as $(c_{Bi} - c_{Be})/\tau$ are also shown. The load is defined as c_{Bi}/τ. The model predicted values for the exit concentration and the removal rate are also shown in Table 6.6. The value of parameter A_{SB} was determined as 23.3 m^{-1} by using two data sets, and was then used in predicting the values of concentrations for the four other sets. One can easily see that the experimental and model predicted values of c_{Be} and R are very close in almost all cases. Judging the performance of a biofilter on the basis of only the removal rate achieved, as is usually the case, may be misleading when the removal

Table 6.5 Parameter values used for solving the model equations for the case of hydrophobic solvents.

Parameter	Value	Units
A_{SB}	23.3	m^{-1}
A_{ST}	40.0	m^{-1}
c_{Oi}	275.0×10^{-3}	kg m^{-3}
D_{BW}	1.04×10^{-9}	m^2 s^{-1}
D_{OW}	2.41×10^{-9}	m^2 s^{-1}
D_{TW}	1.03×10^{-9}	m^2 s^{-1}
D_j/D_{jW}	0.195	--
K_B	12.22	g m^{-3}
K_{IT}	78.94	g m^{-3}
K_{OB}	0.26	g m^{-3}
K_{OT}	0.26	g m^{-3}
K_T	11.03	g m^{-3}
m_B	0.23	--
m_O	34.4	--
m_T	0.27	--
X_v	100.0	kg m^{-3}
Y_B	0.708	kg kg^{-1}
Y_{OB}	0.336	kg kg^{-1}
Y_{OT}	0.341	kg kg^{-1}
Y_T	0.708	kg kg^{-1}
μ_B^*	0.68	h^{-1}
μ_T^*	1.50	h^{-1}

rate is not compared to the load. It is better to compare the observed percent removal, as well as the removal rate, against the model predictions of the same quantities. Results reported in Table 6.6 indicate that complete removal of benzene vapor requires substantial space times.

The agreement between experimentally measured and model predicted concentration values is good not only at the exit of the biofilter bed as shown in Table 6.6,

Table 6.6 Steady state biofiltration of benzene vapors: Experimental data and model predictions.

τ	c_{Bi}	$c_{Be,1}$	$c_{Be,2}$	E_1 %	X %	L	R_1	R_2	E_2 %
(min)		($g\ m^{-3}$)				(gm^{-3}-packing h^{-1})			
4.1	0.28	0.19	0.16	-15.8	32.1	4.1	1.3	1.6	23.1
4.5	0.43	0.23	0.25	8.7	46.5	5.7	2.7	2.5	-7.4
4.7	0.56	0.21	0.31	47.6	62.5	7.1	4.5	3.1	-31.1
2.7	0.13	0.09	0.09	0.0	30.8	2.9	0.9	0.8	-11.1
2.7	0.12	0.08	0.09	-11.1	33.3	2.7	0.9	0.8	-11.1
4.1	0.07	0.04	0.04	0.0	42.8	1.0	0.5	0.4	-20.0

τ : residence time; c_{Bi} : inlet benzene concentration; $c_{Be,1}$, $c_{Be,2}$: exit benzene concentrations, experimental and predicted, respectively; E_1 : percent error in exit concentration defined as $(c_{Be,2} - c_{Be,1}) / c_{Be,1} x100$; X : percent removal defined as $(c_{Bi} - c_{Be,1}) / c_{Bi} x100$; R_1 and R_2 : removal rates based, respectively, on experimental and model values; L: load; E_2 : percent error in removal rate defined as $(R_2 - R_1) / R_1 x100$.

but along the length (or height) as well. This is demonstrated in Figure 6.12. The model also predicts the concentration profiles of oxygen and benzene in the biolayer at any position along the biofilter length. Figure 6.13 shows such profiles at the middle point of a column. This graph shows that benzene is depleted much faster than oxygen in the biolayer. This was found to be always the case with both benzene and toluene, and it is opposite to what was found in the case of methanol (see Figure 6.4). In the latter case, oxygen was depleted first and thus, it was determining the effective biolayer thickness. For the case shown in Figure 6.13, the effective biolayer thickness (θ = 1) is predicted to be 53μm, and is determined by the depletion of benzene.

The results from the experiments with toluene, along with model predictions are shown in Table 6.7. The model parameter values used for solving the model equations are shown in Table 6.5. In this case, the specific surface area, A_{ST}, was found to be $40m^{-1}$.

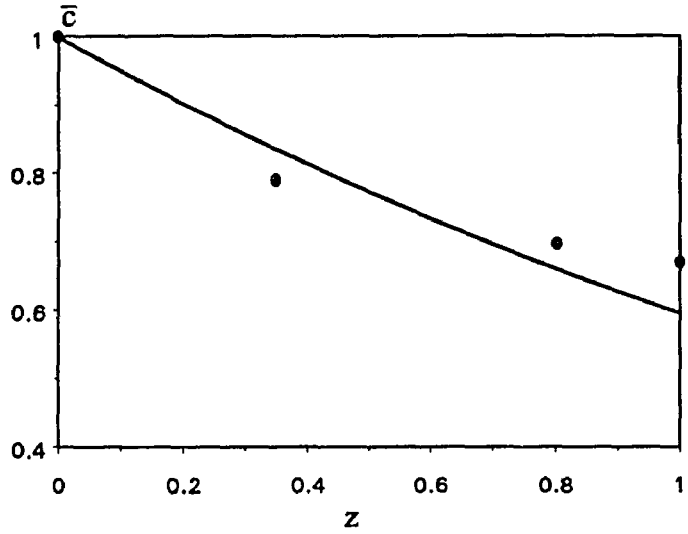

Figure 6.12 Benzene vapor concentration profile along the biofilter under steady state conditions : data and model predictions (curve). For this experiment, $c_{Bi} = 0.28$ gm^{-3}, $\tau = 4.1$ min.

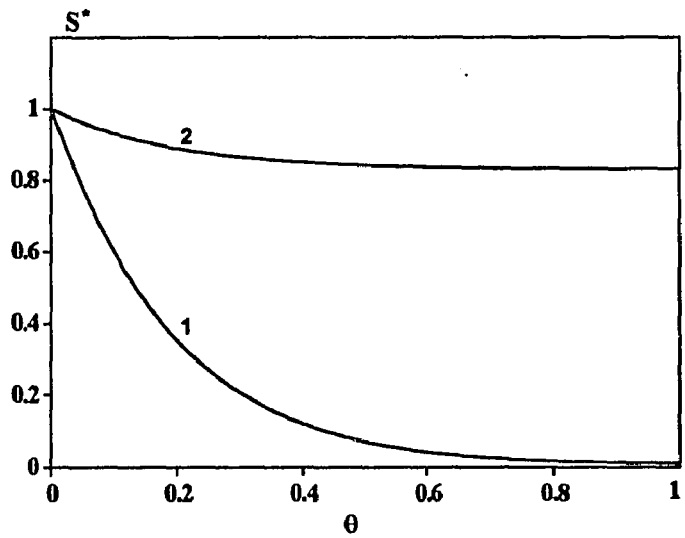

Figure 6.13 Model predicted concentration profiles in the biolayer at h = 0.5H. Curves 1 and 2 are for benzene and oxygen, respectively. These profiles are for the case where $c_{Bi} = 0.43$ gm^{-3}, and $\tau = 4.5$ min.

This value is higher than the one for benzene, but lower than the one for methanol. As can be seen from Table 6.7, the toluene percent removal was very high, leading to low measured exit concentration values. The likelihood of an experimental error in measuring

such low concentrations is high. This may be explaining the high percentage error (E_1) between experimental and model predicted exit concentrations. On the other hand, the percent error between experimentally observed, and model predicted removal rates (column E_2 in Table 6.7) is very reasonable.

Table 6.7 Steady state biofiltration of toluene vapors: Experimental data and model predictions.

τ	c_{Ti}	$c_{Te,1}$	$c_{Te,2}$	E_1 %	X %	L	R_1	R_2	E_2 %
(min)		($g\ m^{-3}$)				(gm^{-3}-packing h^{-1})			
6.3	2.81	0.20	0.55	175.0	92.7	26.8	24.8	21.5	-13.3
4.2	0.92	0.19	0.29	52.6	79.7	13.1	10.4	9.0	-13.5
2.7	0.62	0.21	0.29	38.1	66.5	13.8	9.4	7.4	-21.3
8.6	0.68	0.00	0.05	--	100.0	4.8	4.8	4.4	-8.3
7.7	1.65	0.07	0.19	171.4	95.6	12.8	12.2	11.3	-7.4

c_{Ti} : inlet toluene concentration; $c_{Te,1}$, $c_{Te,2}$: exit toluene concentrations, experimental and predicted, respectively; all other symbols as in Table 6.6

The results indicate that biofiltration of toluene is much easier when compared to benzene.

Except at the exit conditions, the agreement between model predicted and experimentally measured toluene concentrations is remarkably good as shown, for example, in Figure 6.14.

Concentration profiles of toluene and oxygen in the biolayer, are very much similar to those of benzene and oxygen (Figure 6.13).

Data from biofilters are presented in many cases in the form of a diagram showing the removal rate as a function of the load. Usually, a line or a curve is passed through the

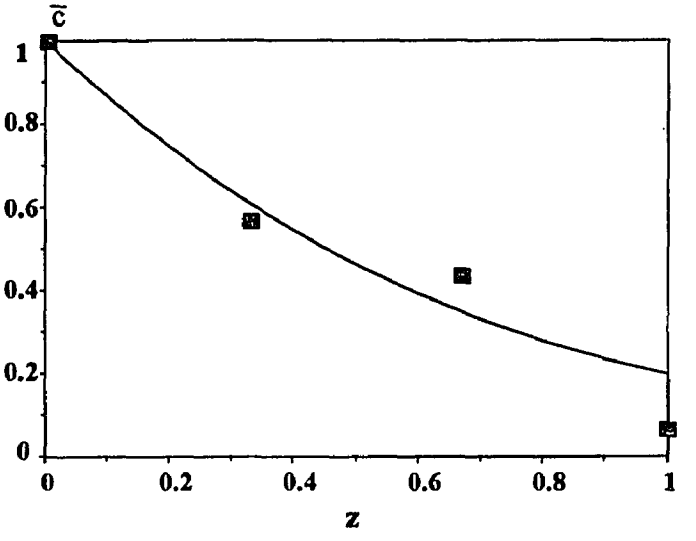

Figure 6.14 Toluene vapor concentration profile along a biofilter column under steady state conditions when $c_{Ti} = 2.81$ g m^{-3}, $\tau = 6.3$ min, $V_p = 5150$ cm^{-3}. Data are compared to the model predictions (curve).

data points by simple interpolation or some type of prediction. It seems that this approach is incorrect. Since variation in the load can be due to either a change in space time, or in the inlet concentration, the data cannot fall on a single straight line, or curve, except if all were obtained under the same space time, or inlet concentration. If both quantities were varied during the experiments, the data should fall in a region rather than a curve (or line), in the removal rate-load space. This is demonstrated in Figure 6.15 for benzene, and Figure 6.16 for toluene. The boundaries of the regions (curves 1 and 2 in the graphs) are predictions under same minimum and maximum space time values used in the experiments. With one exception for benzene, all data points fall in the regions predicted by theory.

Regarding the model parameter values, the highest uncertainty seems to be associated with the biofilm density (X_V), and the biofilm surface area per unit volume of packing (A_{Sj}). For this reason, a sensitivity study on these parameters was performed, similar to the studies reported in section 6.4.3 for methanol. As baseline for this investigation, the experiment reported as last entry in Table 6.7 was used. The results are

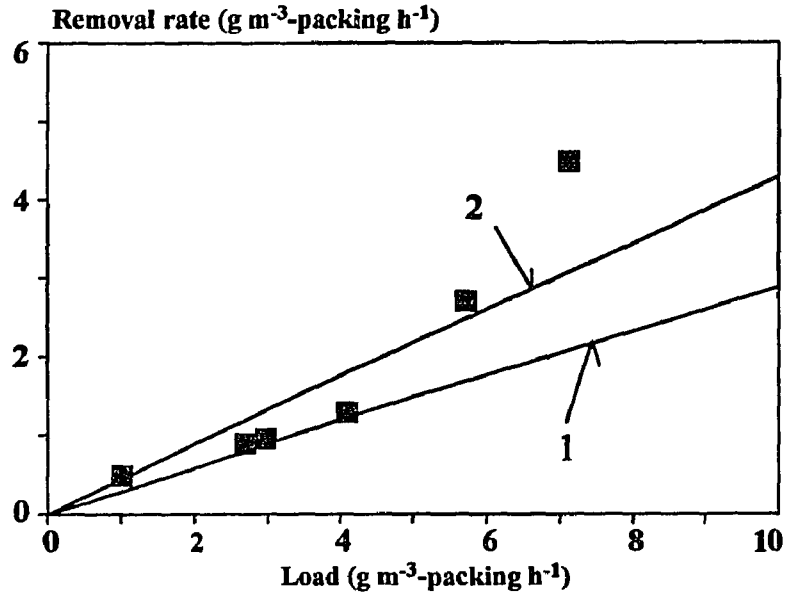

Figure 6.15 Removal rate of benzene as a function of load. Data from experiments under various c_{Bi} and τ values. The two curves represent model predictions for the minimum and maximum τ values used in the experiments. For curve 1, τ = 2.7 min; for curve 2, τ = 4.7 min.

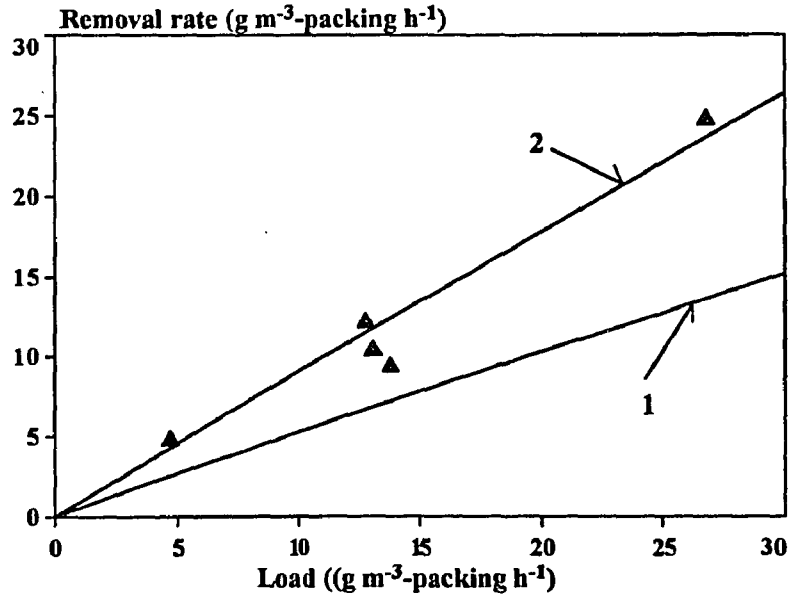

Figure 6.16 Removal rate of toluene as a function of load. Data from experiments under various c_{Ti} and τ values. The curves represent model predictions for the minimum and maximum τ values used in the experiments. For curve 1, τ = 2.7 min; for curve 2, τ = 8.6 min.

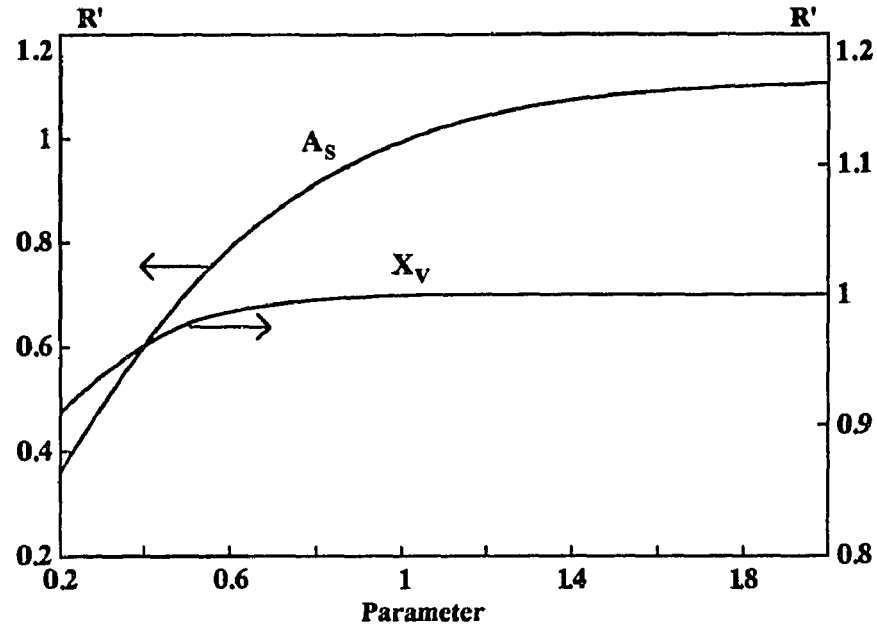

Figure 6.17 Sensitivity of the model to the values of parameters A_S and X_V. Results of simulations compare the removal rate with a reference value when the parameters are changed relative to a reference value. The point of reference (1,1) corresponds to an actual biofiltration experiment with toluene for which $c_{Ti} = 1.65$ g m^{-3}, $\tau = 7.7$ min, and the experimentally observed removal rate was 12.2 g m^{-3}-packing h^{-1}.

shown in Figure 6.17. As can be seen from this graph, for relative X_V values above 0.6, i.e., actual X_V values above 60 kgm^{-3} the predicted removal rate would be practically the same for any X_V. If the real X_V was between 20 and 60 kgm^{-3} the error in the removal rate would be less than 10%. The value of A_{Sj} seems to be very important as shown also in Figure 6.17. It appears that if the real A_{Sj} is larger than the one estimated (relative value larger than 1), the impact on the prediction of the removal rate is less than 10%. On the other hand, if the real value is less than the estimated one, the error in predicting removal rates can be very substantial. It is for this reason that a careful approach needs to used in estimating A_{Sj}.

From the results reported in this section, it is clear that biofiltration can be successfully used for removing benzene and toluene vapors from airstreams. Benzene

appears to be harder to remove than toluene, at least with the culture used in this study. Steady state biofiltration can be nicely described and predicted with the model introduced in this study. Comparing the results from methanol, benzene, and toluene, one can conclude that biofiltration of hydrophobic compounds appears to be less affected by oxygen limitation, when compared to treatment of hydrophilic compounds. Furthermore, removal rates achieved for hydrophilic compounds are at least one order of magnitude higher than those achieved for hydrophobic ones.

CHAPTER 7

STEADY-STATE BIOFILTRATION OF VOC MIXTURES

In Chapter 6 of this dissertation, a detailed model describing biofiltration of single VOC vapors from airstreams was introduced, analyzed, and experimentally validated with three different solvent vapors. Validation of the theory proved that its underlying principles are correct and thus, it was decided to generalize the theory for cases where mixed VOCs are present in airstreams. It was felt that such a generalization is necessary, since in practical applications, airstreams carry -usually- a variety of VOCs. Furthermore, as discussed in the literature review, there is only one model for mixtures, and assumes a simple additive approach. This approach is probably incorrect since, as also discussed in prior chapters, there is a growing evidence of kinetic interactions among compounds which are subjected to simultaneous biodegradation.

7.1 General Theory of Biofiltration of Mixed VOCs

The assumptions made in deriving the general model equations are as follows.

1. Supplemental nutrients, such as nitrogen and phosphorous sources are not exerting rate limitation on the process.
2. All compounds exerting rate limitation on the biofiltration process are transported within the biolayer by a diffusional process.
3. Biodegradation of VOCs occurs only aerobically.
4. Compounds affecting the biofiltration process are oxygen and the VOCs present in the untreated steam.

5. No metabolites accumulate in the filter bed.
6. Biodegradation rates are functions of oxygen, and the VOCs. These rates are the same as in suspended cultures (free cells).
7. The biolayer is formed on the exterior surface of the particles, and its thickness (δ^*) is small when compared to the particle size; hence, planar geometry can be used. At least one of the rate-limiting substrates gets depleted before it reaches the biolayer/solid support interface. Thus, there is an effective biolayer thickness (δ) in the sense of Williamson and McCarty (77).
8. There is no boundary layer at the air/biolayer interface, and the concentration of component j (j : VOC, oxygen), c_j , in the gas phase is related to the concentration of that component in the biolayer (at the air/biolayer interface) through the expression $s_j = c_j/m_j$, where m_j is the distribution coefficient for the component j /water system.
9. The gas phase is in plug flow in the biofilter bed.
10. The biofilm density, X_V , is constant throughout the column.
11. The microbial consortium is stable, and its composition does not vary either in time, or in space. Hence, the specific biofilm area is the same for all VOCs.
12. There is no net biomass accumulation, except during the first stages of process start-up.
13. The diffusivities of compounds in the biolayer, are equal to the diffusivities of the same compounds in water, multiplied by a correction factor, $f(X_V)$, given by the correlation of Fan et al. (29).

For a case of n VOCs, the equations describing the process can be written as follows, when the assumptions above are considered.

In the biolayer, at a position h along the biofilter column:

$$f(X_V)D_{jw}\frac{d^2s_j}{dx^2} = \frac{X_V}{Y_j}\mu_j(s_O, s_1, \ldots, s_n); \qquad j = 1,\ldots,n \tag{7.1}$$

$$f(X_V)D_{ow}\frac{d^2s_O}{dx^2} = \sum_{j=1}^{n}\frac{X_V}{Y_{Oj}}\mu_j(s_O, s_1, \ldots, s_n) \tag{7.2}$$

with boundary conditions,

$$s_j = \frac{c_j}{m_j}, \qquad j = 1,\ldots,n \quad \text{and} \quad s_O = \frac{c_O}{m_O} \quad \text{at} \quad x = 0 \tag{7.3}$$

$$\frac{ds_O}{dx} = \frac{ds_j}{dx} = 0, \qquad j = 1,\ldots,n \quad \text{at} \quad x = \delta \tag{7.4}$$

Along the biofilter column, the following equations hold:

$$u_g\frac{dc_j}{dh} = A_S f(X_V)D_{jw}\left[\frac{ds_j}{dx}\right]_{x=0}; \qquad j = 1,\ldots,n \tag{7.5}$$

$$u_g\frac{dc_O}{dh} = A_S f(X_V)D_{ow}\left[\frac{ds_O}{dx}\right]_{x=0} \tag{7.6}$$

with boundary conditions,

$$c_O = c_{Oi} \quad \text{and} \quad c_j = c_{ji}, \qquad j = 1,\ldots,n \quad \text{at} \quad h = 0 \tag{7.7}$$

Depending on the particular mixture, the only things which change in equations (7.1) through (7.4), are the specific forms of expressions $\mu_j(s_O, s_1, \ldots, s_n)$, $j = 1,\ldots,n$. These kinetic expressions need to be known for the model equations to be solved.

7.2 Biofiltration of a Mixture of Two VOCs Involved in a Competitive Kinetic Interaction

In order to test the theory for biofiltration of VOC mixtures, it was decided to perform experiments with a mixture of benzene and toluene. These solvents are of particular interest since they are constituents of BTEX (benzene/toluene/ethyl-benzene/xylene) mixtures, which are frequently encountered in industrial operations, and in contaminated sites. Furthermore, this mixture was an obvious choice since, as discussed in Chapter 6, experiments were performed with each one of the two solvents individually for validation of the theory concerning biofiltration of single VOCs. Kinetic experiments, discussed in Chapter 5, have shown that simultaneous biodegradation of benzene and toluene follows inhibitory kinetics involving cross-inhibitory, competitive interaction. For this reason, the general equations (7.1) through (7.7) had to be written specifically for such kinetics, and for the mixture of interest.

7.2.1 Theory

The equations describing steady state biofiltration of benzene/toluene mixtures constitute a set of six differential equations. Three of them, equations (7.8) through (7.10), along with boundary conditions (7.11) and (7.12), describe mass balances for benzene, toluene, and oxygen in the biolayer at any cross-section of the biofilter column. The remaining three differential equations, (7.13) through (7.15), along with boundary conditions (7.16), describe mass balances for benzene, toluene, and oxygen in the gas phase (air) along the biofilter length. These equations are as follows.

$$f(X_V)D_{BW}\frac{d^2s_B}{dx^2} = \frac{X_V}{Y_B}\mu_B(s_B, s_T, s_O) \qquad (7.8)$$

$$f(X_V)D_{TW}\frac{d^2s_T}{dx^2}=\frac{X_V}{Y_T}\mu_T(s_B,s_T,s_O) \tag{7.9}$$

$$f(X_V)D_{OW}\frac{d^2s_O}{dx^2}=\frac{X_V}{Y_{OB}}\mu_B(s_B,s_T,s_O)+\frac{X_V}{Y_{OT}}\mu_T(s_B,s_T,s_O) \tag{7.10}$$

$$s_B=\frac{c_B}{m_B};\qquad s_T=\frac{c_T}{m_T};\qquad \text{and}\qquad s_O=\frac{c_O}{m_O}\qquad \text{at}\quad x=0 \tag{7.11}$$

$$\frac{ds_B}{dx}=\frac{ds_T}{dx}=\frac{ds_O}{dx}=0\qquad \text{at}\quad x=\delta \tag{7.12}$$

$$\frac{dc_B}{dh}=\frac{A_S f(X_V)D_{BW}S}{F}\left[\frac{ds_B}{dx}\right]_{x=0} \tag{7.13}$$

$$\frac{dc_T}{dh}=\frac{A_S f(X_V)D_{TW}S}{F}\left[\frac{ds_T}{dx}\right]_{x=0} \tag{7.14}$$

$$\frac{dc_O}{dh}=\frac{A_S f(X_V)D_{OW}S}{F}\left[\frac{ds_O}{dx}\right]_{x=0} \tag{7.15}$$

$$c_B=c_{Bi},\qquad c_T=c_{Ti},\qquad \text{and}\qquad c_O=c_{Oi}\qquad \text{at}\quad h=0 \tag{7.16}$$

The specific forms of the kinetic expressions $\mu_B(s_B,s_T,s_O)$, and $\mu_T(s_B,s_T,s_O)$ which appear in equations (7.8) through (7.10), are given as,

$$\mu_B(s_B,s_T,s_O)=\frac{\mu_B^{*}s_Bs_O}{(K_B+s_B+K_{BT}s_T)(K_O+s_O)} \tag{7.17}$$

$$\mu_T(s_B,s_T,s_O)=\frac{\mu_T^{*}s_Ts_O}{\left(K_T+s_T+\frac{s_T^2}{K_{IT}}+K_{TB}s_B\right)(K_O+s_O)} \tag{7.18}$$

Expression (7.17) involves four kinetic constants, while expression (7.18) involves five. The values of these kinetic constants have been determined as discussed in Chapter 5, and are listed in Table 7.1. The implication of expression (7.17) is that in the absence of toluene, and when oxygen is present at high, non-changing concentration levels, benzene is removed according to a Monod expression (44). Expression (7.18) implies that in the absence of benzene, and when oxygen does not affect the kinetics, toluene is removed according to an Andrews inhibitory expression (2). Parameters K_{BT} and K_{TB} indicate the interference of toluene and benzene, respectively, with the kinetics of benzene and toluene removal, respectively.

By introducing the following dimensionless quantities,

$$\theta = \frac{x}{\delta}, \qquad z = \frac{h}{H}, \qquad \bar{s}_B = \frac{s_B}{K_B}, \qquad \bar{s}_T = \frac{s_T}{K_T}, \qquad \bar{s}_O = \frac{s_O}{K_O}$$

$$\bar{c}_B = \frac{c_B}{c_{Bi}}, \qquad \bar{c}_T = \frac{c_T}{c_{Ti}}, \qquad \bar{c}_O = \frac{c_O}{c_{Oi}}, \qquad \varepsilon_B = \frac{c_{Bi}}{K_B m_B}$$

$$\varepsilon_T = \frac{c_{Ti}}{K_T m_T}, \quad \varepsilon_O = \frac{c_{Oi}}{K_O m_O}, \qquad \gamma = \frac{K_T}{K_{IT}}, \qquad \sigma_1 = \frac{K_{BT} K_T}{K_B}$$

$$\sigma_2 = \frac{K_{TB} K_B}{K_T}, \qquad \phi_1^2 = \frac{\mu_B^* X_V \delta^2}{D_{BW} f(X_V) K_B Y_B}, \qquad \phi_2^2 = \frac{\mu_T^* X_V \delta^2}{D_{TW} f(X_V) K_T Y_T}$$

$$\lambda_1 = \frac{D_{BW} K_B Y_B}{Y_{OW} K_O D_{OW}}, \quad \lambda_2 = \frac{D_{TW} K_T Y_T}{Y_{OT} K_O D_{OW}}$$

$$\eta = \frac{A_S f(X_V) D_{BW} H K_B}{u_g \delta c_{Bi}}, \qquad \omega_1 = \frac{K_T D_{TW} c_{Bi}}{K_B D_{BW} c_{Ti}}, \qquad \omega_2 = \frac{K_O D_{OW} c_{Bi}}{K_B D_{BW} c_{Oi}}$$

equations (7.8) through (7.18) can be written as,

$$\frac{d^2\bar{s}_B}{d\theta^2} = \phi_1^2 \frac{\bar{s}_B \bar{s}_O}{(1+\bar{s}_B+\sigma_1\bar{s}_T)(1+\bar{s}_O)} \tag{7.19}$$

$$\frac{d^2\bar{s}_T}{d\theta^2} = \phi_2^2 \frac{\bar{s}_T \bar{s}_O}{(1+\bar{s}_T+\gamma\bar{s}_T^{\,2}+\sigma_2\bar{s}_B)(1+\bar{s}_O)} \tag{7.20}$$

$$\frac{d^2\bar{s}_O}{d\theta^2} = \lambda_1\phi_1^2 \frac{\bar{s}_B \bar{s}_O}{(1+\bar{s}_B+\sigma_1\bar{s}_T)(1+\bar{s}_O)} + \lambda_2\phi_2^2 \frac{\bar{s}_T \bar{s}_O}{(1+\bar{s}_T+\gamma\bar{s}_T^{\,2}+\sigma_2\bar{s}_B)(1+\bar{s}_O)} \tag{7.21}$$

$$\bar{s}_B = \varepsilon_B\bar{c}_B; \quad \bar{s}_T = \varepsilon_T\bar{c}_T; \quad \bar{s}_O = \varepsilon_O\bar{c}_O \quad \text{at} \quad \theta = 0 \tag{7.22}$$

$$\frac{d\bar{s}_B}{d\theta} = \frac{d\bar{s}_T}{d\theta} = \frac{d\bar{s}_O}{d\theta} = 0 \quad \text{at} \quad \theta = 1 \tag{7.23}$$

$$\frac{d\bar{c}_B}{dz} = \eta\left[\frac{d\bar{s}_B}{d\theta}\right]_{\theta=0} \tag{7.24}$$

$$\frac{d\bar{c}_T}{dz} = \eta\omega_1\left[\frac{d\bar{s}_T}{d\theta}\right]_{\theta=0} \tag{7.25}$$

$$\frac{d\bar{c}_O}{dz} = \eta\omega_2\left[\frac{d\bar{s}_O}{d\theta}\right]_{\theta=0} \tag{7.26}$$

$$\bar{c}_B = \bar{c}_T = \bar{c}_O = 1 \quad \text{at} \quad z = 0 \tag{7.27}$$

Using equations (7.19) through (7.22), one can show that

$$\bar{s}_O = \lambda_1\left[\bar{s}_B(\theta) - \varepsilon_B\bar{c}_B\right] + \lambda_2\left[\bar{s}_T(\theta) - \varepsilon_T\bar{c}_T\right] + \varepsilon_O\bar{c}_O \tag{7.28}$$

Differentiating equation (7.28) with respect to θ, one gets

$$\frac{d\bar{s}_O}{d\theta} = \lambda_1 \frac{d\bar{s}_B}{d\theta} + \lambda_2 \frac{d\bar{s}_T}{d\theta} \tag{7.29}$$

Using equations (7.24) through (7.27), along with equation (7.29), one can show that

$$\bar{c}_O(z) = \lambda_1 \omega_2 \left(\bar{c}_B(z) - 1\right) + \frac{\lambda_2 \omega_2}{\omega_1}\left(\bar{c}_T(z) - 1\right) + 1 \tag{7.30}$$

Finally, equations (7.28) and (7.30), lead to

$$\bar{s}_O(\theta) = \lambda_1 \bar{s}_B(\theta) + \lambda_2 \bar{s}_T(\theta) + \lambda_1(\varepsilon_O \omega_2 - \varepsilon_B)\bar{c}_B(z) + \lambda_2\left[\frac{\varepsilon_O \omega_2}{\omega_1} - \varepsilon_T\right]\bar{c}_T(z)$$

$$-\varepsilon_O\left[\lambda_1 \omega_2 + \frac{\lambda_2 \omega_2}{\omega_1} - 1\right] \tag{7.31}$$

Equations (7.30) and (7.31), allow for a reduction of the original 6-dimensional system of differential equations, to a system of dimension 4. This is done by keeping differential equations (7.19), (7.20), (7.24), and (7.25), along with those conditions in (7.22), (7.23), and (7.27) which refer to benzene and toluene only. In the differential equations which are kept, and in their boundary conditions, $\bar{s}_O$ should be substituted for by the right-hand side of equation (7.31), and $\bar{c}_O$ by the right-hand side of equation (7.30). The physical meaning of this dimensional reduction is that stoichiometric relations among benzene, toluene, and oxygen are always valid while mathematically, it means that the solutions of the original differential equations are always found on a hyperplane of

dimension 4 in the 6-dimensional space. This dimensional reduction greatly facilitates the numerical work needed for solving the model equations.

7.2.2 Numerical Methodology

In order to solve equations (7.19), (7.20), (7.24), and (7.25), along with the appropriate boundary conditions, a computer code was generated and is given as Appendix B of this dissertation. The code is based on the use of the method of orthogonal collocation (30, 76) (for the biolayer), and the Runge-Kutta algorithm (for the gas phase).

The principles of the numerical methodology are as follows. Equations (7.19) and (7.20), for the biolayer are first solved at the entrance conditions ($z = 0$), where the values of gas phase concentrations are known through equations (7.27). The biolayer concentration profiles allow for determination of their slope at $\theta = 0$. These slopes are used for solving equations (7.24) and (7.25), to produce the gas phase concentrations at a position Δz from the entrance. At this position the biolayer equations are solved again and the procedure is repeated up to the point where a Δz increment leads to the exit position from the biofilter. The step in height (Δz) is equal to 0.01 thus, the procedure involves 100 iterations. At every point, the equations in the biolayer are solved by trial and error in order to determine δ. The value of δ is the position in the biolayer where either oxygen is depleted while benzene and/or toluene concentrations are still non-zero, or both benzene and toluene have been depleted while oxygen is still available.

7.2.3 Results and Discussion

Experiments with benzene/toluene mixtures were performed in a specially designed pilot-scale column. This column, as well as the experimental methodology, have been discussed in Chapter 4 of this thesis. During the experiments, the flowrate (or residence time) of the airstream was varied, as well as the absolute and relative composition of the inlet airstream regarding benzene and toluene. Each experiment, under a given set of conditions, lasted

for at least three weeks in order to reach steady state conditions. Experimental data showing the behavior of the pilot-scale unit during start-up under a given set of experimental conditions is shown in Figure 7.1.

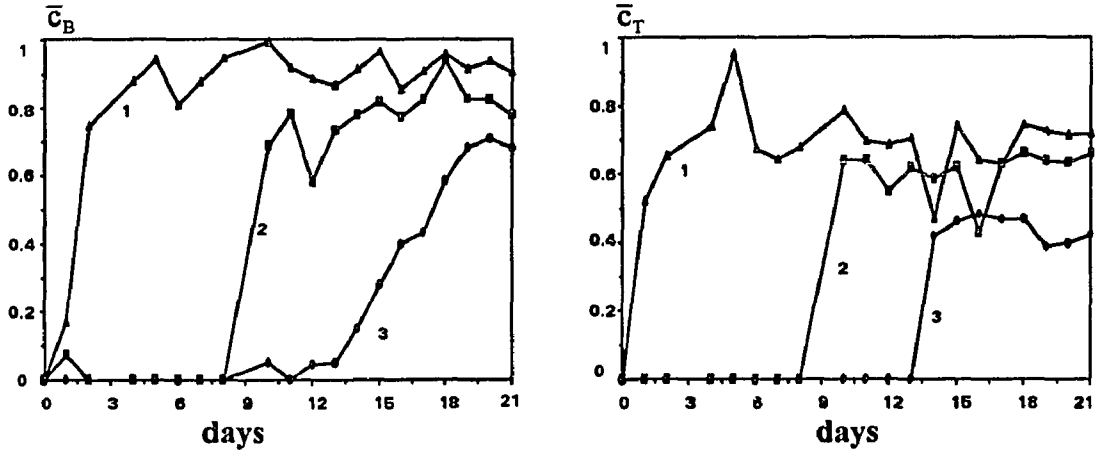

Figure 7.1 Transient data from the start-up of the pilot-scale biofilter unit when c_{Bi} = 0.367 gm^{-3}, c_{Ti} = 0.225 gm^{-3}, τ = 3.1 min, V_P = 15,291 cm^3. Concentration data for benzene (left), and toluene (right), from the exit of the first, second, and third segment of the unit (curves 1, 2, and 3, respectively). The concentrations have been made dimensionless by dividing actual values with their corresponding value at the inlet.

The experimental results were compared to the theoretical predictions obtained by solving the model equations. Model parameters which were not measured, were estimated as explained in Chapter 8, with one exception. In the case of mixtures no fitting approach was used in estimating the specific biolayer surface area (A_S). Since the pilot-scale column was in many ways similar to the intermediate-scale columns used in the experiments with either benzene, or toluene (see Chapter 6), it was decided to use the value of A_S determined for the intermediate columns. As discussed in Chapter 6, the value of A_S was different for the benzene case, and the toluene case. Because of assumption 11, stated in section 7.1, the value of A_{ST} was used as A_S for the mixture. The value of A_{ST} is larger than that of A_{SB}, and the rationale for using the larger of the two was the following. Toluene is biodegraded easier than benzene. As a result, during the initial stages of

toluene biofiltration, the consortium develops on the packing material more than when benzene is passed through the column; this is why A_{ST} is larger than A_{SB}. When a mixture of benzene and toluene is passed through the column, the consortium develops on the packing as in the case where it is exposed to the preferred substrate (toluene) only. If it is a stable consortium (and this is the assumption made), then benzene and toluene degraders are found at any point in the column where a biolayer has been formed, so the larger of the A_S values should be valid. It should be mentioned that due to the inhibition exerted from benzene on toluene, the value of A_S may be lower than that of A_{ST}. On the other hand, as discussed in Chapter 5, the influence of benzene on toluene is not so severe; for this reason, and since no better estimate was available, a value of 40 m^{-1} was used as A_S for the case of the pilot column. The entire list of model parameter values used in solving the model equations, is given in Table 7.1.

Table 7.2 lists experimental conditions, and experimentally obtained exit concentrations and removal rates for benzene and toluene. On the same table, the model predicted values for the same quantities are also shown along with the percent error between experimental and predicted values. The agreement between theory and experiments is very good, especially when one takes into account the complexity of the process. It should be mentioned that in some cases, the discrepancy between experimentally obtained and model predicted removal rates appears to be very substantial. Nonetheless, this is really an artifact due to the small removal rate values involved in the calculations. In fact, a close look at the experimentally obtained and model predicted exit concentration values will convince the reader that the model is really doing an almost perfect job in practically all cases.

Comparisons between experimental and model predicted values which are reported in Table 7.2 refer to the conditions at the exit of the unit. Comparisons can be also made for other locations along the unit where actual measurements were made.

Table 7.1 Parameter values used for solving the model equations for the case of benzene-toluene mixtures.

Parameter	Value	Units
A_S	40.0	m^{-1}
c_{Oi}	275.0×10^{-3}	kg m^{-3}
D_{BW}	1.04×10^{-9}	m^2 s^{-1}
D_{OW}	2.41×10^{-9}	m^2 s^{-1}
D_{TW}	1.03×10^{-9}	m^2 s^{-1}
$f(X_V)$	0.195	--
K_B	12.22	g m^{-3}
K_{BT}	4.50	--
K_{IT}	78.94	g m^{-3}
K_{OB}	0.26	g m^{-3}
K_{OT}	0.26	g m^{-3}
K_T	11.03	g m^{-3}
K_{TB}	0.20	--
m_B	0.23	--
m_O	34.4	--
m_T	0.27	--
S	1.82×10^{-2}	m^2
X_v	100.0	kg m^{-3}
Y_B	0.708	kg kg^{-1}
Y_{OB}	0.336	kg kg^{-1}
Y_{OT}	0.341	kg kg^{-1}
Y_T	0.708	kg kg^{-1}
$\dot{\mu_B}$	0.68	h^{-1}
$\dot{\mu_T}$	1.50	h^{-1}

Table 7.2 Steady state biofiltration of benzene-toluene mixtures: Experimental data and model predictions.

τ	j	c_{ji}	$c_{je,1}$	$c_{je,2}$	E_1	R_1	R_2	E_2
(min)			[a](gm^{-3})		(%)	($g\ m^{-3}$-pack.h^{-1})		(%)
0.9[b]	B	0.162	0.146	0.136	-6.8	1.1	1.7	54.5
	T	0.515	0.300	0.399	33.0	14.3	7.7	-46.2
1.0	B	0.130	0.108	0.105	-2.8	1.3	1.5	15.4
	T	0.212	0.169	0.157	-7.1	2.6	3.3	26.9
1.3	B	0.205	0.164	0.160	-2.4	1.9	2.1	10.5
	T	0.403	0.267	0.283	6.0	6.3	5.5	-12.7
1.4	B	0.165	0.130	0.125	-3.8	1.5	1.7	13.3
	T	0.382	0.239	0.258	7.9	6.1	5.3	-13.1
1.5	B	0.194	0.149	0.143	-4.0	1.8	2.0	11.11
	T	0.272	0.186	0.177	-4.8	3.4	3.7	8.8
2.0	B	0.150	0.119	0.099	-16.8	0.9	1.5	66.7
	T	0.298	0.158	0.167	5.7	4.2	3.9	-7.1
3.1	B	0.367	0.186	0.194	4.3	3.5	3.3	-5.7
	T	0.225	0.102	0.092	-9.8	2.4	2.6	8.3

[a]Concentrations in gm^{-3} can be converted to ppm (mg of compound kg^{-1} air) if they are multiplied by a factor of 854.7; [b]Volume of packing material used for this set of data is 5,097 cm^3, and for all other sets, 15,291 cm^3; τ : residence time; j : compounds, B-benzene and T-toluene; c_{ji} : inlet benzene/toluene concentration; $c_{je,1}$, $c_{je,2}$: exit benzene/toluene concentrations, experimental and predicted, respectively; E_1 : percent error in exit concentration defined as $(c_{je,2} - c_{je,1}) / c_{je,1} x100$; R_1 and R_2 : removal rates based, respectively, on experimental and model values; E_2 : percent error in removal rate defined as $(R_2 - R_1) / R_1 x100$.

Two such examples are shown in Figure 7.2. From the graphs, one can see that the agreement between theory and experimental data is excellent for benzene, and quite good for toluene. It should be mentioned that although the concentration profiles shown

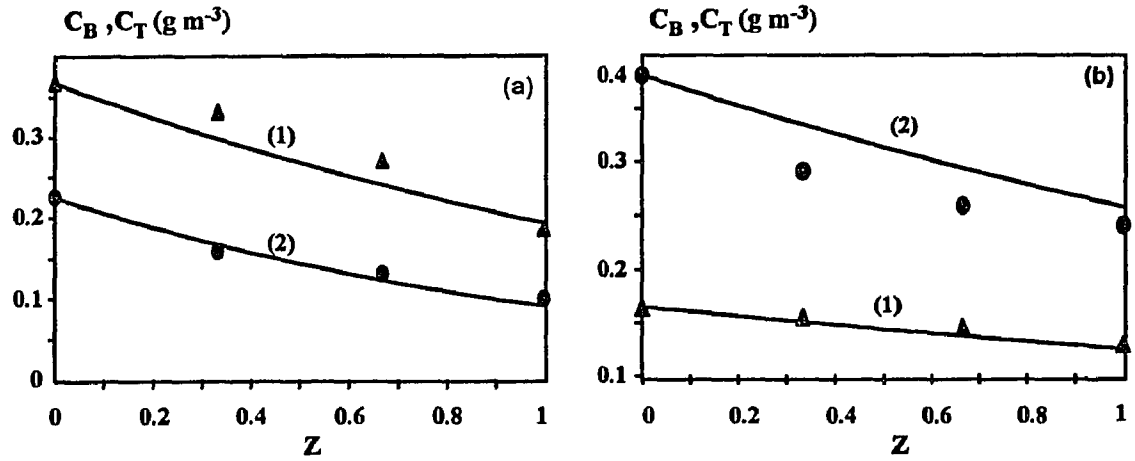

Figure 7.2 Concentration profiles of benzene (curves 1), and toluene (curves 2) along the biofilter are compared with experimental points at the entrance of the column and the exits of each one of its three sections. The experimental conditions for graph (a) are c_{Bi} = 0.367 gm^{-3}, c_{Ti} = 0.225 gm^{-3}, τ = 3.1 min; for graph (b), c_{Bi} = 0.165 gm^{-3}, c_{Ti} = 0.382 gm^{-3}, τ = 1.4 min; in all cases, V_P = 15,291 cm^3.

in Figure 7.2 look as being almost perfectly linear, computer simulations have shown that this is not the case for other values of inlet benzene and toluene concentrations.

Typical concentration profiles in the biolayer, predicted by the model, are shown in Figure 7.3. As in the case of individual benzene or toluene vapor biofiltration (see Chapter 6), it is predicted that the VOCs are depleted much before oxygen is. In the particular example shown in Figure 7.3, benzene and toluene are depleted at almost exactly the same location in the biolayer. Higher benzene and/or toluene concentrations in the air would result in a reversal of the order in which oxygen and VOCs are depleted in the biolayer. Such high concentrations though, are unlikely to happen for these particular solvents, at least in cases of usual emissions.

The fact that oxygen concentration does not appear to drop a lot within the biolayer, does not necessarily imply that the oxygen factor is not important for the biofiltration of benzene/toluene mixtures. This was concluded from simulation studies on

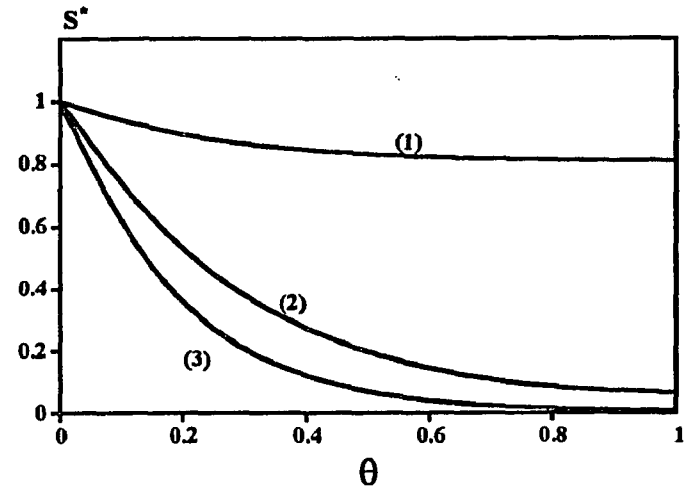

Figure 7.3 Model predicted concentration profiles in the biolayer at the middle point of a biofilter operating under the conditions of the experiment shown in Figure 7.2a. Curves 1, 2, and 3 are for oxygen, benzene, and toluene, respectively.

the sensitivity of the model to parameters K_O and c_{Oi}. The results of these studies are shown in graphical form in Figure 7.4, and indicate that K_O, in particular, may have a considerable impact on the removal rate. In fact, it is predicted that if the value of K_O is an order of magnitude higher than the one valid for the culture used in the experiments reported here, the removal rate may be 15% less than what was obtained during the experiment used as a basis for the these calculations (reference point (1,1) in the graph). This suggests that microbial culture selection should not only be based on its ability to remove VOCs, but also on the affinity of the culture for oxygen.

One of important differences between the model proposed here, and the one used by some researchers as discussed in Chapter 2, is the fact that kinetic interactions are taken into account. In order to further investigate the impact of cross-inhibition on the removal rate, computer simulation studies were performed for the sensitivity of the model to the interaction constants K_{BT} and K_{TB}. The results of these studies are shown in Figure 7.5.

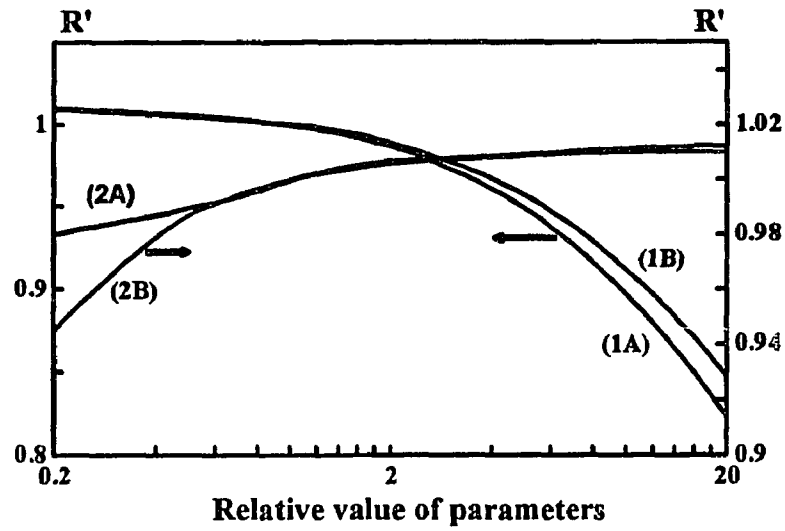

Figure 7.4 Model sensitivity studies on the effect of oxygen on the removal rate. Curves 1A and 1B are for benzene and toluene, respectively, and indicate the effect of kinetic constant K_O. Curves 2A and 2B are for benzene and toluene, respectively, and indicate the effect of the inlet air oxygen concentration on the removal rate. R' is the relative removal rate with respect to the experimental conditions. Conditions are those of Figure 7.2a, and the (1,1) point represents removal of 3.3 g-benzene and 2.6 g-toluene m^{-3}-packing h^{-1}.

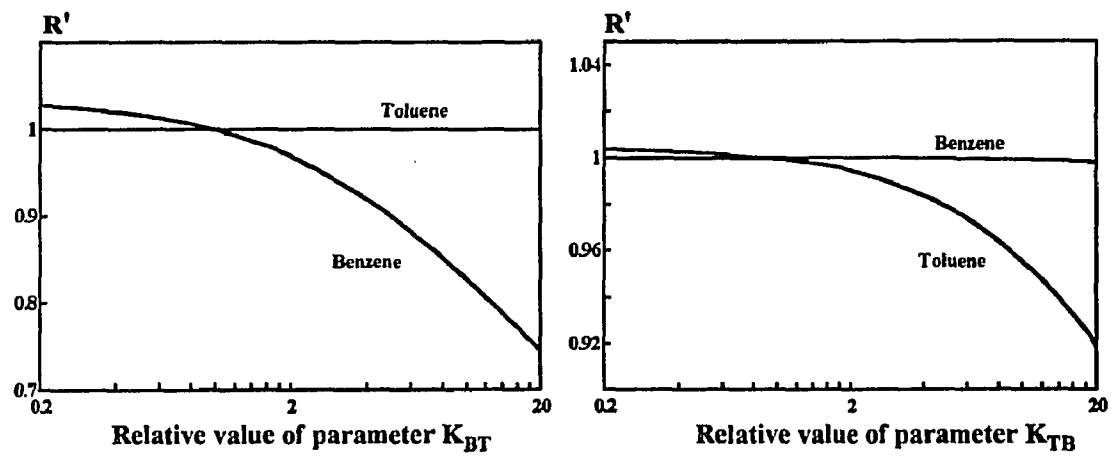

Figure 7.5 Sensitivity studies on the effect of the kinetic interaction constants K_{BT} (left) and K_{TB} (right), on the removal rate of benzene and toluene vapors. R' is the relative removal rate with respect to the experimental conditions as in Figure 7.2a.

The results of these studies indicate that the removal rate of benzene is much more sensitive to the presence of toluene, than the removal of toluene is to the presence to benzene. An order of magnitude increase in the interference parameter K_{BT} can make an almost 30% difference (decrease) in the removal rate of benzene. On the other hand, an order of magnitude increase in K_{TB} can make an almost 10% difference (decrease) in the removal rate of toluene. Clearly, these interaction parameters can have a significant impact on the removal rates and thus, they should not be neglected.

The results of the study reported in this chapter lead to the conclusion that the proposed model can very nicely describe biofiltration of benzene/toluene mixtures under various operating conditions. The fact that the model was validated in a relatively large scale unit, suggests that the proposed theory, and the equations associated with it, can be used with a good amount of confidence in designing actual units.

CHAPTER 8

TRANSIENT BIOFILTRATION OF SINGLE VOCs

In practice, a biofilter often experiences fluctuations in the inlet gas concentration of the VOCs, flow rate, discontinuity of the process due to shut down, etc. Hence, it is very important to have mathematical tools to study the response of biofilters to the variations of these parameters. As discussed in Chapter 2, some experimental studies (72, 80), have been performed to test the operational stability of biofilters. However except for the just published work of Deshusses and Dunn (16), there is absolutely no study published in the literature on modeling the biofiltration process under transient conditions. In this chapter, a detailed model is developed for the case where a single VOC is treated via biofiltration under transient conditions. At the limit, i.e., when the transients decay, this model reduces to the steady-state one discussed in Chapter 6. The model equations have been solved, and the predictions tested against toluene biofiltration data under transient conditions. These data were obtained from the experiments with toluene discussed -but not used or analyzed- in Chapter 6.

8.1 Development of the Mathematical Model

In most cases, a model which describes a process under steady-state conditions can be easily extended to describe the same process under transient conditions by introducing accumulation terms. Biofiltration is an example of cases where such simple extensions are not possible. The first problem is that some amounts of VOCs are physically adsorbed on the packing material. Under steady state conditions, the adsorption process is in equilibrium and thus, it does not need to be taken into consideration in the steady-state

model derivation. Under transient conditions though, equilibrium conditions are not valid and the adsorption process needs to be explicitly accounted for in the model derivation. The second problem is even more complex, and has to deal with process start-up. During start-up of a biofilter unit, the formation of biolayers around solid particles has not been completed. Some biomass accumulation does occur, and this is why one experimentally measures a pressure drop at the very beginning of experiments performed immediately after column inoculation. During this period, as the actual biolayer is still in formation, its thickness varies. Bare parts of particle surface area get covered with biomass during this period, and such phenomena cannot easily be described.

The transient model proposed here would be really applicable only for transitions from one set of operating conditions to another, and cannot describe the very first start-up of a biofilter unit.

The assumptions made in deriving the model are as follows.

1. The biolayer is formed on the exterior surface of the particles. Biomass does not grow in the pores of the particles and thus, no reaction occurs in the pores.
2. The biolayer is not uniformly formed around particles. In actuality, there are patches of biofilm on the solids, leaving the bare surface of the solids in direct contact with the airstream.
3. Adsorption of VOCs on the solid particles occurs only through the direct bare solid/air interface. Adsorption does not occur on the biofilm.
4. Oxygen does not get adsorbed on the solid particles.
5. The thickness of the biolayer is small relative to the main curvature of the solid particle and thus, planar geometry can be used.

6. The extent of the biofilm patch is much larger than its depth. Hence, VOCs and oxygen transported into the biolayer through the side surfaces of the biofilm patch can be neglected, and diffusion/reaction in the biofilm can be considered in a single direction only.
7. Adsorption is a reversible process and its characteristics are determined through the adsorption isotherms.
8. VOCs and oxygen at the biolayer/air interface are always in equilibrium which is dictated by Henry's law. The distribution coefficients are the same as if the biolayer was made of water only.
9. VOCs and/or oxygen are depleted in a fraction of the actual biolayer.
10. Diffusivities of VOCs and oxygen in the biolayer are equal to the diffusivities of the same compounds in water, corrected by a factor depending on the biofilm density according to the expression of Fan et al. (28).
11. The biofilm density is constant.
12. There is no accumulation of biomass in the filter bed thus, the specific biolayer surface area is constant.
13. Biodegradation rates depend on the concentrations of VOCs and oxygen, and their functional forms can be determined from suspended culture experiments.
14. The airstream passes through the biofilter bed in plug flow.

As can be seen from Chapters 6 and 7, some of the assumptions above are also made in deriving the steady state models. Furthermore, it is because of assumptions 9 and 12 that the model described here cannot be valid under start-up conditions of a biofilter unit.

A schematic of the model concept, especially as it relates to assumptions 1, 2, 3, 5, and 6, is shown in Figure 8.1.

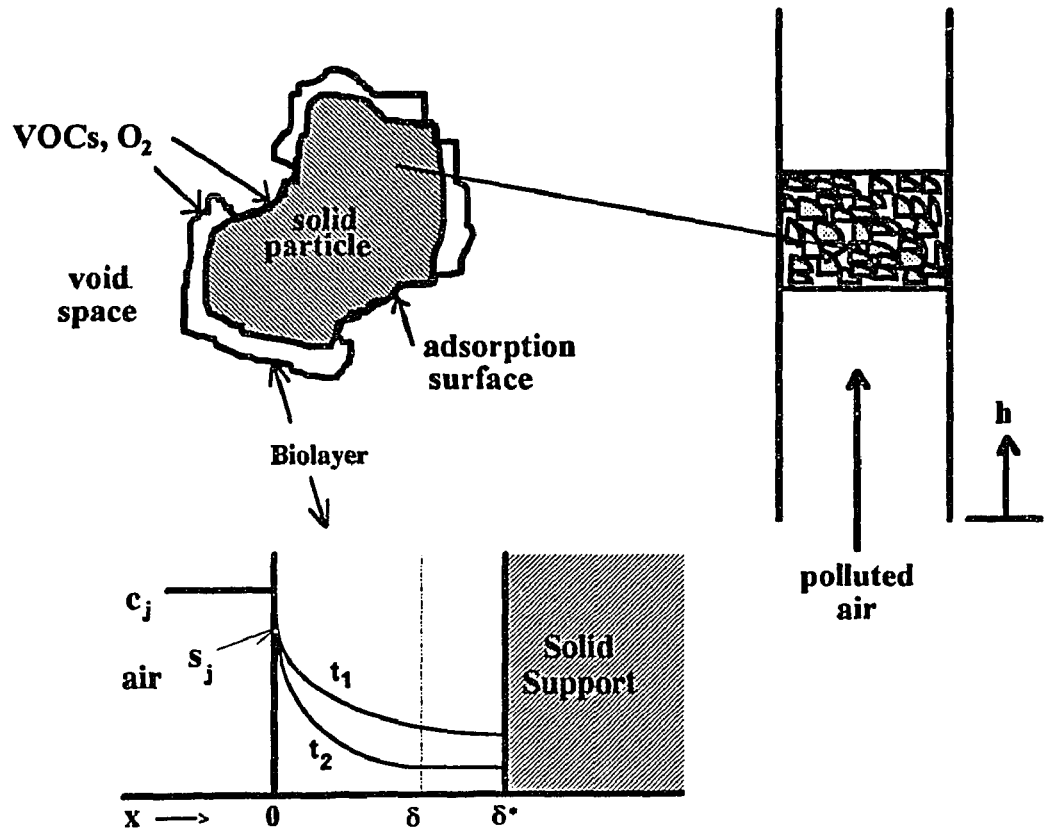

Figure 8.1 Model concept for description of biofiltration under transient conditions. Only part of the surface area is covered with biolayer. VOCs transferred to the biofilm undergo degradation. VOCs are also reversibly adsorbed on the solid packing through the bare surface of the particles.

Considering an airstream carrying vapor of a single pollutant j, the model equations can be written as follows under the assumptions above.

I. Mass balances in the biofilm :

$$\frac{\partial s_j}{\partial t} = f(X_v) D_{jw} \frac{\partial^2 s_j}{\partial x^2} - \frac{X_v}{Y_j} \mu_j(s_j, s_o) \tag{8.1}$$

$$\frac{\partial s_o}{\partial t} = f(X_v) D_{ow} \frac{\partial^2 s_o}{\partial x^2} - \frac{X_v}{Y_o} \mu_j(s_j, s_o) \tag{8.2}$$

with initial and boundary conditions,

$$t = 0,\ h = 0,\ x = 0: \qquad s_j = \frac{c_{ji,0}}{m_j} \qquad s_o = \frac{c_{oi,0}}{m_o} \tag{8.3}$$

$$t = 0,\ 0 < h \le H,\ x = 0: \qquad s_j = \frac{c_{j,0}(h)}{m_j} \qquad s_o = \frac{c_{o,0}(h)}{m_o} \tag{8.4}$$

$$t = 0,\ 0 < x \le \delta: \qquad s_j = s_{j,0}(x) \qquad s_o = s_{o,0}(x) \tag{8.5}$$

$$0 < t < \tau \qquad h > u_g t \qquad x = 0 \qquad s_j = \frac{c_{j,0}(h)}{m_j} \qquad s_o = \frac{c_{o,0}(h)}{m_o} \tag{8.6a}$$

$$0 < t < \tau \qquad 0 < h < u_g t \qquad x = 0 \qquad s_j = \frac{c_j(h)}{m_j} \qquad s_o = \frac{c_o(h)}{m_o} \tag{8.6b}$$

$$t > \tau \qquad h > 0 \qquad x = 0 \qquad s_j = \frac{c_j(h)}{m_j} \qquad s_o = \frac{c_o(h)}{m_o} \tag{8.6}$$

$$t > 0 \qquad h > 0 \qquad x = \delta \qquad \frac{\partial s_j}{\partial x} = 0 \qquad \frac{\partial s_o}{\partial x} = 0 \tag{8.7}$$

II. Mass balances in the gas phase

$$\upsilon \frac{\partial c_j}{\partial t} = -u_g \frac{\partial c_j}{\partial h} + D_{jw} f(X_v) \alpha A_s^* \left(\frac{\partial s_j}{\partial x} \right)_{x=0} - k_a (1-\alpha) A_s^* \left(c_j - c_j^* \right) \tag{8.8}$$

$$\upsilon \frac{\partial c_o}{\partial t} = -u_g \frac{\partial c_o}{\partial h} + D_{ow} f(X_v) \alpha A_s^* \left(\frac{\partial s_o}{\partial x} \right)_{x=0} \tag{8.9}$$

with initial and boundary conditions,

$$t = 0, \quad h = 0 \qquad c_j = c_{ji,o} \qquad c_o = c_{oi,o} \tag{8.10}$$

$$t = 0 \quad 0 < h \le H \qquad c_j = c_{j,0}(h) \qquad c_o = c_{o,0}(h) \tag{8.11}$$

$$t > 0 \quad h = 0 \qquad c_j = c_{ji} \qquad c_o = c_{oi} \tag{8.12}$$

III. Mass balance in the solid phase (particles)

$$(1-\upsilon)\rho_p \frac{\partial c_{jP}}{\partial t} = k_a(1-\alpha)A_S^*\left(c_j - c_j^*\right) \tag{8.13}$$

with initial condition

$$t = 0, h \ge 0, \quad c_{jp} = c_{jp,0}(h) \tag{8.14}$$

When biodegradation of pollutant j follows Andrews (2), kinetics under excess oxygen conditions, and when under both substrate (VOC j), and oxygen limiting conditions the reaction rate can be expressed through an interactive model (5), then the expression of $\mu_j(s_j, s_o)$, which appears in equations (8.1) and (8.2), is

$$\mu_j\left(s_j, s_o\right) = \frac{\mu_j^* s_j}{K_j + s_j + \dfrac{s_j^2}{K_{Ij}}} \frac{s_o}{K_{oj} + s_o} \tag{8.15}$$

When the adsorption isotherm of pollutant j on the solid packing can be described by the Freundlich equation (57), one can write,

$$c_{jp} = k_d \left(c_j^*\right)^n \tag{8.16}$$

Usually, transients of the biofiltration process last very long (even days), while the space time (τ) is in the order of minutes. For this reason, and without any loss of accuracy, one can omit equations (8.6a) and (8.6b), and use equation (8.6) for any $t > 0$ rather than for $t > \tau$ only.

Equations (8.1), (8.2), (8.8), (8.9), and (8.13), along with their initial and boundary conditions constitute a system of coupled partial differential equations in three directions (time, biolayer, bed height), the dynamical dimensionality of which is 5. Solving a system of coupled PDEs is something which is very involved. For this reason, and as the proposed model is the first of its kind, it was decided to simplify it as discussed in the next section.

8.1.1 Simplification of the model

In cases where reaction and diffusion is involved, the notion of effectiveness factor (e), can be introduced as follows (40, 71).

$$e = \frac{\text{amount of a reactant consumed after been transferred into the biofilm via diffusion}}{\text{amount of the reactant consumed under no diffusional limitations}} \tag{8.17}$$

Using definition (8.17), for the cases of VOC j and oxygen, one can write,

$$e_j = \frac{f(X_v) D_{jW} \left(\frac{\partial s_j}{\partial x}\right)_{x=0}}{\delta \frac{X_v}{Y_j} \left[\mu_j(s_j, s_o)\right]_{x=0}} \tag{8.18}$$

$$e_O = \frac{f(X_V)D_{ow}\left(\frac{\partial s_O}{\partial x}\right)_{x=0}}{\delta\frac{X_V}{Y_{Oj}}\left[\mu_j(s_j,s_O)\right]_{x=0}} \tag{8.19}$$

The importance of the effectiveness factors is that they permit omission of equations (8.1) and (8.2). Taking this into account, and after introducing the dimensionless quantities,

$$\bar{c}_j = \frac{c_j}{c_{ji}} \qquad \bar{c}_j^* = \frac{c_j^*}{c_{ji}} \qquad \bar{c}_O = \frac{c_O}{c_{Oi}} \qquad \bar{c}_{jp} = \frac{(1-\upsilon)\rho_p c_{jp}}{\upsilon c_{ji}} \qquad z = \frac{h}{H}$$

$$\theta = \frac{x}{\delta} \qquad \zeta = \frac{u_g t}{H} \qquad \varepsilon_1 = \frac{c_{ji}}{m_j K_j} \qquad \varepsilon_2 = \frac{c_{Oi}}{m_O K_O} \qquad \gamma = \frac{K_j}{K_{1j}}$$

$$\beta_1 = \frac{e_j\alpha\delta A_S^* X_V H\mu^*}{Y_j u_g c_{ji}\upsilon} \qquad \beta_2 = \frac{e_O\alpha\delta A_S^* X_V H\mu^*}{Y_O u_g c_{Oi}\upsilon}$$

$$\beta_3 = \frac{k_a(1-\alpha)A_S^* H}{u_g\upsilon} \qquad \psi = \frac{1}{c_{ji}}\left[\frac{\upsilon c_{ji}}{(1-\upsilon)\rho_P k_d}\right]^{\frac{1}{n}}$$

the model can be reduced to the following system of three differential equations, when Freundlich's isotherm is valid.

$$\frac{\partial\bar{c}_j}{\partial\zeta} = -\frac{1}{\upsilon}u_g\frac{\partial\bar{c}_j}{\partial z} - \beta_1 g(\bar{c}_j,\bar{c}_O) - \beta_3(\bar{c}_j - \bar{c}_j^*) \tag{8.20}$$

$$\frac{\partial\bar{c}_O}{\partial\zeta} = -\frac{1}{\upsilon}u_g\frac{\partial\bar{c}_O}{\partial z} - \beta_2 g(\bar{c}_j,\bar{c}_O) \tag{8.21}$$

$$\frac{\partial\bar{c}_{jp}}{\partial\zeta} = \beta_3(\bar{c}_j - \bar{c}_j^*) \tag{8.22}$$

where

$$g\left(\bar{c}_j, \bar{c}_O\right) = \frac{\varepsilon_1 \bar{c}_j}{\left(1 + \varepsilon_1 \bar{c}_j + \varepsilon_1^2 \gamma \bar{c}_j^2\right)} \frac{\varepsilon_2 \bar{c}_O}{\left(1 + \varepsilon_2 \bar{c}_O\right)} \tag{8.23}$$

and

$$\bar{c}_j^* = \psi\left(\bar{c}_{jp}\right)^{\frac{1}{n}} \tag{8.24}$$

The initial and boundary conditions for equations (8.20) through (8.22) are as follows.

$$\text{at } \zeta = 0 \text{ and } z = 0: \quad \bar{c}_j = 1 \qquad \bar{c}_O = 1 \qquad \bar{c}_{jp} = \bar{c}_{jp,0}(0) \tag{8.25}$$

$$\text{at } \zeta = 0 \text{ and } 0 < z \le 1: \quad \bar{c}_j = \bar{c}_{j,0}(z) \quad \bar{c}_O = \bar{c}_{O,0}(z) \quad \bar{c}_{jp} = \bar{c}_{jp,0}(z) \tag{8.26}$$

$$\zeta \ge 0 \text{ and } z = 0: \quad \bar{c}_j = 1 \qquad \bar{c}_O = 1 \tag{8.27}$$

8.2 Numerical Methodology

By looking at equations (8.20) through (8.22), one could expect that they constitute a system of PDEs which should be easy to solve. One could for example, use a finite differences approach in the z-direction, and then solve the resulting system of ordinary differential equations through a Runge-Kutta algorithm, or any other ODE-solver available in software packages such as IMSL (International Mathematical Software Library). Codes based on this approach were generated, but failed to produce results. The reason was that expression (8.23) for the biodegradation kinetics makes the problem stiff from the

numerical point of view. The problem was resolved by using ODESSA (Ordinary Differential Equation Solver with explicitly Simultaneous Sensitivity Analysis). ODESSA is a subroutine within the AUTO software package (23). A computer code was developed, and is offered as Appendix C of this dissertation. The code is based on finite differences in the z-direction, and integration of the resulting system of ODEs. If twenty points are used for discretizing z (from z = 0 to z = 1), ODESSA solves a system of sixty simultaneous differential equations. An indication of the stiffness of the problem is the fact that one needs to select within ODESSA the option for highest stiffness [MF = 21, this option requires supplying the Jacobian matrix of the ODE system; with 20 points in the z-direction, the Jacobian is a 60x60 matrix]. With this option, convergence was always obtained, even when the error tolerance was set to as low as 10^{-12}.

8.3 Determination of Model Parameters

Kinetic parameters, distribution coefficients, yield coefficients, diffusivities, biofilm density can be either measured, or estimated as discussed in Chapters 5, 6 and 7. Parameters which appear only in the transient model, were either measured or estimated as follows.

The first problem is that the effective biolayer thickness, δ, and the effectiveness factors e_j and e_O are not constant. The value of δ varies along the biofilter column. The values of effectiveness factors depend on δ, as well as on the concentrations of oxygen and the VOC at any particular location. One can then use the following approach : use the steady state version of the problem (Chapter 6), and solve the equations for various inlet VOC concentrations in the range of interest; since these equations yield values for concentrations, as well as for δ, try to find a simple correlation between the gas phase concentration of the pollutant and the quantities of interest (δ, e_j, e_O). For the case of toluene, it was found that these correlations are simple linear expressions (see Table 8.1).

This approach disregards the fact that δ may be time dependent. However, this seems to be a reasonable assumption since, as discussed in Chapter 6 in conjunction with the study on methanol, the time scale of events in the biolayer is order of magnitudes smaller than that in the gas phase.

The parameters involved in the adsorption isotherm (k_d and n, in the case of Freundlich's isotherm), can be determined from independent kinetic experiments. For the case of toluene, experiments were performed using the methodology described in Chapter 4. The results of these experiments are shown in Figure 8.2. From this figure it appears as if there is a perfectly linear relationship between c_{jP} and c_j^*. In reality, when the data are plotted on a logarithmic scale, as suggested by equation (8.16), they yield a value of n = 1.04.

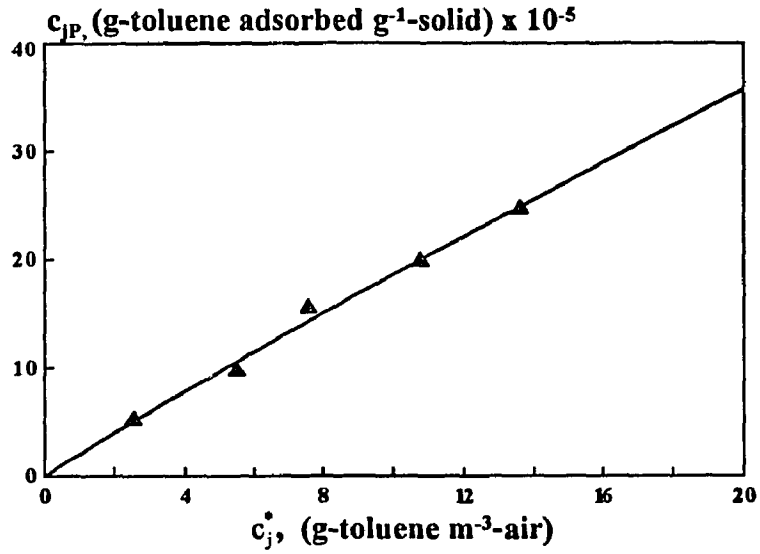

Figure 8.2 Adsorption isotherm of toluene on a peat/perlite mixture (2:3 volume ratio). Symbols represent experimental points. The curve represents a fit of the data to the Freundlich isotherm.

Porosity of the bed was taken from a reported value (52), as 0.3. The fraction of the external surface area of particles which is covered by biofilm (α) is extremely hard to

estimate. In this study, the following crude assumption was made. Since before packing the column, an amount of thick suspension of volume V_1 was mixed with the packing material of volume V_2, and $V_1:V_2 = 0.3$, a value of $\alpha = 0.3$ was used. Having the value of α, one can estimate A_S^* as A_S / α, where A_S is the value obtained from steady state data as explained in Chapter 6.

Regarding the mass transfer coefficient (k_a), there is a correlation available in the literature for packed-beds (36). This correlation is a function of the flow conditions, and characteristics of the particles (density, size etc.). The type of packing materials used in the present study had a wide size distribution. For this reason, an average particle size (2 mm) was first assumed, and a value of k_a was obtained. This value was used as an initial guess in the following procedure. Data from one experimental run were fitted to the solution of equations (8.20) through (8.22) by varying the value of k_a. The objective was to not only get a good fit of the transient data, but to also converge (at large times) to the steady state solution predicted by the steady-state model discussed in Chapter 6. This fitted value of k_a was subsequently used unchanged, in predicting the transient data in all other experiments.

The entire list of model parameter values used in analyzing the transient toluene biofiltration data is given in Table 8.1.

8.4 Results and Discussion

As mentioned earlier, transient data from toluene biofiltraion experiments were used for validating the model. These are the same experiments which were discussed in Chapter 6 in conjunction with steady-state performance. Data from one experiment were originally used for determining the value of the mass transfer coefficient following the methodology described in the preceding section. This value is given in Table 8.1. The data from the exit of the column, and from a location along the bed at one third of the

column height are shown in the Figure 8.3. In the same figure the curves which were generated through the fitting approach discussed earlier, are also shown. As can be seen

Table 8.1 Parameter values used for solving the transient model equations.

Parameter	Value	Units
A_s^*	133.3	m^{-1}
c_{Oi}	275.0×10^{-3}	kg m^{-3}
D_{OW}	2.41×10^{-9}	m^2 s^{-1}
D_{TW}	1.03×10^{-9}	m^2 s^{-1}
$f(X_V)$	0.195	--
k_a	6.04×10^{-3}	m h^{-1}
k_d	2.25×10^{-5}	g/g-particle
K_{IT}	78.94	g m^{-3}
K_O	0.26	g m^{-3}
K_T	11.03	g m^{-3}
m_O	34.4	--
m_T	0.27	--
n	1.04	--
V_P	5.15×10^{-3}	m^3
X_v	100.0	kg m^{-3}
Y_{OT}	0.341	kg kg^{-1}
Y_T	0.708	kg kg^{-1}
α	0.3	--
δ	$1.5c_j+33.4$	μm (c_j in g m^{-3})
e_T or e_O	$0.03c_j+0.2$	(c_j in g m^{-3})
υ	0.3	--
ρ_P	4.28×10^5	g m^{-3}
μ_T^*	1.50	h^{-1}

from the graph, the agreement between the data and model predictions at 1/3 of the column height (curve a) is very good, while at the exit of the column the agreement is not great. This should not be surprising if one considers the fact that during the fitting approach, the objective was to not only minimize the error between data and predictions at all sampling points, but also get a fit which at large times predicts the same concentration along the column as the steady state model does. The steady state profile for the same experimental set is shown in Figure 6.14. As one can see from that graph, the agreement between predicted and experimentally measured toluene concentrations is very good at the 1/3-height sampling point, but not very good at the exit. The same thing happens for the transient behavior shown in Figure 8.3.

Once the value of k_a was determined from the experimental set shown in Figure 8.3, it was kept constant; thus, the remaining figures in this chapter show curves representing model predictions based on the model parameter values shown in Table 8.1 No fitting, or correction procedure was used.

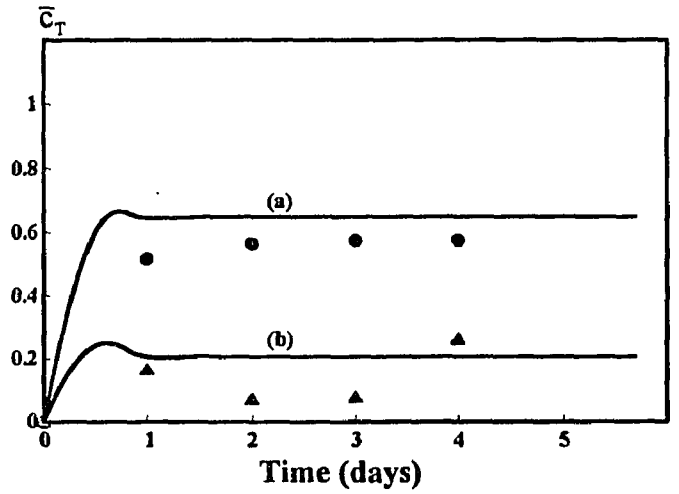

Figure 8.3 Removal of toluene vapor under F = 0.049 $m^3 h^{-1}$, and c_{Ti} = 2.81 gm^{-3}. Transient behavior, to steady state conditions. Model predictions (curves) and experimental data (symbols) are given at two locations; (a) one-third height of the biofilter (b) exit of the biofilter.

Figure 8.4 shows another data set, along with model predictions. The agreement seems to be reasonably good. It is unfortunate that more data were not obtained during the first day. It was not expected that concentrations would reach levels close to the steady state ones so fast. One should also see that there is some fluctuation in the data from day to day. keeping in mind that the temperature was not controlled, and humidity of the air not closely monitored, one should be expecting fluctuations.

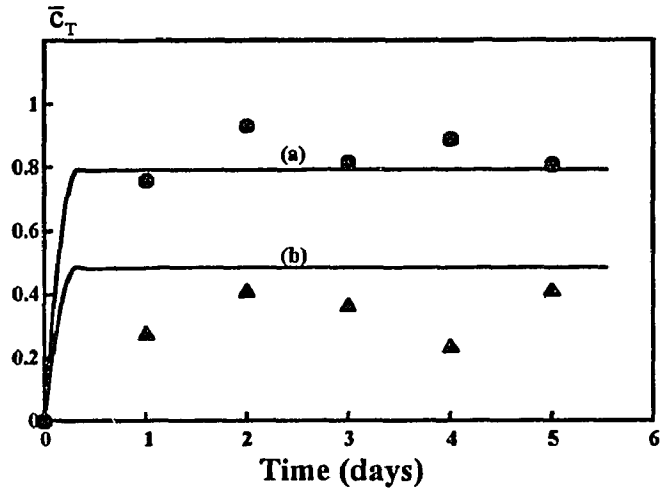

Figure 8.4 Removal of toluene vapor under F = 0.116 $m^3 h^{-1}$, and c_{Ti} = 0.625 gm^{-3}. Transient behavior, to steady state conditions. Model predictions (curves) and experimental data (symbols) are given at two locations; (a) one-third height of the biofilter (b) exit of the biofilter.

Figures 8.5 and 8.6 show data and model predictions from two sets of consecutive experiments. In Figure 8.5 the first experiment is the same as the one shown in Figure 8.4. The concentration profiles predicted from the model under the conditions of this experiment at day 5, were used as initial conditions for predicting the behavior after the flowrate was changed from 0.116 to 0.074 $m^3 h^{-1}$, and the inlet concentration from 0.625 to 0.919 g-toluene m^{-3}-air. The same approach was used for generating the curves of Figure 8.6. The agreement between data and predictions is good, especially in the sense

that the model can capture the qualitative features of the transient behavior. Given the fact that experiments lasted for days under operating conditions which were not perfectly

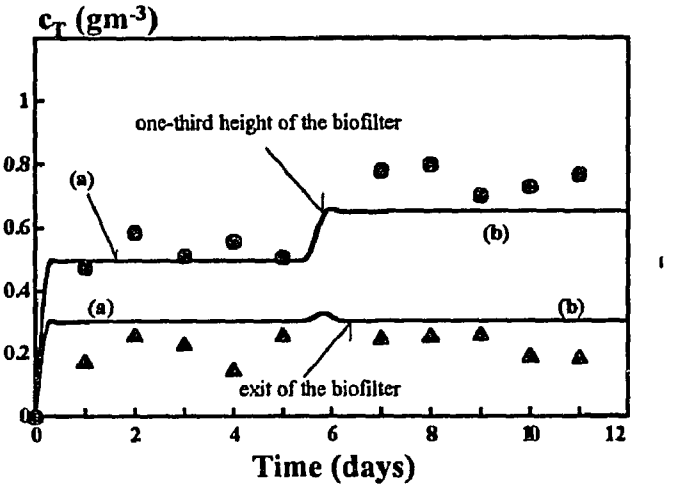

Figure 8.5 Experimental data and model predictions for two consecutive experiments with toluene vapor. Conditions for the first experiment (curves a), were F = 0.116 m^3h^{-1}, and c_{Ti} = 0.625 gm^{-3}. Five days after this experiment started, the conditions were changed to F = 0.074 $m^3 h^{-1}$, and c_{Ti} = 0.919 gm^{-3} (curves b). Data and model predictions refer to one-third height (top curve), and exit of the biofilter bed.

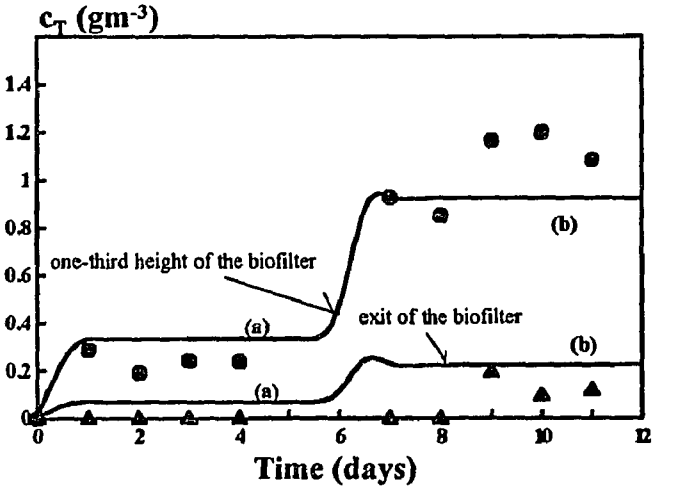

Figure 8.6 Experimental data and model predictions for two consecutive experiments with toluene vapor. Conditions for the first experiment (curves a), were F = 0.036 m^3h^{-1}, and c_{Ti} = 0.684 gm^{-3}. Five days after this experiment started, the conditions were changed to F = 0.04 $m^3 h^{-1}$, and c_{Ti} = 1.65 gm^{-3} (curves b). Data and model predictions refer to one-third height (top curve), and exit of the biofilter bed.

controlled (fluctuations in flowrate, inlet concentration, temperature, humidity of the bed), one could say that the agreement between theory and experimental data is very reasonable.

It should be mentioned that the results presented in this chapter should be viewed as a preliminary effort to model the transient behavior of biofiltration. Clearly, a number of simplifying assumptions were made in deriving the model, and two of the parameters (α and υ), were estimated almost on an arbitrary basis. Finally, sampling should had been done more frequently. Nonetheless, a model which captures the transient features of the process has been developed, and can be used as a basis for designing more elaborate experiments in the future. The practical implication of both the data and the predictions, is that transients last for long time, and since variations in operating parameters are bound to happen, biofilter units should be expected to be operating under transient conditions at all times.

CHAPTER 9

CONCLUSIONS AND RECOMMENDATIONS

Biofiltration is a very complex process. It involves reactions, mass transfer, physical adsorption/desorption, multiple phases (solids, air, biolayer), flow of air through macro- and possibly micro-pores, microbial consortia which may exhibit spatial and temporal variations in their compositions, etc. The work performed in this study was an attempt to systematically investigate some aspects of this complex process. Use of simplifying assumptions is unavoidable, but in this study some assumptions made by other investigators were relaxed, and this relaxation revealed phenomena which are of importance for the design of actual units.

Regarding kinetics of biodegradation, it was found that usage of simple first- or zero-order expressions is wrong. More often than not, kinetics are complex even with consortia which in general are thought of as having good capabilities of degrading pollutants. With single VOCs, Andrews inhibitory kinetics are common (methanol, toluene), and nothing simpler than Monod kinetics (benzene), should be used. In cases of mixtures, biodegradation rate expressions may be even more complex, as kinetic interactions such as competitive inhibition (benzene/toluene mixtures) arise. Although detailed kinetic studies may be impractical (if at all possible) in some cases, e.g., multicomponent gasoline emissions, some understanding of the kinetics is needed. Sensitivity studies performed in this dissertation have shown that errors (even up to 30%), can be made in expected removal rates when some of the kinetic parameters are wrongly estimated.

This is the first study which considered oxygen as a possible limiting factor for the process. The assumption that since there is plenty of oxygen in the air (relative to the VOCs presence), the same should also hold in the biolayer is incorrect. Differences in

thermodynamic properties such as the distribution coefficient, can reverse the situation in the biofilm, i.e., oxygen presence is much less than that of the VOC. In fact, it was found here that with water soluble VOCs (e.g., methanol), oxygen is depleted in the biolayer before the VOC. This oxygen limitation should be expected to happen at relatively high VOC concentrations in airstreams, and in positions close to the entrance of the biofilter bed. These predictions are based on a mathematical model which described very well the macro quantities (e.g., measured gas phase concentrations). It would be of interest to experimentally verify the predicted biofilm concentration profiles in future studies. If the predictions are correct, they would suggest some possible solutions to practical problems. For example, one could try to enhance degradation rates by reducing the oxygen limitation through the use of oxygen enriched air, or membrane-based biofilms for higher oxygen retention.

This study introduced a detailed model for single compounds. This is an improvement over the single existing model in the literature. It was validated with three compounds in experiments performed within this study (benzene, toluene), and with data obtained from another laboratory (methanol). The agreement between model predicted, and experimentally obtained concentration profiles was remarkably good. It is a model which could be used with confidence, as its predictions are based on a rational approach to parameter measurement/estimation, and does not involve any fitting approach once all parameters have been determined. This model was the basis for developing another one which is more realistic for practical applications, that is one which describes biofiltration of VOC mixtures.

The general model for steady state biofiltration of VOC mixtures developed during this study, takes into account potential oxygen effects, as well as potential interactions among VOCs during their biodegradation. It was validated through experiments in a large (pilot-scale) column with benzene/toluene mixtures. These two components are involved in cross-inhibitory, competitive, interactions, and led to a proof (both experimentally and

numerically) of the fact that biofiltration of mixtures is not the same as, and cannot be predicted from data, on single VOC removal. Thus, the additive approach proposed earlier in the literature, leads to errors in the design of biofilters.

Clearly, biofiltration is a process subject to frequent variations in the operating parameters. The model developed in this study can be used in cases where the fluctuations are not wide and thus, when quasi-steady state operation is expected. Further studies should involve more complex mixtures (e.g., BTEX), chlorinated solvent vapors, compounds degraded via cometabolism, etc.

Experimentally, the results of the present study show that biofilters seem to have a long life span. Continuous experiments were performed over a period of almost two years, without adding any supplemental nutrients, and without development of any significant pressure-drop over the bed. These results suggest that this technology will have a negligible operating cost. Hence, future studies should consider factors for capital cost minimization; for example, design methodologies for removal rate increases which could result in decreases of biofilter size.

The final part of this study dealt with biofiltration under transient conditions. If biofiltration is complex to analyze under steady state conditions, it becomes even more complex under transient operation. Transient operation involves an extra process, namely adsorption on the solid packing. This extra process results in very lengthy transients. One should possibly consider using packing materials which do not adsorb VOCs of interest. This is a question which should be investigated in the future. Future experiments should be carefully planned; frequent sampling, and good control of operating parameters should be applied. Unambiguous transient data will help provide a better understanding of the process, and may lead to new insights into the process. From the modeling view point, methodologies for solving coupled PDEs should be used, so that the simplifications made in this study are avoided. Nonetheless, this study produced the first detailed transient model which seems to be able to capture and predict the basic trends of experimental data.

It is believed that this study contributes significantly towards fundamental understanding of biofiltration, a technology which will play a significant future role in air pollution control.

APPENDIX A

COMPUTER CODE FOR SOLVING THE STEADY-STATE BIOFILTRATION MODEL FOR A SINGLE VOC

```
c*************************************************************
c
c  Purpose      : "Solution of the Steady-State Biofitration
c                  Model for a Single VOC"
c
c  Method       :  Multiple Shooting Technique
c
c  Language     :  FORTRAN
c
c  Requirement  :  IMSL Subroutine Package
c
c  By           :  Zarook Shareefdeen
c
c*************************************************************
      INTEGER LDY,NEQNS,NMAX
      PARAMETER (NEQNS=2,NMAX=21,LDY=NEQNS,NHMAX=21)
c
      parameter (n=20)
      REAL height(n+1),gas(n+1,1)
c
      INTEGER I,MAXIT,NFINAL,NINIT,NOUT
      REAL    FCNBC,FCNEQN,FCNJAC,FLOAT,TOL,
     &  X(NMAX),XLEFT,XRIGHT,Y(LDY,NMAX),H(NHMAX)
      EXTERNAL BVPMS,FCNBC,FCNEQN,FCNJAC
c
      EXTERNAL   F
      external tdate
c
      COMMON /gas/deri,an
      common /sur/ sur
      COMMON /cg/ cg
      COMMON /prm/ ak,al,g,e1,e2,w
      common /del/ del
      common /acg0/ acg01
C
c
      open(6,file='bmvmsw.out',status='new')
c
      call today
c
      cg = 1.0
      sur = 85.15
c
c  gas
c
      delz=1./float(n)
      z= 0.0
      height(1)=z
      gas(1,1)=cg
c
      index = 1000
c
      do 100 igas=2,n+1
      del = 20.0
      write(6,55)  z
 55   format(' ','Height = ',5x, f7.2)
c
  6   call prm (index,ak,al,g,e1,e2,an,w)
      index = 2000
C
      WRITE(6,1)
  1   FORMAT(' LIQUID PHASE CONC. ALONG THE FILM OF THE BIOLAYER')
      WRITE(6,*)
```

```
      WRITE(6,*)
      WRITE(6,2)
    2 FORMAT('          ',',     X    ',',    ',',     meoh (ppm)     ',
     & '    ',',  O2 (PPM)    ',//)
      WRITE(6,*)
C
C  BOUNDARY CONDITIONS
C
      XLEFT  =   1.0e-3
      XRIGHT =   1.0
      TOL    =   1.0E-4
      MAXIT  =   20
      NINIT  =   NMAX
C
C  INITIAL SHOOTING POINTS
C
      DO 10 I=1,NINIT
      X(I)=XLEFT+FLOAT(I-1)/FLOAT(NINIT-1)*(XRIGHT-XLEFT)
      Y(1,I)=30.0
      Y(2,I)=-0.01
   10 CONTINUE

C
C  CALL IMSL SUBROUTINE
C
      CALL BVPMS (FCNEQN,FCNJAC,FCNBC,NEQNS,XLEFT,XRIGHT,TOL,
     & TOL,MAXIT,NINIT,X,Y,LDY,NMAX,NFINAL,X,Y,LDY)
C
      sof  = y(1,ninit)*0.26
      cob = al*w*(cg-1)+1
      smf  = ((sof/0.26-e2*cob)/al+e1*cg)*631.78
      uplm1 = e2*cob/100*0.26
      uplm2 = e1*cg/100*631.78
      alcg  = cg*acg01
c
      del = del/1e-6
c
      if (sof.ge.0.0.and.sof.le. uplm1)then
      go to 5
      elseif (smf.ge.0.0.and.smf.le. uplm2) then
      go to 5
      elseif (alcg.le.0.5.and.del.le.150.0)then
      del = del + 0.1
      go to 6
      elseif (alcg.gt.0.5.and.del.le.150.0)then
      del = del + 1.0
      go to 6
      elseif (del.gt.150)then
      del = 150.
      go to 6
      else
      endif
c
  5   DO 4 I = 1,NINIT
      so  = y(1,I)*0.26
      cob = al*w*(cg-1)+1
      sm  = ((so/0.26-e2*cob)/al+e1*cg)*631.78
      WRITE(6,*) X(I),sm,so
    4 CONTINUE
    3 FORMAT('          ',F7.3,3x,e10.6,3x,f10.6)
      deri = y(2,1)/al
c
C CALCULATE GAS PHASE CONCENRATION
```

```
c
      CALL RK4(F,z,cg,delz)
      height(igas)=z
      gas(igas,1)=cg
 100  continue
c
      write(6,123)
      WRITE(6,22)
 22   format(//,5x,'        Gas Phase Concent. Profile',//)
      WRITE(6,13)
 13   FORMAT (' ',8x, 'Height   ','    Concentration',/)
      do 44 igas=1,n+1
      cob = al*w*(gas(igas,1)-1)+1
      write(6,33) height(igas), gas(igas,1),cob
 44   continue
 33   format(' ',F14.6,3x,F14.6,3x,f14.6)
c
       call lsq (gas, alsq)
       write(6,66) alsq
  66   format(' sum of sq. = ', 4x, f10.6)
c
  123 FORMAT(' ____________________________________________________',/)
      stop
      end
c*************************************************************
       subroutine today
       EXTERNAL   TDATE
       CALL TDATE (IDAY, MONTH, IYEAR)
       write(6,123)
       WRITE (6,66) month,iday,iyear
  66   Format( ' Date of Simulation :    ',i2,'/',i2,'/',I4,//)
  123  FORMAT(' ____________________________________________________',/)
       return
       end

c*************************************************************
c purpose :  solve the gas phase concentration profile
c            using the fourth order runge kutta method
cc************************************************************
        SUBROUTINE RK4(F,z,cg,H)
        H2=0.5*H
        START=z
        F1=F(z,cg)
        F2=F(z+H2,cg+H2*F1)
        F3=F(z+H2,cg+H2*F2)
        F4=F(z+H,cg+H*F3)
        cg=cg+H*(F1+2.*F2+2.*F3+F4)/6.
        z=z+H
        RETURN
        END
c*************************************************************
c purpose : give the function for RK method, in the gas phase
c           balance
cc************************************************************
        FUNCTION F(z,cg)
        COMMON/gas/deri,an
        F= an*deri
        RETURN
        END
*****************************************************************
c purpose : compare the model predicitons with the exp. and
c           minimize the error to find the best surface area.
cc************************************************************
```

```
      subroutine lsq (ycal, alsq)
      REAL       ycal(21,1),yexp(4)
      data yexp/.860,.657,.448,.149/
      x2=ycal(6,1)-yexp(1)
      x3=ycal(11,1)-yexp(2)
      x4=ycal(16,1)-yexp(3)
      x5=ycal(21,1)-yexp(4)
      alsq=(x2**2+x3**2+x4**2+x5**2)
      return
      end
C*************************************************************
      SUBROUTINE FCNEQN (NEQNS,X,Y,P,DYDX)
      INTEGER NEQNS
      REAL X,Y(NEQNS),P,DYDX(NEQNS)
c
      COMMON /cg/ cg
      COMMON /prm/ ak,al,g,e1,e2,w
C
      cob  = al*w*(cg-1)+1
      alp  = -e2*cob+al*e1*cg
      bet1 = al**2+al*alp+g*alp**2
      bet2 = al+2.*alp*g
      bet3 = al**2*ak
c
      DYDX(1)=Y(2)*p
      DYDX(2)=(bet3*y(1)/(bet1+p*bet2*Y(1)+p*Y(1)**2*G))*
     &          (alp+p*y(1))/(1.+p*y(1))*p
      RETURN
      END
C
      SUBROUTINE FCNBC(NEQNS,YLEFT,YRIGHT,P,F)
      INTEGER NEQNS
      REAL  YLEFT(NEQNS),YRIGHT(NEQNS),P,F(NEQNS)
c
      COMMON /cg/ cg
      COMMON /prm/ ak,al,g,e1,e2,w
c
      cob = al*w*(cg-1)+1
c
      F(1)=YLEFT(1)-cob*E2*p
      F(2)=YRIGHT(2)
      RETURN
      END
C
      SUBROUTINE FCNJAC(NEQNS,X,Y,P,DYPDY)
      INTEGER NEQNS
      REAL X,Y(NEQNS),P,DYPDY(NEQNS,NEQNS)
c
c
      COMMON /cg/ cg
      COMMON /prm/ ak,al,g,e1,e2,w
C
      cob = al*w*(cg-1)+1
      alp = -e2*cob+al*e1*cg
      bet1 = al**2+al*alp+g*alp**2
      bet2 = al+2.*alp*g
      bet3 = al**2*ak
C
      x1 = bet1+p*bet2*y(1)+p*g*y(1)**2
      x2 = 1.+y(1)*p
      x3 = alp+2.*y(1)*p
      x4 = p*bet2+2.*g*y(1)*p
c
```

```
      DYPDY(1,1)=0
      DYPDY(1,2)=1.0*p
      DYPDY(2,1)=bet3*(x1*x2*x3-y(1)*(p*y(1)+alp)*(x1*p+x2*x4))/
     &           x1**2/x2**2*p
      DYPDY(2,2)=0.0
      RETURN
      END

c*****************************************************************
      subroutine prm (index,ak,al,g,e1,e2,an,w)
      common /del/ del
      common /sur/ sur
      common /acg0/ acg01
c
c 1-methanol
c 2-oxygen
c
      del = del*1e-6
c
      b0     = 100e3
c
      xv     = b0/1000
      fd     = 1-0.43*xv**0.92/(11.19+0.27*xv**0.99)
c
      df1  = 1.30e-9 *3600.*fd
      df2  = 2.41e-9 *3600.*fd
      ay1    = 0.28
      ay2    = 0.26
      akii1 = 20.002*1000
      akss1 = 0.63178*1000
      amu1  = 0.22244
      akss2 = 0.26
c
      ACG01 = 6.56
      aug    = .0155
      vv     = 932e-6
c
      acg02 = 275
      amm1 = 0.0034
      amm2 =  34.4
      if (index.eq.1000)then
      CALL SVARI(sur,b0,vv,df1,df2,ay1,ay2,AKII1,AKSS1,
     &  amu1,akss2,acg01,acg02,aug, amm1,amm2,phi)
      else
      endif
c
      ak=amu1*del**2*b0/df1/ay1/akss1
      al=df1*ay1*akss1/ay2/akss2/df2
      g =akss1/akii1
      e1=acg01/amm1/akss1
      e2=acg02/amm2/akss2
      an=df1*sur*akss1*vv/del/aug/acg01
      w=akss2*df2*acg01/akss1/df1/acg02
c
      write(6,123)
      WRITE(6,1)
    1 FORMAT ('  ', '     Parameters Used :', /)
      WRITE(6,2) ak, g
      WRITE(6,3) e1, AN
    2 FORMAT ('  ', '  k    =   ',e14.3,3x,'gama = ',3x,f7.3)
    3 FORMAT ('  ', ' Eps1 =   ',f14.6,3x,'n    = ',3x,f7.3)
      WRITE(6,4) al,del*1e6
      WRITE(6,5) e2,w
```

```
     4   FORMAT ('  ', ' lamda =   ',e14.3,5x,'delta (mic.m)=', f10.6,/)
     5   FORMAT ('  ', ' Eps2 =   ',e14.3,3x,'omega  = ',3x,e14.3,/)
   123   FORMAT(' ____________________________________________________',/)
         return
         end
C*********************************************************************
         subroutine SVARI(sur,b0,vv,df1,df2,ay1,ay2,AKII1,AKSS1,
      &  amu1,akss2,acg01,acg02,aug, amm1,amm2,phi)
c
         write(6,123)
         WRITE(6,1)
     1   FORMAT ('  ',//, ' VARIABLES IN THE MODEL',//)
         WRITE(6,19) Aug
    19   format ('  ', 'Gas Flow Rate (m3/hr)        = ', e14.3)
         WRITE(6,3) vv*1e6
     3   FORMAT ('  ', 'Volume of the column(cm3)    = ', f14.3)
         WRITE(6,4) SUR
     4   FORMAT ('  ', 'Biolayer Sur.Area( m2/m3)    = ', f14.3)
         write(6,44) b0
    44   format ('  ', 'Biomass Conc. (g/m3)         = ', e14.3)
c         WRITE(6,5) del*1e3
c     5   FORMAT ('  ', 'Film thickness (mm)          = ', f14.3)
         WRITE(6,2) ACG01
         WRITE(6,22) ACG02
     2   FORMAT ('  ', 'Inlet conc. (g/m3 of air)(m) = ', f14.3)
    22   FORMAT ('  ', 'Inlet conc. (g/m3 of air)(o) = ', f14.3)
         write(6,31) ay1
    31   format ('  ', 'Yield Coefficient (m)        = ', f14.3)
         write(6,32) ay2
    32   format ('  ', 'Yield Coefficient (o)        = ', f14.3)
         WRITE(6,51) df1*1e9/3600
         WRITE(6,54) df2*1e9/3600
    51   format ('  ', 'Diff. Coefficient (m)*1e9    = ', f14.3)
    54   format ('  ', 'Diff. Coefficient (o)*1e9    = ', f14.3)
         WRITE(6,56) amm1
    56   FORMAT ('  ', 'Dist. Coeff.        (m)      = ', e14.3)
         WRITE(6,566) amm2
   566   FORMAT ('  ', 'Dist. Coeff.        (o)      = ', e14.3)
         write(6,123)
         write(6,*) '          Andrews and other  Parameters'
         WRITE(6,6) akii1,akss1,amu1, akss2
     6   format(' ',/, ' Kil (g/m3) = ',e14.3,3x,'Ks1 (g/m3) = ', f7.3,
      &  /,' Sp. Growth Rate-1 (1/hr)=',f14.3,3x,/,' ',
      &  'aKd (g/m3) = ', f7.3,//)
   123   FORMAT(' ____________________________________________________',/)
         return
         end
C*********************************************************************
```

APPENDIX B

COMPUTER CODE FOR SOLVING THE STEADY-STATE BIOFILTRATION MODEL FOR A MIXTURE OF TWO VOCs

```
c*************************************************************
c
c  Purpose      : "Solution of the Steady-State Biofitration
c                  Model for Mixed (Binary) VOCs"
c
c  Method       :  Orthogonal collocation
c
c  Language     :  FORTRAN
c
c  Requirements :  1) IMSL package
c                  2) Modified version of the subroutine
c                     package given in the appendix A
c                     of the ref. (76)'
c
c  By           :  Zarook Shareefdeen
c
c*************************************************************
        Implicit Real*8 (a-h,o-z)
        parameter (n  = 10)
        parameter (ng = 20)
        REAL height(ng+1),gas1(ng+1), gas2(ng+1), gas3(ng+1)
        real*8 a(0:n+1,0:n+1),b(0:n+1,0:n+1),v1(n+2),v2(n+2)
        real*8 xold(2*n),xintp(n+2),y(n+2)
        real*8 xdat(n+1),yb(n+1),yt(n+1)
        real*8 s(n,n+1),eig(n,2),nr(n)
        real*8 root(n+2),dif1(n+2),dif2(n+2),dif3(n+2)
c
        EXTERNAL   TDATE
        EXTERNAL   fun1,fun2
c
        common /del/ del
        common /sur/ sur
        common /index/ indx
c
        common /prm1/ ph12,ph22,al1,al2,w1,w2,g,sg1,sg2,bt,
     &                  e1,e2,e3
        common /prm2/ a,b
        common /prm3/ cg1,cg2,cg3
        COMMON /gas/deri1,deri2,an
c
        open(6,file='btcolw.out',status='new')
c
c  for othogonal collacation method..
c
        alpha=0.0
        beta=0.0
c
        n0=1
        n1=1
        nt=n+n0+n1
c
c   ----calculate the collocation point----
        call jcobi(nt,n,n0,n1,alpha,beta,dif1,dif2,dif3,root)
c   ----calculate the discretization matrices a & b----
c
        do 50 i=1,nt
        call dfopr(nt,n,n0,n1,i,1,dif1,dif2,dif3,root,v1)
        call dfopr(nt,n,n0,n1,i,2,dif1,dif2,dif3,root,v2)
        do 60 j=1,nt
        a(i-1,j-1)=v1(j)
   60   b(i-1,j-1)=v2(j)
   50   continue
c
```

```
C DATE
c
      indx = 100
      CALL today
c
      WRITE (6,67) n
  67  Format( ' Solution of the Model using Orthogonal
     & Collocation ',/,' with [',i3,'] col. points',/)
c
      sur = 40.0
      cg1 = 1.0
      cg2 = 1.0
      cg3 = 1.0
c
c
c  gas
c
      delz=1./float(ng)
      z= 0.0
      height(1)=z
      gas1(1)=cg1
      gas2(1)=cg2
      gas3(1)=cg3
c
      do 100 igas=2,ng+1
      write(6,55)  z
  55  format(3x,'Height = ',5x, f14.3)
c
      del = 30.0
c
   6  call prm (ph12,ph22,a11,a12,an,w1,w2,g,sg1,sg2,bt,
     &                  e1,e2,e3)
c
      if (igas.eq.ng)then
      indx = 1000
      else
      indx = 200
      endif
c
c  initial guess for y
c
      do 10 i=1,2*n
      xold(i)=.1
  10  continue
c

      itmax  =  100
      iprint =  -1
      eps1   =  1.e-9
      eps2   =  1.e-9
c
c
c   *** iprint=1 all iterations are printed ***
      call newton(itmax,2*n,iprint,eps1,eps2,xold)
c
c     interpolation at desired values
c
      call interp (xold,nt,root, dif1,xdat,yb,yt)
c
c

      sbf   = yb(n+1)
      stf   = yt(n+1)
      sof   = a11*(sbf-e1*cg1)+a12*(stf-e2*cg2)+e3*cg3
```

```
        uplm1 = e1*cg1*0.01
        uplm2 = e2*cg2*0.01
        uplm3 = e3*cg3*0.01
        del   = del*1e6
c
        if (sof.gt.0.0.and.sof.le.uplm3)then
        go to 5
        elseif ((sbf.gt.0.0.and.sbf.le. uplm1).or.
     &  (stf.gt.0.0.and.stf.le. uplm2).or.
     &  (sof.gt.0.0.and.sof.le. uplm3)) then
        go to 5
        elseif(del.lt.150)then
        del = del+ 1.0
        go to 6
        elseif(del.ge.150)then
        del = 150
        go to 6
        else
        endif
c
   5    indx = 3000
        call interp (xold,nt,root, difl,xdat,yb,yt)
        call deri (xold, deri1, deri2)
c
C CALCULATE GAS PHASE CONCENRATION
C
      CALL RK4(Fun1,z,cg1,delz)
      z = z-delz
      CALL RK4(fun2,z,cg2,delz)
      height(igas)=z
      cg3 = al1*w2*(cg1-1)+al2*w2/w1*(cg2-1)+1
      gas1(igas)=cg1
      gas2(igas)=cg2
      gas3(igas)=cg3
 100  continue
c
      write(6,123)
      WRITE(6,22)
 22   format(//,5x,'        Gas Phase Concentration Profile',//)
      WRITE(6,13)
 13   FORMAT ('  ',12x, 'Height',10x,'Cg(B)',10x,'Cg(T)',10x,'Cg(O)'/)
      do 44 igas=1,ng+1
c      write(6,33) height(igas),(1-gas1(igas)), (1-gas2(igas)),
c     &            (1- gas3(igas))
      write(6,33) height(igas), gas1(igas), gas2(igas), gas3(igas)
 44   continue
 33   format(4x,F14.6,2x,F14.6,1x,f14.6,1x,f14.6)
c
      call lsq (gas1,gas2,alsq1,alsq2,alsq)
      write(6,56) alsq1,alsq2,alsq
c
   56 format(//,' ','lsq1 = ', e14.3,'lsq2 = ',e14.3,/,
     & 'lsq = ',e14.3,//)
  123 FORMAT(' ____________________________________________________',/)
      stop
      end
c*******************************************************
c purpose : interpolating the results that you get from
c           newton raphson subroutine
c
c*******************************************************
      subroutine interp (xold,nt,root, difl,xdat,yb,yt)
      Implicit Real*8 (a-h,o-z)
```

```
      parameter(n=10)
      real*8 xold(2*n),xintp(n+2),y1(n+2),y2(n+2)
      real*8 xdat(n+1), yb(n+1), yt(n+1),yo(n+1)
      real*8 root(n+2),dif1(n+2),dif2(n+2),dif3(n+2)
      common /prm1/ ph12,ph22,a11,a12,w1,w2,g,sg1,sg2,bt,
     &              e1,e2,e3
      common /prm3/ cg1,cg2,cg3
      common /index/ indx
c
      if (indx.eq.3000)then
      write(6,123)
      WRITE(6,12)
 12   FORMAT ('  ',10x, 'Concentration Profiles in the Biofilm ', /)
      WRITE(6,13)
 13   FORMAT (5x,'   x   ',11x,'s(B)',14x,'s(T)',11x,'s(O)'//)
      else
      endif
c
       y1(1)=e1*cg1
       y2(1)=e2*cg2
c
       do 15 i=1,n
 15    y1(i+1)=xold(i)
       y1(nt)=y1(nt-1)
c
       do 16 i=1,n
 16    y2(i+1)=xold(i+n)
       y2(nt)=y2(nt-1)

c
       do 20 i=1,n+1
       dist=float(i-1)/n
       call intrp(nt,nt,dist,root,dif1,xintp)
       sb=0.0
       st=0.0
       do 30 j=1,nt
       sb = sb+xintp(j)*y1(j)
       st = st+xintp(j)*y2(j)
 30    continue
       if (indx.eq.3000)then
       so = a11*(sb-e1*cg1)+a12*(st-e2*cg2)+e3*cg3
       write(6,40) dist,sb,st,so
       else
       endif
c plot
       xdat(i)=dist
       yb(i)=sb
       yt(i)=st
c
 20    continue
 40    format(5x,f7.2,5x,E14.6,5x,E14.6,5x,e14.6)
123    FORMAT(' ____________________________________________________',/)
       return
       end
c*************************************************************
c purpose : construct the jacobian matrix and on the last
c           column vector -f
c
cc************************************************************
C   SUBROUTINE CALCN FOR EVALUTING THE AUGMENTED JACOBIAN MATRIX
C      JAC*DEL=-F  SOLVING DEL
c
       SUBROUTINE CALCN(dXOLD,DF,N)
```

```
      implicit real*8 (a-h,o-z)
      parameter(m=10)
      real*8 xold(2*m),dxold(2*m),df(2*m,2*m+1), sum1(2*m),
     &  sum2(2*m)
      real*8 a(0:m+1,0:m+1),b(0:m+1,0:m+1)
      common /prm1/ ph12,ph22,al1,al2,w1,w2,g,sg1,sg2,bt,
     &              e1,e2,e3
      common /prm2/ a,b
      common /prm3/ cg1, cg2,cg3
c
      cob  = al1*w2*(cg1-1)+al2*w2/w1*(cg2-1)+1
      alp  = -al1*e1*cg1-al2*e2*cg2+e3*cob
c
      do 1 i=1,2*n
      xold(i)=dxold(i)
      do 1 j=1,(2*n+1)
    1 df(i,j)=0.0
c
      do 3 i=1,2*n
      sum1 (i)=0.0
    3 sum2 (i)=0.0
c
      do 10 i=1,n
      do 20 j=1,n
      if(i.eq.j)then
      p1=1.+xold(i)+sg1*xold(i+n)
      p2=1.+alp+al1*xold(i)+al2*xold(i+n)
      p3=2*al1*xold(i)+alp+al2*xold(i+n)
      p4=p1*al1+p2
      p5=al1*xold(i)+al2*xold(i+n)+alp
      df(i,j)=b(i,j)-b(i,n+1)/a(n+1,n+1)*a(n+1,j)
     & -ph12*(p1*p2*p3-xold(i)*p5*p4)/p1**2/p2**2
      else
      df(i,j)=b(i,j)-b(i,n+1)/a(n+1,n+1)*a(n+1,j)
      endif
      sum1(i)=sum1(i)+(b(i,j)-b(i,n+1)/a(n+1,n+1)*a(n+1,j))*xold(j)
   20 continue
      df(i,(2*n+1))=-(sum1(i)+b(i,0)*e1*cg1-b(i,n+1)*
     & a(n+1,0)*e1*cg1/a(n+1,n+1)-
     & ph12*p5*xold(i)/p1/p2)
   10 continue
c
      do 12 i=n+1,2*n
      do 22 j=n+1,2*n
      if(i.eq.j)then
c
      q1=1.+xold(i)+g*(xold(i))**2+sg2*xold(i-n)
      q2=bt+alp+al1*xold(i-n)+al2*xold(i)
      q3=al1*xold(i-n)+alp+2*al2*xold(i)
      q4=q1*al2+q2*(1.+2*g*xold(i))
      p5=al1*xold(i-n)+al2*xold(i)+alp
c
      df(i,j)=b(i-n,j-n)-b(i-n,n+1)/a(n+1,n+1)*a(n+1,j-n)
     & -ph22*(q1*q2*q3-xold(i)*p5*q4)/q1**2/q2**2
      else
      df(i,j)=b(i-n,j-n)-b(i-n,n+1)/a(n+1,n+1)*a(n+1,j-n)
      endif
      sum2(i)=sum2(i)+(b(i-n,j-n)-
     &         b(i-n,n+1)/a(n+1,n+1)*a(n+1,j-n))*xold(j)
   22 continue
      df(i,(2*n+1))=-(sum2(i)+b(i-n,0)*e2*cg2-b(i-n,n+1)*
     & a(n+1,0)*e2*cg2/a(n+1,n+1)-
     & ph22*p5*xold(i)/q1/q2)
```

```
   12   continue
        return
        end
C*************************************************************
c purpose : newton raphson to solve the algebric equations
c
C*************************************************************
      subroutine newton(itmax,n,iprint,eps1,eps2,xold)
      implicit real*8 (a-h,o-z)
      parameter (m=10)
      dimension xold(2*m),xinc(2*m),a(2*m,2*m+1)
c     newton raphson iteration
c      write(6,200)itmax,iprint,2*n,eps1,eps2,2*n,(xold(i),i=1,2*n)
      write(6,123)
      do 9 iter=1,itmax
c     call on calcn to set up the a matrix
      call calcn(xold,a,m)
c     call simul to compute jacobian and correction in xinc
      nn=n+1
      indic=1
      deter=simul1 (n,a,xinc,eps1,indic,nn)
      if (deter.ne.0)goto 3
      write(6,201)
      return
c     check for convergence and update xold value
3     itcon=1
      do 5 i=1,n
      if(dabs(xinc(i)).gt.eps2) itcon=0
5     xold(i)=xold(i)+xinc(i)
      if(iprint.eq.1) write(6,202)iter,deter,n,(xold(i),i=1,n)
      if(itcon.eq.0) goto 9
c     write(6,203)iter,n,(xold(i),i=1,n)
      write(6,2203)iter
      return
9     continue
      write(6,204)
      return
c     formats for input and output statements
200   format(' itmax  = ',i8,/' iprint = ',i8/' n      = ',i8/
     &' eps1   = ',1pe14.1/' eps2   = ',1pe14.1/10x,'xold(1)...xold(',
     &i2,')'//(1h ,1p4e16.6))
201   format(38h0matrix is ill-conditioned or singular)
202   format(' iter   =',i8/  10h deter  = ,e18.5/
     $   26h           xold(1)...xold(,i2,1h) / (1h ,1p4e16.6) )
203   format(' successful convergence'/'   iter   =',i3/10x,
     $'xold(1)...xold(',i2,')'//  (1h ,1p4e16.6) )
2203  format(' successful convergence'/'   iter   =',i3/)
204   format(' no convergence' )
123   FORMAT(' ____________________________________________________',/)
      end

C*********************************************************************
      subroutine SVARI (sur,b0,vv,df1,df2,df3,ay1,ay2,ay13,ay23,AKSS1,
     &  amu1,akii2,akss2,amu2,akss12,akss21,akss13,akss23,acg01,
     &  acg02,acg03,aug, amm1,amm2,amm3,del)
      Implicit Real*8 (a-h,o-z)
c
      write(6,123)
      WRITE(6,1)
1     FORMAT ('  ',//, ' VARIABLES IN THE MODEL',//)
      WRITE(6,2)
2     FORMAT (3x,'1 - benzene',/,3x,'2 - Toluene',/,3x,'3 - oxygen',/)
      WRITE(6,19) Aug
```

```
 19   format ('  ', 'Gas Flow Rate (m3/hr)        = ', e14.3)
      WRITE(6,3) vv*1e6
  3   FORMAT ('  ', 'Volume of the column(cm3)    = ', f14.3)
      WRITE(6,4) SUR
  4   FORMAT ('  ', 'Biolayer Sur.Area( m2/m3)    = ', f14.3)
      write(6,44) b0
 44   format ('  ', 'Biomass Conc. (g/m3)         = ', e14.3)
      WRITE(6,5) del*1e3
  5   FORMAT ('  ', 'Film thickness (mm)          = ', f14.3)
      WRITE(6,18) ACG01
      WRITE(6,21) ACG02
      WRITE(6,22) ACG03
 18   FORMAT ('  ', 'Inlet conc. (g/m3 of air)(1) = ', f14.3)
 21   FORMAT ('  ', 'Inlet conc. (g/m3 of air)(2) = ', f14.3)
 22   FORMAT ('  ', 'Inlet conc. (g/m3 of air)(3) = ', f14.3)
      write(6,31) ay1
 31   format ('  ', 'Yield Coefficient (1)        = ', f14.3)
      write(6,32) ay2
 32   format ('  ', 'Yield Coefficient (2)        = ', f14.3)
      write(6,33) ay13
 33   format ('  ', 'Yield Coefficient (13)       = ', f14.3)
      write(6,34) ay23
 34   format ('  ', 'Yield Coefficient (23)       = ', f14.3)
      WRITE(6,51) df1*1e9/3600
      WRITE(6,54) df2*1e9/3600
      WRITE(6,55) df2*1e9/3600
 51   format ('  ', 'Diff. Coeff.(1)*1e9 (m2/s)   = ', f14.3)
 54   format ('  ', 'Diff. Coeff.(2)*1e9 (m2/s)   = ', f14.3)
 55   format ('  ', 'Diff. Coeff.(3)*1e9 (m2/s)   = ', f14.3)
      WRITE(6,56) amm1
 56   FORMAT ('  ', 'Dist. Coeff.        (1)      = ', e14.3)
      WRITE(6,566) amm2
566   FORMAT ('  ', 'Dist. Coeff.        (2)      = ', e14.3)
      WRITE(6,567) amm3
567   FORMAT ('  ', 'Dist. Coeff.        (3)      = ', e14.3)
      write(6,123)
      write(6,*) '          Andrews and other  Parameters'
      WRITE(6,6) akss1,amu1, akss2,akii2,amu2, akss12,akss21,
     & akss13,akss23
  6   format (' ',/,' Ks1 (g/m3) = ',e14.3,3x,'mu1 (1/hr) = ',f14.3,/,
     &                ' Ks2 (g/m3) = ',e14.3,3x,'Ki2 (g/m3) = ',e14.3,/,
     &                ' mu2 (1/hr) = ',f14.3,/,
     &                ' Ks12(g/m3) = ',e14.3,3x,'Ks21(g/m3) = ',e14.3,/,
     &                ' Kob (g/m3) = ',e14.3,3x,'Kot (g/m3) = ',f14.3)
123   FORMAT(' ____________________________________________________',/)
      return
      end
c*************************************************************
      subroutine today
      EXTERNAL   TDATE
      CALL TDATE (IDAY, MONTH, IYEAR)
      write(6,123)
      WRITE (6,66) month,iday,iyear
 66   Format( 3x, ' Date :    ',i2,'/',i2,'/',I4,//,
     &          '      Model Predictions for Benzene-Toluene Mixture',/,
     &          '            by Collocation Method                  ',/,
     &          '      ---------------------------------------------' //)
123   FORMAT(' ____________________________________________________',/)
      return
      end
c*************************************************************
c     Subroutine for evaluating the derivative
c     necessary for gas phase profiles
```

```
c
c*****************************************************************
        subroutine deri (xold, deri1, deri2)
        Implicit Real*8 (a-h,o-z)
        parameter (n=10)
        real*8 a(0:n+1,0:n+1),b(0:n+1,0:n+1)
        real*8 xold(2*n)
        common /prm1/ ph12,ph22,al1,al2,w1,w2,g,sg1,sg2,bt,
     &                e1,e2,e3
        common /prm2/ a,b
        common /prm3/ cg1,cg2,cg3
c
         sum1 = 0.0
         sum2 = 0.0
         do 10 j =1,n
         sum1 = sum1+(a(0,j)-a(0,n+1)*a(n+1,j)/a(n+1,n+1))*xold(j)
         sum2 = sum2+(a(0,j)-a(0,n+1)*a(n+1,j)/a(n+1,n+1))*xold(j+n)
   10    continue
         deri1 = sum1+(a(0,0)-a(0,n+1)*a(n+1,0)/a(n+1,n+1))*e1*cg1
         deri2 = sum2+(a(0,0)-a(0,n+1)*a(n+1,0)/a(n+1,n+1))*e2*cg2
c         write(*,*) deri1, deri2
         return
         end
c*****************************************************************
c            for gas phase
c            using the fourth order runge kutta method
cc****************************************************************
        SUBROUTINE RK4(F,z,cg,H)
        Implicit Real*8 (a-h,o-z)
        H2=0.5*H
        START=z
        F1=F(z,cg)
        F2=F(z+H2,cg+H2*F1)
        F3=F(z+H2,cg+H2*F2)
        F4=F(z+H,cg+H*F3)
        cg=cg+H*(F1+2.*F2+2.*F3+F4)/6.
        z=z+H
        RETURN
        END
C
c*****************************************************************
c purpose : give the function for RK method, in the gas phase
c           balance ; benzene
cc****************************************************************
        FUNCTION Fun1(z,cg1)
        Implicit Real*8 (a-h,o-z)
        COMMON /gas/deri1,deri2,an
        Fun1 = an*deri1
        RETURN
        END
C
c*****************************************************************
c purpose : give the function for RK method, in the gas phase
c           balance ; Toluene
cc****************************************************************
        FUNCTION Fun2(z,cg2)
        Implicit Real*8 (a-h,o-z)
        COMMON /gas/deri1,deri2,an
        common /prm1/ ph12,ph22,al1,al2,w1,w2,g,sg1,sg2,bt,
     &                e1,e2,e3
        Fun2 = an*w1*deri2
        RETURN
        END
```

```
c*********************************************************************
        subroutine lsq (ycal1,ycal2, alsq1,alsq2,alsq)
        REAL       ycal1(21),yexp1(3),ycal2(21), yexp2(3)
        data yexp1/.939,.90,.869/
        data yexp2/.800,.671,.583/
c
        x1=3.3/5*(ycal1(8)-ycal1(7))+ycal1(7)-yexp1(1)
        x2=1.6/5*(ycal1(15)-ycal1(14))+ycal1(14)-yexp1(2)
        x3=ycal1(21)-yexp1(3)
        alsq1=(x1**2+x2**2+x3**2)
c
        x1=3.3/5*(ycal2(8)-ycal2(7))+ycal2(7)-yexp2(1)
        x2=1.6/5*(ycal2(15)-ycal2(14))+ycal2(14)-yexp2(2)
        x3=ycal2(21)-yexp2(3)
        alsq2=(x1**2+x2**2+x3**2)
c
        alsq = alsq1+alsq2
c
        return
        end
c*********************************************************************
        subroutine prm (ph12,ph22,al1,al2,an,w1,w2,g,sg1,sg2,bt,
     &                  e1,e2,e3)
        Implicit Real*8 (a-h,o-z)
        common /del/ del
        common /sur/ sur
        common /index/ indx
        common /cg0 / acg01, acg02,acg03
c
c 1-benzene
c 2-toluene
c 3-oxygen
c
        del  = del*1e-6
        write(6,52) del*1e6
c
        b0     = 100e3
c
        xv     = b0/1000
        fd     = 1-0.43*xv**0.92/(11.19+0.27*xv**0.99)
c
        df1  = 1.0374e-9 *3600.*fd
        df2  = 1.0315e-9 *3600.*fd
        df3  = 2.41e-9 *3600.*fd
c
        ay1    = 0.708
        ay2    = 0.708
        ay13   = 0.336
        ay23   = 0.341
c
        akss1 = 12.220
        amu1  = 0.6765
c
        akii2 = 78.9437
        akss2 = 11.0317
        amu2  = 1.5036
c
        akss12 = 4.5
        akss21 = 0.2
c
        akss13 = 0.26
        akss23 = 0.26
c
```

```
c
      ACG01 = 0.194
      ACG02 = 0.272
      ACG03 = 275.0
      aug   = 10.0e-3*60
      vv    = 15291*1e-6
c
      amm1 = .2266
      amm2 = .27
      amm3 =  34.4
c
      if (indx.eq.100)then
      CALL SVARI(sur,b0,vv,df1,df2,df3,ay1,ay2,ay13,ay23,AKSS1,
     &  amu1,akii2,akss2,amu2,akss12,akss21,akss13,akss23,acg01,
     &  acg02,acg03,aug, amm1,amm2,amm3,del)
      else
      endif
c
      ph12=amu1*del**2*b0/df1/ay1/akss1
      ph22=amu2*del**2*b0/df2/ay2/akss2
      a11=df1*ay1*akss1/ay13/akss13/df3
      a12=df2*ay2*akss2/ay23/akss13/df3
      g =akss2/akii2
      e1=acg01/amm1/akss1
      e2=acg02/amm2/akss2
      e3=acg03/amm3/akss13
      an=df1*sur*akss1*vv/del/aug/acg01
      w1=akss2*df2*acg01/akss1/df1/acg02
      w2=akss13*df3*acg01/akss1/df1/acg03
      sg1 = akss12*akss2/akss1
      sg2 = akss21*akss1/akss2
      bt  = akss23/akss13
c
      if (indx.eq.1000)then
      write(6,123)
      WRITE(6,1)
    1 FORMAT ('  ', '     Parameters Used :', /)
      WRITE(6,2) ph12,ph22, g
      WRITE(6,3) e1, e2,e3,AN
    2 FORMAT (3x,'ph1^2   =   ',e14.6,
     &        3x,'ph2^2   =   ',e14.6,/,
     &        3x,'gama    =   ',f14.6)
    3 FORMAT (3x,'Eps1    =   ',f14.6,
     &        3x,'Eps2    =   ',f14.6,/,
     &        3x,'Eps3    =   ',f14.6,
     &        3x,'n       =   ',f14.6)
      WRITE(6,4) a11,a12
      WRITE(6,5) w1,w2
    4 FORMAT (3x,'lamda1  =   ',e14.6,
     &        3x,'lamda2  =   ',e14.6)
      WRITE(6,51) sg1,sg2,bt
    5 FORMAT (3x,'omega1  =   ',e14.6,
     &        3x,'omega2  =   ',e14.6)
   51 FORMAT (3x,'sigma1  =   ',e14.6,
     &        3x,'sigma2  =   ',e14.6,
     &      /,3x,'beta    =   ',f14.3,/)
   52 format (3x,'del.(um)=     ',f14.3,/)
  123 FORMAT(' ____________________________________________________',/)
      else
      endif
      return
      end
c*******End of main program*****************************************
```

APPENDIX C

COMPUTER CODE FOR SOLVING BIOFILTRATION OF A SINGLE VOC UNDER TRANSIENT CONDITIONS

```
c*************************************************************
c
c  Purpose      : "Solution of the Transient Biofitration
c                  Model for a Single VOC"
c
c  Method       :  ODESSA-Ordinary Differential Equation
c                  Solver with explicit Sensitivity Analysis;
c                  Stiff mode with user supplied jacobian
c                  option is used
c
c  Language     :  FORTRAN
c
c  Requirement  :  ODESSA package which is a part of AUTO
c                  given in ref. (23)
c
c  By           :  Zarook Shareefdeen
c
c*************************************************************
      implicit double precision(a-h,o-z)
      parameter(nt=100)
      parameter(nh=20)
      external fun,dfun,jfun
      dimension par(7),y(3*nh,8),atol(3*nh,8),rtol(3*nh,8),
     1          rwork(5000),iwork(100),neq(2),iopt(3)
      dimension cg(nt,nh+1), co(nt,nh+1), cp(nt,nh+1),
     1          time(nt), ht(nh+1)
c
      common /ef1/ ef1
      common /del/ del
      common /dz / dz
      common /acg01/ acg01,tau
c
      open (5, file = 'trtol.dat', status='old')
      open (6, file = 'trtola.out', status='new')
      open (7, file = 'trtolb.out', status='new')
c
c  conditions of pdes
c
      n=3*nh
      npar=7
      neq(1)=n
      neq(2)=npar
      nsv=npar+1
c
c  initial conditions of the problem
c
      do 30 ih = 1,nh+1
      read (5,*) ht(ih),cg(1,ih),co(1,ih)
   30 continue
c
       isw = 1
c 1 = for startup
c
c for start-up only
c
       if (isw.eq.1)then
       do 31 ih = 2,nh+1
       cg(1,ih) = 1.0e-2
       co(1,ih) = 1.0e-2
   31  continue
       else
       endif
c
```

```
c
c  film thickness and effectiveness factors are
c  estimated from steady state models and correlations
c  are used
c
      avcg = acg01
      call pdelef ( avcg, del, ef1)
      call prm (1000,ak1,ak2,g,e1,e2,bet,rho)
c
      do 32 ih = 1,nh+1
      cp(1,ih) = cg(1,ih)/rho
   32 continue
c
      do 35 ih = 1,nh
      y(ih,1)       = cg(1,ih+1)
      y(ih+nh,1)    = co(1,ih+1)
      y(ih+2*nh,1)  = cp(1,ih+1)
   35 continue
c
      ht(1)   = 0.0
      time(1) = 0.0
      dz      = 1.0/float(nh)
c
c   error control
c
      err=1.d-12
      itol=4
      do 20 i=1,n
      do 20 j=1,nsv
      rtol(i,j)=err
   20 atol(i,j)=err
c
c   parameters for odessa
c
      itask=1
      iopt(1)=0
      iopt(2)=0
      iopt(3)=1
      lrw=5000
      liw=100
      mf=21
c
      do 69 it =1,nt
      cg(it,1) = 1.0
      co(it,1) = 1.0
      cp(it,1) = cg(it,1)/rho
  69  continue
c
      par(1) = e1
      par(2) = e2
      par(3) = g
      par(4) = ak1
      par(5) = ak2
      par(6) = bet
      par(7) = rho
c
      T       = time(1)
      delta   = 100.0
      istate  = 1
c
      do 60 it = 2,nt
c
      tout    = t + delta
```

```
      time(it) = tout
c
      CALL ODESSA(fun,dfun,NEQ,Y,PAR,T,TOUT,ITOL,RTOL,ATOL,
     1    ITASK,ISTATE, IOPT,RWORK,LRW,IWORK,LIW,jfun,MF)
      do 65 ih = 1, nh
      cg (it,ih+1) = y(ih,1)
      co (it,ih+1) = y(ih+nh,1)
      cp (it,ih+1) = y(ih+2*nh,1)
   65 continue
c
c     checking if steady state is reached
c
      d1 = abs (cg(it, nh+1)-cg(it-1, nh+1))
      d2 = abs (co(it, nh+1)-co(it-1, nh+1))
      d3 = abs (cp(it, nh+1)-cp(it-1, nh+1))
      if(d1.le.1.0e-4.and.d2.le.1.0e-4.and.
     &  d3.le.1.0e-4) then
      go to 46
      else
      endif
c
      avcg = cg(it,nh/2)*acg01
c
      call pdelef (avcg, del, ef1)
      call prm (2000,ak1,ak2,g,e1,e2,bet,rho)
      par(4) = ak1
      par(5) = ak2
      if(istate.lt.0)then
      go to 45
      else
      endif
   60 continue
c
c     output your results
c
   46 ntlast = it
      call print (cg,co,cp,time,ht,ntlast)
      call printxxx (cg,co,cp,time,ht,ntlast)
      write(7,47) tout*tau*24, it, nt
   47 format(//,5x,'Steady state has reached in',f10.3,
     &' hrs',/,5x,'Iterations = ',i10,/,5x,'Maximum
     &  Iterations = ',i10,//)
   45 write(6,*) '  istate=  ',istate
      stop
      end
c*************************************************************************
c print concentration changes along the column time
c*************************************************************************
      subroutine print(cg,co,cp,time,ht,ntlast)
      implicit double precision(a-h,o-z)
      parameter(nt=100)
      parameter(nh=20)
      dimension cg(nt,nh+1), co(nt,nh+1), cp(nt,nh+1),
     1          time(nt), ht(nh+1)
      write (6,84)
   84 format(//,5x,'Solution of the Transient Model',//)
      do 85 it = 1, ntlast
      write (6,86) time(it)
   86 format (/, 10x, 'At Time  =  ', f14.3,/)
      write (6,89)
   89 format(//,8x,'h/H',9x,'cg',13x,'co',13x,'cp',//)
      do 95 ih = 1, nh+1
      write (6,96) ht(ih), cg(it,ih), co(it,ih), cp(it,ih)
```

```
   96 format (5x, f7.3,3x,f10.4,5x,f10.4,5x,f10.4)
   95 continue
   85 continue
c
      return
      end
c*************************************************************************
c print concentration changes at the exit of the column with time
c*************************************************************************
      subroutine printx(cg,co,cp,time,ht,ntlast)
      implicit double precision(a-h,o-z)
      parameter(nt=100)
      parameter(nh=20)
      dimension cg(nt,nh+1), co(nt,nh+1), cp(nt,nh+1),
     1          time(nt), ht(nh+1)
      common /acg01/ acg01,tau
      write (7,84)
   84 format(//,5x,'Solution of the Transient Model',//)
      write (7,89)
   89 format(//,8x,'time',9x,'cge',13x,'coe',13x,'cpe',//)
      do 85 it = 1, ntlast
      write (7,96) time(it), cg(it,nh+1), co(it,nh+1), cp(it,nh+1)
   96 format (5x, f7.3,3x,f10.4,5x,f10.4,5x,f10.4)
   97 format (5x, e7.3,3x,e10.4)
   85 continue
c
      return
      end
c*************************************************************************
c print concentration changes at the selected locations
c*************************************************************************
      subroutine printxxx (cg,co,cp,time,ht,ntlast)
      implicit double precision(a-h,o-z)
      parameter(nt=100)
      parameter(nh=20)
      dimension cg(nt,nh+1), co(nt,nh+1), cp(nt,nh+1),
     1          time(nt), ht(nh+1)
      common /acg01/ acg01,tau
      write (7,84)
   84 format(//,5x,'Solution of the Transient Model',//)
      write (7,89)
   89 format(//,8x,'t (d)',7x,'cg-0.333',7x,'cg-0.666',8x,'cge',//)
      do 85 it = 1, ntlast
      days = time(it)*tau
      cg333 = 0.66*(cg(it,8)-cg(it,7))+cg(it,7)
      cg666 = 0.32*(cg(it,13)-cg(it,12))+cg(it,13)
      write (7,96) days, cg333,cg666,cg(it,nh+1)
   96 format (5x, f7.3,3x,f10.4,3x,f10.4,5x,f10.4)
   97 format (5x, e7.3,3x,e10.4)
   85 continue
c
      return
      end
C*************************************************************************
c  this subroutine computes the vectorfield
c*************************************************************************
      subroutine fun(neqn,t,y,par,ydot)
      IMPLICIT DOUBLE PRECISION (A-H,O-Z)
      dimension y(neqn),ydot(neqn),par(7)
      common /por/ por
      common /dz / dz
      common /fp / an
c
```

```
      nh = neqn/3
c
      do 10 i = 1,nh
      y1   = par(1)*par(2)*y(i)*y(i+nh)
      y2   = 1.+par(1)*y(i)+par(1)**2*y(i)**2*par(3)
      y3   = 1+par(2)*y(i+nh)
      fun1 = y1/y2/y3
      fun2 = y(i)-par(7)*(y(i+2*nh))**an
c
      if (i.eq.1)then
      der1  = (y(i)-1)/dz
      else
      der1  = (y(i)-y(i-1))/dz
      endif
c
      ydot(i)= -der1/por-par(4)*fun1-par(6)*fun2
  10  continue
c
      do 20 i = nh+1, 2*nh
      y1   = par(1)*par(2)*y(i-nh)*y(i)
      y2   = 1.+par(1)*y(i-nh)+par(1)**2*y(i-nh)**2*par(3)
      y3   = 1+par(2)*y(i)
      fun1 = y1/y2/y3
c
      if (i.eq.(nh+1))then
      der2  = (y(i)-1)/dz
      else
      der2  = (y(i)-y(i-1))/dz
      endif
c
      ydot(i)= -der2/por-par(5)*fun1
  20  continue
c
      do 30 i = 2*nh+1,3*nh
      fun2 = y(i-2*nh)-par(7)*(y(i))**an
      ydot(i)= par(6)*fun2
  30  continue
c
      RETURN
      END
C*******************************************************************************
c  this subroutine computes the jacobian
c  of the vectorfield
c*******************************************************************************
      subroutine jfun(neqn,t,y,par,ml,mu,pd,nrpd)
      implicit double precision (a-h,o-z)
c
      dimension y(neqn),pd(nrpd,neqn),par(7)
c
      common /por/ por
      common /dz / dz
      common /fp/ an
c
      nh = neqn/3
c
c
c  jacobian of the vectorfield
c
      do 9 i=1,neqn
      do 9 j=1,neqn
   9  pd(i,j)=0.
c
c for i = 1
```

```
c
      i    = 1
      y1   = par(1)*par(2)*y(i)*y(i+nh)
      y2   = 1.+par(1)*y(i)+par(1)**2*y(i)**2*par(3)
      y3   = 1+par(2)*y(i+nh)
      y4   = y1*y3*par(1)*(1.+2.*par(1)*y(i)*par(3))
      dfyi = (y1*y2*y3/y(i)-y4)/y2**2/y3**2
      pd(1,1) = -1/por/dz-par(4)*dfyi-par(6)
c
      dfyn = (y1*y2*y3/y(1+nh)-y1*y2*par(2))/y2**2/y3**2
      pd(1, nh+1) = -par(4)*dfyn
      pd(1,2*nh+1) = par(6)*par(7)*an*(y(i+2*nh))**(an-1)
c
c for i = 2, nh
c
      do 10 i = 2, nh
      pd (i, i-1) = 1/por/dz
c
      y1   = par(1)*par(2)*y(i)*y(i+nh)
      y2   = 1.+par(1)*y(i)+par(1)**2*y(i)**2*par(3)
      y3   = 1+par(2)*y(i+nh)
      y4   = y1*y3*par(1)*(1.+2.*par(1)*y(i)*par(3))
      dfyi = (y1*y2*y3/y(i)-y4)/y2**2/y3**2
c
      pd(i,i) = -1/por/dz-par(4)*dfyi-par(6)
c
      dfyn = (y1*y2*y3/y(i+nh)-y1*y2*par(2))/y2**2/y3**2
      pd(i, nh+i) = -par(4)*dfyn
c
      pd(i,2*nh+i) = par(6)*par(7)*an*(y(i+2*nh))**(an-1)
 10   continue
c
c for i = nh+1
c correct i value dont change....
c
      i    = 1
      y1   = par(1)*par(2)*y(i)*y(i+nh)
      y2   = 1.+par(1)*y(i)+par(1)**2*y(i)**2*par(3)
      y3   = 1+par(2)*y(i+nh)
      y4   = y1*y3*par(1)*(1.+2.*par(1)*y(i)*par(3))
      dfyi = (y1*y2*y3/y(i)-y4)/y2**2/y3**2
      pd(nh+1,1) = -par(5)*dfyi
c
      dfyn = (y1*y2*y3/y(1+nh)-y1*y2*par(2))/y2**2/y3**2
      pd(nh+1, nh+1) = -1/por/dz-par(5)*dfyn
c
c
c for i = nh+2 to 2*nh
c
      do 20 i = nh+2, 2*nh
      pd (i, i-1) = 1/por/dz
c
      y1   = par(1)*par(2)*y(i-nh)*y(i)
      y2   = 1.+par(1)*y(i-nh)+par(1)**2*y(i-nh)**2*par(3)
      y3   = 1+par(2)*y(i)
      y4   = y1*y3*par(1)*(1.+2.*par(1)*y(i-nh)*par(3))
      dfyi = (y1*y2*y3/y(i-nh)-y4)/y2**2/y3**2
c
      pd(i,i-nh) = -par(5)*dfyi
c
      dfyn = (y1*y2*y3/y(i)-y1*y2*par(2))/y2**2/y3**2
      pd(i, i) = -1/por/dz-par(5)*dfyn
 20   continue
```

```
c
c
c
c for i = 2*nh+1 to 3*nh
c
      do 30 i = 2*nh+1, 3*nh
      pd (i, i-2*nh) = par(6)
      pd (i,i) = -par(6)*par(7)*an*(y(i))**(an-1)
  30  continue
c
      RETURN
      END
C*********************************************************************
      subroutine dfun(neqn,t,y,par,dfdp,jpar)
c*****************************************
c      partial derivatives wrt. parameters of interest
c
      implicit double precision(a-h,o-z)
      dimension y(neqn),par(20),dfdp(20)
      return
      end
c*********************************************************************
c-----------------------------------------------------------
c     dummy subroutines
c-----------------------------------------------------------
      subroutine bcnd
      return
      end
      subroutine fopt
      return
      end
      subroutine icnd
      return
      end
c***********************************************************
        subroutine prm (index,ak1,ak2,g,e1,e2,bet,rho)
        implicit double precision (a-h,o-z)
        common /por/ por
        common /del/ del
        common /ef1/ ef1
        common /acg01/ acg01,tau
        common /fp/ an
c
c 1-compound
c 2-oxygen
c
        del = del*1e-6
c
        b0     = 100e3
c
        xv     = b0/1000
        fd     = 1-0.43*xv**0.92/(11.19+0.27*xv**0.99)
c
        call compm (fd,  df1, ay1, ay2, akii1,
     &  akss1, amu1,amm1)
c
        amm2 =  34.4
        df2  = 2.41e-9 *3600.*fd
        akss2 = 0.26
c
        ACG01 = 2.806
        aug   = 0.049
        vv    = 5150e-6
```

```
c
c in days
c
      tau   = vv/aug/24.0
c
      acg02 = 275
c
      ef2  = ef1
      alp  = 0.3
      por  = 0.3
      aka  = 0.302
      rp   = 0.428e6
c
c  Freundlich Isotherm,
c
      akd  = 2.254e-5
      an   = 0.96
c
      sur = 40.0/alp
c
      if (index. eq. 1000) then
      CALL SVARI(sur,b0,vv,df1,df2,ay1,ay2,AKII1,AKSS1,
     &  del,amu1,akss2,acg01,acg02,aug, amm1,amm2,
     &  ef1, ef2, alp, por, aka, an, rp, akd)
      else
      endif
c
      ak1=ef1*alp*sur*del*b0*vv*amu1/ay1/aug/acg01/por
      ak2=ef2*alp*sur*del*b0*vv*amu1/ay2/aug/acg02/por
      g =akss1/akii1
      e1=acg01/amm1/akss1
      e2=acg02/amm2/akss2
c
      factor = 0.02
c
      bet = aka*(1-alp)*sur*vv/aug/por*factor
c
      rho = acg01*(an-1)*(por/rp/akd/(1-por))**an
c
      if (index. eq. 1000)then
      write(6,123)
      WRITE(6,1)
    1 FORMAT (10x,'Parameters Estimated from the Data Above', /)
      WRITE(6,2) ak1, ak2
      WRITE(6,3) e1, e2
    2 FORMAT ('  ', ' ak1   =   ',e14.3,3x,'ak2 = ',3x,f7.3)
    3 FORMAT ('  ', ' eps1 =   ',f14.6,3x,'eps2    = ',3x,f7.3)
      WRITE(6,4) g,bet
      WRITE(6,5) rho
    4 FORMAT ('  ', ' g =   ',e14.3,5x,'bet =', f10.6,/)
    5 FORMAT ('  ', ' rho =   ',e14.3,3x,/)
      write(6,123)
      else
      endif
  123 FORMAT(' ____________________________________________________________',/)
      return
      end
c*********************************************************************
      subroutine pdelef (avcg, del, ef1)
      implicit double precision (a-h,o-z)
      del = 1.513*avcg+33.35
      ef1 = 0.031*avcg+0.190
      return
```

```
      end
C*********************************************************************
      subroutine compm (fd,  df1, ay1, ay2, akii1,
     &  akss1, amu1,amm1)
      implicit double precision (a-h,o-z)
c
      df1   = 1.0315e-9 *3600.*fd
      ay1   = 0.71
      ay2   = 0.341
      akii1 = 78.94
      akss1 = 11.03
      amu1  = 1.50
      amm1 = .27
c
      return
      end
C*********************************************************************
      Subroutine SVARI(sur,b0,vv,df1,df2,ay1,ay2,AKII1,AKSS1,
     &  del,amu1,akss2,acg01,acg02,aug, amm1,amm2,
     &  ef1, ef2, alp, por, aka, an, rp, akd)
c
      write(6,123)
      WRITE(6,1)
    1 FORMAT (5x,/, ' Input data for Transient Biofilter Model',/)
      WRITE(6,19) Aug
   19 format ('  ', 'Gas Flow Rate (m3/hr)        = ', e14.3)
      WRITE(6,3) vv*1e6
    3 FORMAT ('  ', 'Volume of the column(cm3)    = ', f14.3)
      WRITE(6,4) SUR
    4 FORMAT ('  ', 'Biolayer Sur.Area( m2/m3)    = ', f14.3)
      write(6,44) b0
   44 format ('  ', 'Biomass Conc. (g/m3)         = ', e14.3)
      WRITE(6,5) del*1e3
    5 FORMAT ('  ', 'Film thickness (mm)          = ', f14.3)
      WRITE(6,2) ACG01
      WRITE(6,22) ACG02
    2 FORMAT ('  ', 'Inlet conc. (g/m3 of air)(m) = ', f14.3)
   22 FORMAT ('  ', 'Inlet conc. (g/m3 of air)(o) = ', f14.3)
      write(6,31) ay1
   31 format ('  ', 'Yield Coefficient (1)        = ', f14.3)
      write(6,32) ay2
   32 format ('  ', 'Yield Coefficient (o)        = ', f14.3)
      WRITE(6,51) df1*1e9/3600
      WRITE(6,54) df2*1e9/3600
   51 format ('  ', 'Diff. Coefficient (1)*1e9    = ', f14.3)
   54 format ('  ', 'Diff. Coefficient (o)*1e9    = ', f14.3)
      WRITE(6,56) amm1
   56 FORMAT ('  ', 'Dist. Coeff.        (1)      = ', e14.3)
      WRITE(6,566) amm2
  566 FORMAT ('  ', 'Dist. Coeff.        (o)      = ', e14.3)
      WRITE(6,567) ef1
  567 FORMAT ('  ', 'ef-factor (1)                = ', e14.3)
      WRITE(6,568) ef2
  568 FORMAT ('  ', 'ef-factor (2)                = ', e14.3)
      WRITE(6,569) por
  569 FORMAT ('  ', 'porosity                     = ', e14.3)
      WRITE(6,570) aka
  570 FORMAT ('  ', 'mass transfer coef.          = ', e14.3)
      WRITE(6,571) akd
  571 FORMAT ('  ', 'adsorption parameter (akd)   = ', e14.3)
      WRITE(6,572) an
  572 FORMAT ('  ', 'adsorption parameter (an)    = ', e14.3)
      WRITE(6,573) rp/1e6
```

```
  573   FORMAT ('  ', 'particle density (g/cm3)     = ', e14.3)
        WRITE(6,574) alp
  574   FORMAT ('  ', '% area covered by biomass    = ', e14.3)
        write(6,123)
        write(6,*) '          Andrews and other  Parameters'
        WRITE(6,6) akii1,akss1,amu1, akss2
    6   format(' ',/, ' Ki1 (g/m3) = ',e14.3,3x,'Ks1 (g/m3) = ', f7.3,
     &  /,' Sp. Growth Rate-1 (1/hr)=',f14.3,3x,/,' ',
     &  'aKd (g/m3) = ', f7.3,/)
        write(6,123)
  123   FORMAT(' ____________________________________________________',/)
        return
        end
c*********************************************************************
```

REFERENCES

1. Alvarez, P. J. J., and T. M. Vogel, "Substrate Interactions of Benzene, Toluene, and para-Xylene during Microbial Degradation by Pure Cultures and Mixed Culture Aquifer Slurries." *Appl. Environ. Microbiol.* 57 (1991):2981-2985.

2. Andrews, J. F., "A Mathematical Model for the Continuous Culture of Microorganisms Utilizing Inhibitory Substrates." *Biotechnol. Bioeng.* 10 (1968): 707-723.

3. Arcangeli, J. P., and E. Arvin, "Toluene Biodegradation and Biofilm Growth in an Aerobic Fixed-Film Reactor." *Appl. Microbiol. Biotechnol.* 37(1992):510-517.

4. Arvin, E., B. J. Jensen, and A. T. Gundersen, "Substrate Interaction During Aerobic Biodegradation of Benzene." *Appl. Environ. Microbiol.* 55(1989):3221-3225.

5. Bader, F. G., "Kinetics of Double-Substrate Limited Growth." pp.1-32 In: *Microbial Population Dynamics.* M.J. Bazin (ed.), CRC Press, Boca Raton, FL 1982.

6. Bailey, J. E., and D. F., Ollis, *Biochemical Engineering Fundamentals.* 2nd edition. McGraw-Hill, New York, 1986.

7. Barbee, G. C., and K. W. Brown, "Movement of Xylene Through Unsaturated Soils Following Simulated Spills." *Water Air Soil Pollut.* 29(1986):321-331.

8. Bird, R. B., W. E. Stewart, and E. N., Lightfoot, *Transport Phenomena.* John Wiley & Sons, New York, 1960.

9. Bohn, H., "Soil and Compost Filters of Malodorant Gases." *J. Air Pollut. Control Assoc.* 25 (1975) 953-955.

10. Bohn, H., "Consider Biofiltration for Decontaminated Gases." *Chem. Eng. Progress, April* (1992): 34-40.

11. Bohn, H.,"Biofiltration: Design Principles and Pitfalls", 86th Annual Meeting of the Air & Waste Management Association, Paper No. 93-TP-52A.01, Denver, CO, June 13-18, 1993.

12. Bohn, H., and R., Bohn, "Soil Beds Weed Out Air Pollutants." *Chemical Engineer* 95 (4) (1988): 73-76.

13. Chang, M. -K., T. C., Voice, and C. S. Criddle, "Kinetics of Competitive Inhibition and Cometabolism in the Biodegradation of Benzene, Toluene, and *p*-Xylene by Two *Pseudomonas* isolates." *Biotechnol. Bioeng.* 41(1993):1057-1065.

14. Crueger, W., and A. Crueger, *Biotechnology: A Textbook of Industrial Microbiology.* 2nd edition. T.D. Brock, editor of the english edition. Sinauer Associates, Sunderland, MA, 1976.

15. Dean, B. J., "Recent Findings on the Genetic Toxicology of Benzene, Toluene, Xylenes and Phenols." *Mutat. Res.* 145(1985):153-181.

16. Deshusses, M. A., and I. J. Dunn, "Modeling Experiments on the Kinetics of Mixed-solvent Removal from Waste Gas in a Biofilter", In proceedings of the 6th European Congress on Biotechnology, Florence, June 13-17, 1993.

17. Deshusses, M. A., and G. Hamer, "The Removal of Volatile Ketone Mixtures from Air in Biofilters", *Bioprocess Eng.* 9 (1993): 141-146.

18. Dharmavaram, S., "Biofiltration: A Lean Emissions Abatement Technology," 84th Annual Meeting of the Air & Waste Management Association, Paper No. 91-103.2, Vancouver, BC, June 16-21, 1991.

19. DiGiulio, D.C., "Evaluation of Soil Venting Application." *J. Hazard. Mat.* 32(1992): 279-291.

20. Diks, R. M. M., *The Removal of Dichloromethane from Waste Gases in a Biological Trickling Filter*, Ph.D. Thesis, The Eindhoven University of Technology, The Netherlands, 1992.

21. Diks, R. M. M. and S. P. P. Ottengraf, "Process Technological View on the Elimination of Chlorinated Hydrocarbons from Waste gases", Proceedings of the 8th World Clean Air Congress, pp 405-410, In: *Man and his Ecosystem*, L.J. Brasser and W.C. Mulder (Eds)., Elsevier Publishers B.V., Amsterdam, 1989.

22. Diks, R. M. M. and S. P. P. Ottengraf, "Verification Studies of a Simplified Model for Removal of Dichloromethane from Waste Gases Using a Biological Trickling Filter. Part 1," *Bioprocess Engineering* 6 (1991): 93-99.

23. Doedel, E. J., *AUTO: Software for Continuation and Bifurcation Problems in Ordinary Differential Equations.* CIT Press, Pasadena, CA, 1986.

24. Ebinger, M. H., H. L. Bohn and R. W. Puls, "Propane Removal from Propane-Air Mixtures by Soil Beds." *JAPCA*, 37, No. 12 (1987):1486-1489.

25. Environmental Protection Agency, *Test Methods for Evaluating Solid Waste.* SW-846, III. Ed., Vol. I.A. USEPA, Washington, DC, 1986.

26. Ergas, S. J., E. D. Schroeder, and D. P. Y. Chang, "VOC Emission Control from Wastewater Treatment Facilities Using Biofiltration." 84th Annual Meeting of the Air & Waste Management Association, Paper No. 91-105.4, Vancouver, British Columbia, June 16-21, 1991.

27. Ergas, S. J., E. D. Schroeder, and D. P. Y. Chang, "Control of Air Emissions of Dichloromethane, Tricholoroethene, and Toluene by Biofiltration." 86th Annual Meeting of the Air & Waste Management Association, Paper No. 93-WA-52B, Denver, CO, June 13-18, 1993.

28. Fan, L. -S., K. Fujie, T. -R. Long, and W. -T. Tang, "Characteristics of a Draft Tube Gas-Liquid-Solid Fluidized-Bed Bioreactor with Immobilized Living Cells for Phenol Degradation." *Biotechnol. Bioeng.* 30 (1987): 498-504.

29. Fan, L. -S., R. Leyva-Ramos, K. D. Wisecarver, and B. J., Zehner, "Diffusion of Phenol Through a Biofilm Grown on Activated Carbon Particles in a Draft-Tube Three-Phase Fluidized-Bed Bioreactor." *Biotechnol. Bioeng.* 35(1990) : 279-286.

30. Finlayson, B. A., *Nonlinear Analysis in Chemical Engineering,* McGraw-Hill, New York, 1980.

31. Gibson, D. T., and V. Subramanian, "Microbial Degradation of Aromatic Hydrocarbons." pp. 181-252. In: *Microbial Degradation of Organic Compounds.* D.T. Gibson (ed.), Marcel Dekker, Inc., New York, 1984.

32. Gmehling, J., U. Onken, and W. Arlt, *Vapor-Liquid Equilibrium Data Collection: Aqueous-Organic Systems* (supplement 1). In: D. Behrens and R. Eckermann (ed.), Chemistry data series, vol. 1, part 1a. Dechema, Frankfurt, Germany, 1981.

33. Grbic-Galic, D. and T. M. Vogel, "Transformation of Toluene and Benzene by Mixed Methanogenic Cultures." *Appl. Environ. Microbiol.* 53(1987):254-260.

34. Grocco, J. "Methanol : Yesterday, Today and Tomorrow. *Chemistry & Industry* 4(1990): 97-101.

35. Haigler, B. E., C. A., Pettigrew and J. Spain, "Biodegradation of Mixtures of Substituted Benzenes by *Pseudomonas* sp. Strain JS150." *Appl. Environ. Microbiol.* 58(1992):2237-2244.

36. Jones, W. L., J. D. Dockery and C. R. Vogel, "Diffusion and Reaction within Porous Packing Media: A Phenomenological Model", *Biotechnol. Bioeng.* 41(1993):947-956.

37. Karel, S. F., S. B. Libicki, and C. R. Robertson, "The Immobilization of Whole Cells: Engineering Principles." *Chem. Eng. Sci.* 40 (1985): 1321-1354.

38. Leson, G., D. S. Hodge, F. Tabatabai, and A. M. Winer, "Biofilter Demonstration Projects for the Control of Ethanol Emissions." 86th Annual Meeting of the Air & Waste Management Association, Paper No. 93-WP-52C.04, Denver, CO, June 13-18, 1993.

39. Leson, G., and A. M. Winer, "Biofiltration: an Innovative Air Pollution Control Technology for VOC Emissions. *J Air Manage. Assoc.* 41(1991): 1045-1054.

40. Levenspiel, O., *Chemical Reaction Engineering*, John Wiley & Sons, New York, pp. 473-475, 1972.

41. Livingston, A. G., "Biodegradation of 3,4-Dichloroaniline in a Fluidized Bed Bioreactor and a Steady-State Biofilm Kinetic Model." *Biotechnol. Bioeng.* 38(1991): 260-272.

42. Livingston, A. G., and H. A. Chase, "Modeling Phenol Degradation in a Fluidized-Bed Bioreactor." *AIChE J.* 35(1989): 1980-1992.

43. Mackay, D. and W. Y. Shiu, "A Critical Review of Henry's Law Constants for Chemicals of Environmental Interest." *J. Phys. Chem. Ref. Data*, Vol 10, No 4 (1981):1175-1199.

44. Monod, J., *Recherches sur la Croissance des Cultures Bacteriennes, Hermann et Cie*, Paris, 1942.

45. Ockeloen, H. F., T. J. Overcamp, and C. P. L. Grady, Jr., "A Biological Fixed-Film Simulation Model for the Removal of Volatile Organic Air Pollutants," 85th Annual Meeting of the Air & Waste Management Association, Paper No. 92-116.05, Kansas City, MO, June 21-26, 1992.

46. Oh, Y. -S., *Biofiltration of Solvent Vapors from Air*, Ph.D. Thesis, Rutgers University, New Brunswick, NJ, 1993.

47. Ottengraf, S. P. P., "Exhaust Gas Purification." pp. 425-452. In: *Biotechnology*, W. Shonborn (ed.), vol. 8. VCH Verlagsgesellschaft, Weinheim, Germany, 1986.

48. Ottengraf, S. P. P., "Biological Systems for Waste Gas Elimination." *Trends Biotechnol*, 5 (1987): 132-136.

49. Ottengraf, S. P. P. and R. Disks, "Biological Purification of Waste Gases." *Chimicaoggi*, May (1990):41-45.

50. Ottengraf, S. P. P., and J. H. G. Konings, "Emission of Microorganisms from Biofilters." *Bioprocess Eng.* 7 (1991): 89-96.

51. Ottengraf, S. P. P., J. J. P. Meesters, A. H. C. van den Oever, and H. R. Rozema, "Biological Elimination of Volatile Xenobiotic Compounds in Biofilters." *Bioprocess Eng.* 1 (1986): 61-69.

52. Ottengraf, S. P. P., and A. H. C. van den Oever, "Kinetics of Organic Compound Removal from Waste Gases with a Biological Filter." *Biotechnol. Bioeng.* 25 (1983): 3089-3102.

53. Ottengraf, S. P. P., A. H. C. van Den Oever, and F. J. C. M. Kempenaars, "Waste Gas Purification in a Biological Filter Bed." In: *Innovations in Biotechnology*, Elsevier Science Publications, Amsterdam, 1983.

54. Overcamp, T. J., G. R. DeHollander, H. -C. Chang, and C. P. L. Grady, Jr., "A Biologically-Enhanced Scrubber for Volatile Organic Compounds." 84th Annual Meeting of the Air & Waste Management Association, Paper No. 91-180.12, Vancouver, BC, June 16-21, 1991.

55. Overcamp, T. J., H. F. Ockeloen, H.-C. Chang, and C. P. L. Grady, Jr., "Design Criteria for Bioscrubbers: Fixed-Film Versus Suspended-Growth Reactors." 9th World Clean Air Congress and Exhibition, Paper No. IU-18C.11, Montreal, Quebec, Canada, August 30-September 4, 1992.

56. Paul P. G., and C. Roos, "Biological Waste Air Treatment with the Biobox." Proceedings of the 8th World Clean Air Congress, pp 399-404, In: *Man and his Ecosystem*, L. J. Brasser and W.C. Mulder (Eds)., Elsevier Publishers B.V., Amsterdam, 1989.

57. Perry R. H., and D. Green, *Perry's Chemical Engineers' Handbook*, Sixth Edition, McGraw-Hill Inc., New York, 1984.

58. Phipps Jr., D. W., and H. F. Ridgway, "Modular Bioreactor and Computerized Instrumentation Package to Identify Critical Design Parameters for Vapor Phase Bioreactors.", Proceedings of the 2nd International Symposium on In Situ and On-Site Bioreclamation, San Diego, CA, April 5-8 1993.

59. Pomeroy, D., "Biological Treatment of Odorous Air." *J. Water Pollut. Contr. Fed.* 54(1982): 1541-1545.

60. Potter, T. L., "Fingerprinting Petroleum Products: Unleaded Gasolines." pp. 83-92. In: *Petroleum Contaminated Soils*, Vol. 3, P.T. Kostecki and E.J. Calabrese, (Eds.), Lewis Publishers, Chelsea, MI, 1992.

61. Pye, V. I., and R. Patrick, "Groundwater Contamination in the United States." *Science* 221(1983):713-718.

62. Reid, R. C., J. M. Prausnitz, and T. K. Sherwood, *The Properties of Gases and Liquids*. 3rd edition. McGraw-Hill, New York, 1977.

63. Reisch, M. S., "Top 50 Chemicals Production Stagnated Last Year." *Chem. Eng. News* 70 (15)(1992):16-22.

64. Shareefdeen, Z., B. C. Baltzis, Y. -S. Oh and R. Bartha, "Biofiltration of Methanol Vapor." *Biotechnol. Bioeng.* 41(1993): 512-524.

65. Shuler, M. L., and F. Kargi, *Bioprocess Engineering: Basic Concepts.* Prentice-Hall, Englewood Cliffs, NJ, 1992.

66. Smith, R. K., "The Biodegradation of Aromatic Hydrocarbons by Bacteria." *Biodegradation* 1(1990):191-206.

67. Smith, P. J., P. Biswas, M. T. Suidan, and R. C. Brenner, "Treatment of Volatile Organic Compounds in Waste Gases Using a Trickling Biofilter System: A Modeling Approach." 86th Annual Meeting of the Air & Waste Management Association, Paper No. 93-TP-52A.05, Denver, CO, June 13-18, 1993.

68. Sorial, G. A., F. L. Smith, P. J. Smith, M. T. Suidan, and P. Biswas, "Development of Aerobic Biofilter Design Criteria for Treating VOCs.", 86th Annual Meeting of the Air & Waste Management Association, Paper No. 93-TP-52A.04, Denver, CO, June 13-18, 1993.

69. Tang, W. -T., and L. -S. Fan, "Steady State Phenol Degradation in a Draft-Tube, Gas-Liquid-Solid Fluidized-Bed Bioreactor." *AIChE J.* 33(1987): 239-249.

70. Tang, W. -T., K. Wisecarver, and L. -S. Fan, "Dynamics of a Draft Tube Gas-Liquid-Solid Fluidized Bed Bioreactor for Phenol Degradation." *Chem. Eng. Sci.* 42(1987): 2123-2134.

71. Tong, C. C, and L. -S. Fan, "Concentration Multiplicity in a Draft Tube Fluidized-Bed Bioreactor Involving Two Limiting Substrates." *Biotechnol. Bioeng.* 31(1988): 24-34.

72. Togna, A. P., and S. Frisch, "Field-Pilot Study of Styrene Biodegradation Using Biofiltration.", 86th Annual Meeting of the Air & Waste Management Association, Paper No. 93-WP-52C.03, Denver, CO, June 13-18, 1993.

73. Utgikar, V., R. Govind, Y. Shan, S. Safferman, and R. C. Brenner, "Biodegradation of Volatile Organic Chemicals in a Biofilter." pp.233-260. In *Emerging Technologies in Hazardous Waste Management II*, D.W. Tedder and F. G. Pokland, (Eds.) ACS Symposium Series 468, Washington, DC, 1991.

74. van Lith, C., S. L. David, and R. Marsh, "Design Criteria for Biofilters." *Trans. IChemE.* 68(1990.): 127-132.

75. van Lith, C., "Biofiltration, An Essential Technique in Air Pollution Control." Proceedings of the 8th World Clean Air Congress, pp 393-399, In: *Man and his Ecosystem*, L.J. Brasser and W.C. Mulder (Eds)., Elsevier Publishers B.V., Amsterdam, 1989.

76. Villadsen, J. and M. L. Michelsen, *Solution of Differential Equation Models by Polynomial Approximation*, Prentice-Hall Inc., NJ, 1978.

77. Williamson, K., and P. L. McCarty, "A Model of Substrate Utilization by Bacterial Films." *J. Water Pollut. Contr. Fed.* 48(1976): 9-24.

78. Williamson, K., and P. L. McCarty, "Verification Studies of the Biofilm Model for Bacterial Substrate Utilization." *J. Water Pollut. Contr. Fed.* 48(1976): 281-296.

79. Zeyer, J., E. P. Kuhn, P. Eichner, and R. F. Schwarzenbach, "Rapid Microbial Mineralization of Toluene and 1,2-Dimethylbenzene in the Absence of Molecular Oxygen." *Appl. Environ. Microbiol.* 52(1986):944-947.

80. Zilli, M., A. Converti, A. Lodi, M. Del Borghi, and G. Ferraiolo, "Phenol Removal From Waste Gases with a Biological Filter by *Pseudomonas Putida.*" *Biotechnol. Bioeng.* 41 (1993): 693-699.